GEORG-AUGUST-UNIVERSITÄT
GÖTTINGEN

Regulation of Dual Leucine Zipper Kinase (DLK) by Prediabetic Signals

Dissertation
for the award of the degree
"Doctor rerum naturalium" (Dr.rer.nat.)
of the Georg-August-Universität Göttingen

within the doctoral program Biology
of the Georg-August University School of Science (GAUSS)

submitted by
Rohollah Babaeikelishomi

from
Roodbar, Iran

Göttingen, 2013

Thesis Committee

Prof. Dr Ralf Heinrich, Department of Cellular Neurobiology, University Göttingen.

Prof. Dr. Hubertus Jarry, Department of Clinical and Experimental Endocrinology, Universitätmedizin Göttingen, UMG.

Members of the Examination Board

Reviewer: Prof. Dr. Susanne Lutz, Department of Pharmacology, Universitätmedizin Göttingen, UMG.

Second Reviewer: Prof. Dr. Ralph Kehlenbach, Department of Biochemistry and Molecular Biology, Universität Göttingen.

Further members of the Examination Board:

Prof. Dr. Dörthe Katschinski, Department of Heart- and Circulation Phsiology, Universitätmedizin Göttingen, UMG.

Prof. Dr. Sigrid Hoyer-Fender, Johann-Friedrich-Blumenbach-Institut of Zoologie and Anthropologie.

Date of the oral examination: 26.03.2013

Declaration

I declare that this submission is my own work, and it contains no materials which have been published before by another person, except those are clearly cited.

Rohollah Babaeikelishomi

Göttingen, March 2013

List of Figures

List of Tables

Acknowledgements

I deeply thank my scientific advisor, Prof. Elke Oetjen, who initiated and continuously supported the projects. I am grateful for her scientific guidance and technical advisory, which helped me to explore the fields related to this study. I am also grateful to my thesis committee members Prof. R. Heinrich and Prof. H. Jarry for their comments and inspiring discussion during the meetings.

I sincerely thank Dr. Ralph Kehlenbach for helping in protein purification process. I am grateful to all colleges and friends in department of pharmacology in klinikum Goettingen and UKE Hamburg for their help and support: Dr. Annette Heinrich, Dr. Stephan Döker, Dr Diana Keiser, Dr. Phu DT, Julia Meike Krebs, Marie-Jeannette Stahnke, Roland Blume, Anja Pahl.

My special thanks go to Prof. Wolfram Hubertus Zimmermann, Prof. Ali El-Armouche, Prof. Susanne Lutz, Prof Böger, and Prof Eschenhagen.

I would like to thank Mostafa Bakhti, Mehdi Pirouz, Ali Shahmoradi, Zohreh Farsi, Atefeh Pooryasin, Tahereh Ajam, Farnaz Shamsi, Ahmad Mirkhani and for the nice atmosphere we had together during staying in Göttingen.

I sincerely thank Mona Shaghayegh Khoshmehr for her kind help in the translation of the summary.

Finally my special thanks go to my family, especially my parents for their unlimited support and love, and for everything that they have done for me.

Abbreviations

AP-1	**activator protein-1**
APS	**ammonium persulphate**
ATP	**adenosine triphosphate**
BAC	**bacterial artificial chromosome**
BSA	**bovine serum albumin**
CBP	**CREB binding protein**
CiAP	**calf intestine alkaline phosphatase**
cko	**Knock-out**
CN	**calcineurin**
CRD	**carbohydrate rich diet**
CRE	**cAMP response element**
CREB	**CRE binding protein**
CRTC	**CREB- regulated transcription coactivator**
CsA	**cyclosporine A**
DD	**death domain**
DLK	**dual leucine zipper kinase**
DM	**diabetes mellitus**
DMSO	**dimethyl sulfoxide**
dNTP	**deoxynucleoside triphosphates**
DTT	**dithiotreitol**
EPAC	**exchange protein activated by cAMP**
ER	**endoplasmic reticulum**
ERK	**extracellular signal-regulated kinase**
FADD	**Fas-associated death domain protein**
FCS	**fetal calf serum**
FFA	**free fatty acid**
FRT	**flippase recognition target**
GAS	**IFNγ-activated site**
GDM	**gestational diabetes mellitus**
GFPtpz	**green fluorescent protein variant topaz**
GLP	**glucagon like peptide**
GLUT	**glucose transporter**
GST	**Glutathione-s-transferase**
HFD	**High-fat diet**
hIP	**Human insulin promoter**
HIT	**Hamster insulinotropic**
HS	**Horse serum**
IFNGR	**IFNγ receptor**
IFNγ	**Interferon γ**
IGT	**Impaired glucose tolerance**
IKK	**inhibitor of κB kinase**
IL-1R	**IL-1 receptor**
IL-1Ra	**IL-1 receptor antagonist**
IL-1RAcP	**IL-1R accessory protein**
IL-1β	**Interleukin-1β**
IPTG	**Isopropyl-β-D-thiogalactoside**
IRF	**IFN-regulatory factor**
IRS	**insulin receptor substarte**
JIP	**JNK interacting protein**
JNK	**C-jun N-terminal kinase**
LZ	**leucine zipper**
LZK	**leucine zipper-binding kinaser**
MAPK	**mitogen activated protein kinase**
MAPKK	**mitogen activated protein kinase kinase**
MAPKKK	**mitogen activated protein kinase kinase kinase**
MBP	**maltose binding protein**
MLK	**mixed lineage kinase**
MODY	**maturity onset diabetes of the young**
ND	**normal diet**
NFκB	**nuclear factor κB**
NK	**natural killer cells**
NKT	**natural killer T cells**
NLS	**nuclear localization signal**
NOD	**non-obese diabetic**

Nup	**nucleoporin**
OD	**optical density**
PAGE	**poly acrylamide gel electrophoresis**
PBS	**phosphate buffered saline**
pBSK	**bluescript plasmid**
PCR	**polymerase chain reaction**
PDX-1	**pancreatic and duodenal homebox-1**
PFG	**pulsed-field gel**
PI-3K	**phosphoinositide-3 kinase**
RIP	**receptor interacting protein**
PKA	**protein kinase A**
PKB	**protein kinase B**
PKC	**protein kinase C**
PMSF	**phenylmethylsulfonylfluoride**
ROS	**reactive oxygen species**
SAPK	**stress activated protein kinase**
SDS	**sodium dodecylsulphate**
SH3	**SRC homology 3**
SODD	**silencer of death domain**
T1DM	**type 1 diabetes mellitus**
T2DM	**type 2 diabetes mellitus**
TACE	**TNFα converting enzyme**
TBS	**Tris base saline**
TEMED	**tetramethylethylenediamine**
TK	**thymidine kinase**
TNFR	**TNF receptor**
TNFα	**tumor necrosis factor α**
TRADD	**TNFR associated death domain**
TRAF	**TNFR associated factor**
VDCC	**voltage dependent calcium chanel**
WAT	**white adipose tissue**
ZPK	**zipper protein kinase**

1. Introduction

1.1 Diabetes mellitus

Diabetes mellitus (DM) refers to a group of metabolic disorders with the common phenotype of hyperglycemia. Complex interaction of genetic and environmental factors results in distinct types of DM mainly by reduced insulin secretion, decreased glucose utilization, and increased glucose production (Beck-Nielsen 2002). Depending on the etiology, DM is classified into different types. Two major types of DM, type 1 and type 2, are discussed below. Maturity onset diabetes of the young (MODY) is a genetic autosomal dominant disorder which occurs usually in people younger than 25 years and characterized by insulin secretion impairment. Gestational diabetes mellitus (GDM) may develop during pregnancy, in which metabolic changes of late pregnancy resulted in insulin resistance, subsequently the increased insulin requirement may lead to impaired glucose tolerance (IGT). Mutation in insulin receptor, destruction of pancreatic islet due to pancreatic exocrine disease, antagonizing of insulin action by hormones, and viral infection of islets (fulminant diabetes) are the etiologies for some rare subtypes of DM.

1.1.a Type 1 diabetes mellitus

Type 1 diabetes is a chronic autoimmune disease in which the pancreatic insulin-producing β-cells are selectively destroyed by the immune system (Eisenbarth 1986). This type of diabetes is characterized by the progressive infiltration of pancreatic β-cells by $CD4^+$ and $CD8^+$ T-cells, as well as macrophages, which are critical mediators of inflammation by the secretion of cytokines, like IL-1β and TNFα, and reactive oxygen species (ROS)(Miller, Appel et al. 1988; Hutchings, Rosen et al. 1990; El-Sheikh, Suarez-Pinzon et al. 1999; Phillips, Parish et al. 2009). This infiltration can result in insulitis and impaired insulin production, and subsequently in overt disease due to the destruction of the β-cells and absolute insulin deficiency. B-cells and the other cell types like NK (natural killer) cells and NKT (natural killer T) cells may be involved in part or a cross-talk between all cell types determines the establishment of the disease (Lehuen, Diana et al. 2010).

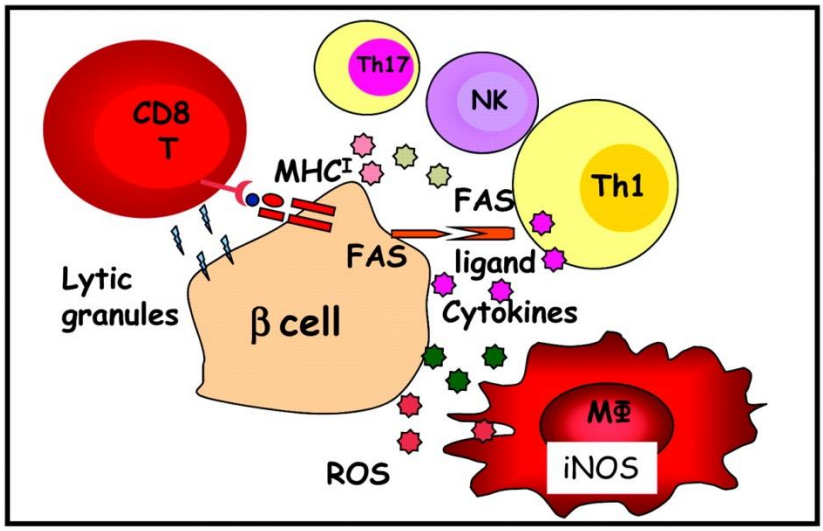

Figure 1. 1 β-cell killing in type 1 diabetes. $CD8^+$ T-cells through recognition of the presented antigens (MHC) may be involved in direct cytotoxicity by production of lytic granules. Cytokines may induce apoptosis through an inflammatory process. T-effector cells may leads to apoptosis by recruiting death domain signaling, such as FAS/FASL signal. ROS derived from activated macrophages may have direct toxic effects on β-cells (Bending, Zaccone et al. 2012).

1.1.b Type 2 diabetes mellitus

Type 2 diabetes becomes clinically apparent when the endocrine pancreas fails to secrete sufficient insulin to overcome the high metabolic demand which has been raised due to insulin resistance followed by hyperglycemia (Lingohr, Buettner et al. 2002; Donath and Halban 2004). This failure of endocrine pancreas may be because of the acquired β-cell secretory dysfunction (Leahy 1990; Kahn 2001; Kahn, Hull et al. 2006) and/or β-cell mass decline (Donath and Halban 2004; Weir and Bonner-Weir 2004).

Insulin resistance refers to the diminished ability of the cells (e.x. adipocytes, myocytes, and hepatocytes) in responding to the action of insulin. In a non-diabetic hyperglycemic patient, β-cells compensate the metabolic demand through morphological changes like hyperplasia and by producing and secretion of more insulin, termed hyperinsulinemia. Short term hyperinsulinemia might be tolerated, but chronic hyperinsulinemia might be detrimental and involved in β-cell failure (White 2003) and insulin insensitivity in adipocytes through strong activation of p42/44 MAPK pathway (Engelman, Berg et al. 2000). Obesity as a risk factor for the development of type 2 diabetes contributes to insulin resistance, since adipocytes secrete adipokines, the proteins may influence the insulin sensitivity (Kahn and Flier 2000).

Nearly 60 years ago, the importance of β-cell loss in pathogenesis of type 2 diabetes was hypothesized (Maclean and Ogilvie 1955). This hypothesis was withdrawn and the insulin resistance was for many years the only acceptable explanation for type 2

diabetes. The role of β-cell decline in pathogenesis of type 2 diabetes has strongly returned to the field of debates few years ago (Donath and Halban 2004). Beside the genetic background, several environmental factors might be involved in β-cell failure and decline, such as glucose, free fatty acids (FFA), and adipose tissue derived factors adipokines. Although glucose is an essential fuel for β-cells' survival and metabolic activity (Hugl, White et al. 1998; Srinivasan, Bernal-Mizrachi et al. 2002) hyperglycemia has severe deleterious effects on β-cells (Sako and Grill 1990; Leahy, Bumbalo et al. 1994) which finally leads to diminished insulin secretion and stores, termed glucotoxicity (Rossetti, Giaccari et al. 1990; Kaiser, Corcos et al. 1991; Eizirik, Korbutt et al. 1992; Leahy, Bonner-Weir et al. 1992; Ling, Kiekens et al. 1996; Marshak, Leibowitz et al. 1999). High glucose concentration participates in β-cells dysfunction by different mechanisms, such as generation of reactive oxygen species (Kaneto, Kawamori et al. 2004; Robertson, Harmon et al. 2004), formation of advanced glycation end products (Tajiri, Moller et al. 1997), activation of mitogen-activated protein kinase (MAPK) family (Briaud, Lingohr et al. 2003; Khoo, Gibson et al. 2004; Maedler, Storling et al. 2004), impairment of insulin gene transcription and proinsulin biosynthesis (Robertson, Zhang et al. 1992; Robertson, Olson et al. 1994), reduction in the binding activity of pancreatic duodenal homebox 1 (PDX-1) (Marshak, Leibowitz et al. 1999), and triggering the endoplasmic reticulum (ER) stress (Wang, Kouri et al. 2005).

Increased plasma level of FFA which have been reported in the state of insulin resistance (Walker, O'Dea et al. 1996), is considered as a toxic element for β-cells, referring to the concept of lipotoxicity (Unger 1995; McGarry and Dobbins 1999; Maedler, Spinas et al. 2001). The mechanism underlying the lipotoxicity in β-cells might include the ER stress (Oyadomari, Araki et al. 2002; Karaskov, Scott et al. 2006). Fig 1.2 depicts some of the factors affecting on the β-cells survival and function (Maedler 2008).

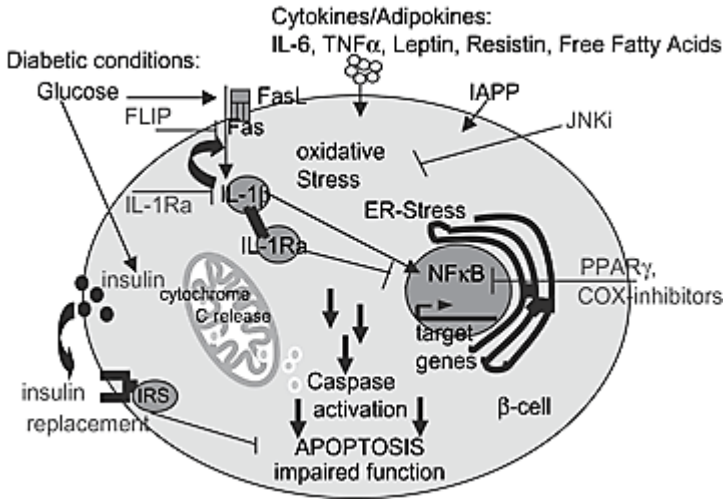

Figure 1. 2 Factors affecting the survival and function of β-cells. In diabetic condition, increased level of glucose, pro-inflammatory cytokines, adipokines and toxic IAPP (Islet Amyloid Polypeptide) oligomers activate downstream pathways leading to apoptosis and impaired function. Interleukin-1β receptor antagonist (IL-1βRa), inhibitors of c-Jun N-terminal kinase (JNKi) and the inhibitors of nuclear factor κB (NFκB) activation (peroxisome proliferator-activated receptor-γ [PPARγ] agonists, cyclooxygenase [COX] inhibitors) might preserve a functional β-cell mass (Maedler 2008).

1.2 Pro-inflammtory cytokines and diabetes mellitus

1.2 a IL-1β

For the first time in 1972, interleukin-1 (IL-1) was introduced as a lymphocyte-activating factor (Gery, Gershon et al. 1972). Later in 1985, IL-1 was classified into two distinct prototypes, IL-1α and IL-1β, which are synthesized in monocytes (March, Mosley et al. 1985). The IL-1 receptor family has been introduced in two type, IL-1RI and IL-1RII, which comprising at least 9 members, IL-1R1 to 1R9 (Sims 2002). IL-1β exerts its inflammatory effects via binding to IL-1RI while IL-1RII appears to act as a decoy molecule, particularly for IL-1β (Mantovani, Locati et al. 2001). The binding of IL-1 to IL-1RI recruits the interleukin-1 receptor accessory protein (IL-1RAcP), which is known as IL-1R3, to the ligand/receptor complex and subsequently induces signal transduction (Wesche, Korherr et al. 1997). Interleukin-1 receptor antagonist (IL-1Ra) is another member of IL-1 family which acts as a natural antagonist for IL-1R via binding to the receptor without inducing signal transduction (Carter, Deibel et al. 1990; Eisenberg, Evans et al. 1990; Dinarello 1991; Dripps, Brandhuber et al. 1991; Granowitz, Clark et al. 1991).

The role of IL-1β in Type 1 and Type 2 diabetes has been demonstrated (Eizirik and Mandrup-Poulsen 2001; Guest, Park et al. 2008; Feve and Bastard 2009). IL-1β alone or in combination with interferon (IFN) γ and/or TNFα induces the pancreatic islet

apoptotic cell death and function impairment (Eizirik and Mandrup-Poulsen 2001). The activation of c-jun N-terminal kinase (JNK) pathway by IL-1β in β-cells (Welsh 1996; Major and Wolf 2001) might be the mechanism by which IL-1β induces β-cell apoptosis, since JNK as a member of mitogen activated protein kinase (MAPK) family transmit the stress and apoptotic signaling in many cells (Miyauchi, Takiyama et al. 2009). The inhibition of JNK pathway prevents the pancreatic β-cell from cytokine-mediated apoptosis (Ammendrup, Maillard et al. 2000; Bonny, Oberson et al. 2000; Bonny, Oberson et al. 2001). It has been also shown that IL-1β induces apoptosis in β-cells through induction of Fas expression, whose signaling activation triggers apoptosis (Loweth, Williams et al. 1998; Giannoukakis, Mi et al. 2000).

A balance between IL1-β and IL-1Ra might be a crucial factor for the improvement of β-cell function in Type 2 diabetic patients. Treatment of these patients with IL-1Ra decreased the plasma level of HbA1c (Larsen, Faulenbach et al. 2007; Larsen, Faulenbach et al. 2009). The expression of IL-1Ra in these patients is reduced, where the production of IL-1β is induced by high glucose concentration in pancreatic β-cells, which indeed leads to impaired insulin secretion, diminishes β-cell proliferation, and induces β-cell apoptosis (Poitout and Robertson 2002; Rhodes 2005; Donath and Mandrup-Poulsen 2008; Dinarello, Donath et al. 2010). A protective effect of exogenous recombinant human (rh) IL-1Ra on high fat diet-induced hyperglycemia (Sauter, Schulthess et al. 2008) and on cultured human islets against IL-1β-mediated apoptosis triggered by glucose has been reported (Maedler, Spinas et al. 2001).

Lipotoxicity along with elevated glucose concentration plays an important role in β-cell destruction by production and secretion of IL-1β in diabetic patients (Federici, Hribal et al. 2001; Maedler, Sergeev et al. 2002).

Another study in pancreatic islet β-cells demonstrated that IL-1β decreases the transcriptional activity of MafA (a pivotal transcription factor for β-cell function) followed by inhibition of insulin transcription, which leads to destruction in insulin biosynthesis and β-cell dysfunction (Oetjen, Blume et al. 2007).

Similar to glucose, low concentrations of IL-1β have a protective effect on human pancreatic β-cells through increase in glucose-stimulated insulin secretion (Maedler, Schumann et al. 2006).

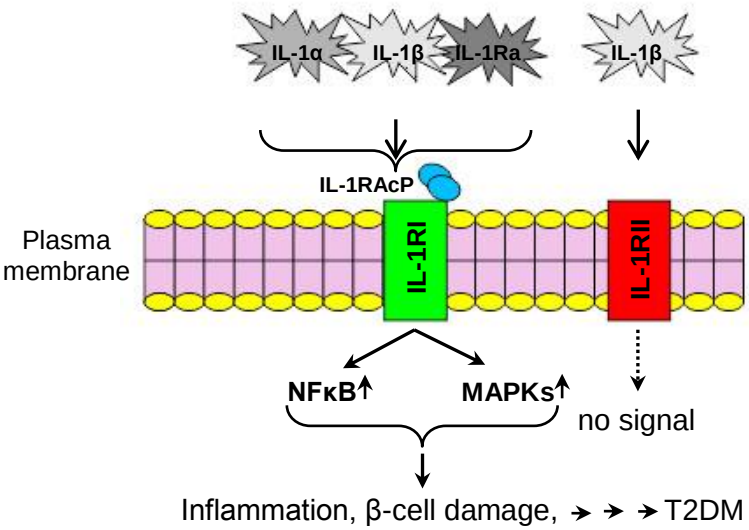

Figure 1. 3 Signaling events triggered by IL-1 family members in β-cells. Binding of IL-1α and IL1-β to IL-1RI triggers the downstream signaling. By activating of nuclear factor (NFκB) and mitogen activated kinases (MAPKs), IL-1β induces apoptosis in β-cells leading to type 2 diabetes mellitus. IL-1Ra is a competitive antagonist of IL-1 on IL-1RI. IL-1RII is an orphan receptor whose binding does not activate any downstream signaling cascade. The figure has been modified from (Banerjee and Saxena 2012).

1.2.b TNFα

Tumor necrosis factor (TNF, known as TNFα) was introduced in 1975 as an endotoxin-induced glycoprotein. The new identified factor showed a haemorrhagic necrosis in transplanted sarcomas in mice (Carswell, Old et al. 1975). 10 years later the human tumor necrosis factor was cloned (Pennica, Hayflick et al. 1985). Activated macrophages and T-lymphocytes are the main source of TNFα production. They produce a 26 kDa pro-TNF molecule which is expressed in plasma membrane. A metalloproteinase, TNFα converting enzyme, (TACE, also known as ADAM-17) cleaves the extracellular domain of pro-TNF and releases a 17 kDa soluble molecule (Black, Rauch et al. 1997). Two distinct receptors have been identified for TNFα, TNFR1 (TNFRSF1A, CD120a) and TNFR2 (TNFRSF1B, CD120b) which are expressed in different cell types (Al-Lamki, Wang et al. 2001). Despite similarity in extracellular cysteine-rich ligand-binding domain the intracellular domains of two receptors show no sign of homology, leading to distinct signal transduction pathways (Ledgerwood, Pober et al. 1999) (Fig. 1.4). TNFR1 has been suggested to be involved in pro-inflammatory and programmed cell death activated by TNFα, while TNFR2 might mediate the tissue repair and angiogenesis. TNFR1 is mainly sequestered in Golgi apparatus in resting cells. Its cell membrane-translocation sensitizes the cell to the action of TNFα (Bennett, Macdonald et al. 1998).

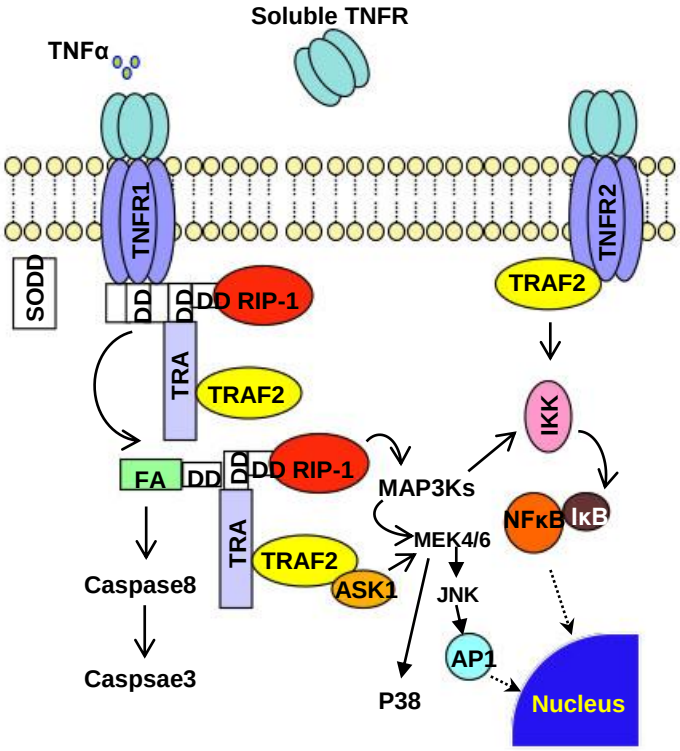

Figure 1. 4 TNFα signaling pathways. TNFR appears as trimer in plasma membrane. TNFR1 contains death domains (DD), the protein motifs which interact with other DDs. SODD (silencer of death domain) might prevent the TNFR1 signaling. Binding of TNFα to TNFR1 results in the release of SODD, leading to recruitment of TNFR-associated DD protein, which initiates the signaling by interacting to RIP-1 (receptor interacting protein-1) and TNFR-associated factor-2 (TRAF2). The signal initiating complex is internalized and interacts with different signal proteins, including MAP3Ks (mitogen activated protein kinase kinase kinase), IKK (inhibitor of κB [IκB] kinase), and FADD (Fas-associated death domain protein). The activation of NFκB (nuclear factor κB) through IKK, JNK and AP-1 (activator protein-1) through MAP3Ks, and caspases through FADD result in cell pro-inflammatory and apoptotic signals. TNFR2 lacks the death domain but can interacts with TRAFs (Hsu, Huang et al. 1996; Takeuchi, Rothe et al. 1996; Ichijo, Nishida et al. 1997; Nishitoh, Saitoh et al. 1998; Jiang, Woronicz et al. 1999; Jones, Ledgerwood et al. 1999; Yang, Lin et al. 2001; Blonska, Shambharkar et al. 2005). The figure has been modified from (Bradley 2008).

The role of TNFα along with some other pro-inflammatory cytokines have been clarified in the pathogenesis of Type 1 and Type 2 diabetes mellitus (Donath, Storling et al. 2003; Hotamisligil 2006; Shoelson, Herrero et al. 2007). Since, most of the type 2 diabetic patients are obese and TNFα is highly expressed in adipose tissues of obese subjects, there might be a link between obesity and the development of insulin resistance, mediated by TNFα (Hotamisligil, Arner et al. 1995). In addition, the obese mice lacking either TNFα or its receptors do not show insulin resistance (Uysal, Wiesbrock et al. 1997). Through an autocrine or/and paracrine mechanism TNFα triggers insulin resistance in

white adipose tissue (WAT) beside inducing IL-6. By activation of sphingomyelinase TNFα increases the production of free fatty acids (FFA) and ceramides, the molecules that contribute to insulin resistance in peripheral tissues (Arner 2003).

The contribution of MAPKs in the insulin resistance induced by TNFα has been reported. In type 2 diabetic subjects the phosphorylation of p38MAPK in adipocytes and muscle accelerates the insulin resistance process and glucose intolerance by down regulation of GLUT-4 (glucose transporter type 4) expression (Carlson, Koterski et al. 2003). TNFα mediates the Ser-Thr phosphorylation of IRS-1 (insulin receptor substrate-1) at Ser-307 residue through activation of the MAPK family members ERK and JNK (Rui, Aguirre et al. 2001; Aguirre, Werner et al. 2002). The MEK1/2-p42/44 MAPK pathway may mediate insulin resistance induced by TNFα in 3T3.L1 adipocytes (Engelman, Berg et al. 2000).

The role of activated IKK (inhibitor of κB kinase) by TNFα in Ser-phosphorylation of IRS-1 has been also reported (Yuan, Konstantopoulos et al. 2001). The inhibition of IKK by salicylate reversed the obesity and diet-induced insulin resistance (Yuan, Konstantopoulos et al. 2001; Gao, Zuberi et al. 2003).

In addition to the involvement of TNFα in insulin resistance some reports clarified the contribution of TNFα in necrotic and apoptotic pancreatic β-cell death. In Type 1 diabetes, the infiltrating cells might play a role in β-cell destruction by producing of cytokines TNFα, IFNγ, and IL-1 (Campbell, Iscaro et al. 1988; Pukel, Baquerizo et al. 1988). A combination of these three cytokines has been reported to induce apoptosis in rat islets and βTC1 cells by forming hypodiploid nuclei and oligonucleosomal DNA fragmentation (Rabinovitch, Suarez-Pinzon et al. 1994; Iwahashi, Hanafusa et al. 1996). DNA strand breaks and apoptosis have been also observed in human pancreatic islet cells after prolonged exposure to a mixture of these cytokines (Delaney, Pavlovic et al. 1997). Through TNFR1, TNFα executes downstream signaling of TRADD, FADD, caspase8 (FLICE: FADD-like interleukin-1 beta-converting enzyme), and ceramide whose activity result in apoptotic β-cell death (Ishizuka, Yagui et al. 1999). The involvement of TNFα in combination with IFNγ and IL-1β in the induction of apoptosis has been shown. Transfection of human pancreatic islets and rat insulin producing cell line (RINm5F) with the anti-apoptotic gen bcl-2 counteracted the apoptosis and β-cell destruction induced by these cytokines (Rabinovitch, Suarez-Pinzon et al. 1999; Saldeen 2000).

1.2.c IFNγ

The interferon (IFN) was discovered as an agent who interferes with virus replication (Isaacs and Lindenmann 1957). Different members of this family were

classified according to their secreting cell type, but today they are classified into two types, type I and type II, according to receptor specificity and sequence homology. The type I consist of multiple subtypes such as IFNα, IFNβ, IFNω, and IFNτ. All members of type I IFN bind to a heterodimeric receptor IFNAR which is comprised of IFNAR1 and IFNAR2 chains (Liu 2005). IFNγ is the only member of type II IFN which has no structural relation to type I IFNs and binds to a different receptor, IFNGR (Gray and Goeddel 1982). Beside the immunomodulatory activities, the role of IFNγ in pancreatic β-cell survival and death has been reported along with other pro-inflammatory cytokines.

The IFNγ receptor (IFNGR) is comprised of two ligand-binding chains, IFNGR1 and IFNGR2. Since both IFNGR chains lack the intrinsic kinase/phosphatase activity they need to recruit signaling machinery for signal transduction. The signaling pathway recruited by this receptor is a well-known pathway called JAK-STAT which is used by over 50 cytokines, growth factors and hormones (Subramaniam, Torres et al. 2001). IFNγ is a noncovalent homodimer in its biologically active form and binds IFNGR1 in 2:2 binding stoichiometry (Ealick, Cook et al. 1991; Fountoulakis, Zulauf et al. 1992; Greenlund, Schreiber et al. 1993; Walter, Windsor et al. 1995; Bach, Tanner et al. 1996). The IFNγ: IFNGR1 complex interact with IFNGR2 (Kotenko, Izotova et al. 1995; Pestka, Kotenko et al. 1997). Ligand binding induces the autophosphorylation of JAK2 and consequently the transphosphorylation of JAK1 by JAK2 (Briscoe, Rogers et al. 1996). The activated JAK1 phosphorylate IFNGR1 at Y440 which leads to the recruitment of STAT1 to the receptor (Greenlund, Farrar et al. 1994; Igarashi, Garotta et al. 1994; Greenlund, Morales et al. 1995; Heim, Kerr et al. 1995). Stat1 is phosphorylated at Y701 probably by JAK2 (Briscoe, Rogers et al. 1996). The activated STAT1 dissociates from receptor as homodimers and enters the nucleus for further transcriptional activity. STAT1 binds DNA at IFNγ-activation site (GAS) elements which control the transcription of IFNγ-responsive genes (Decker, Kovarik et al. 1997; Paludan 1998) (Fig. 1.5).

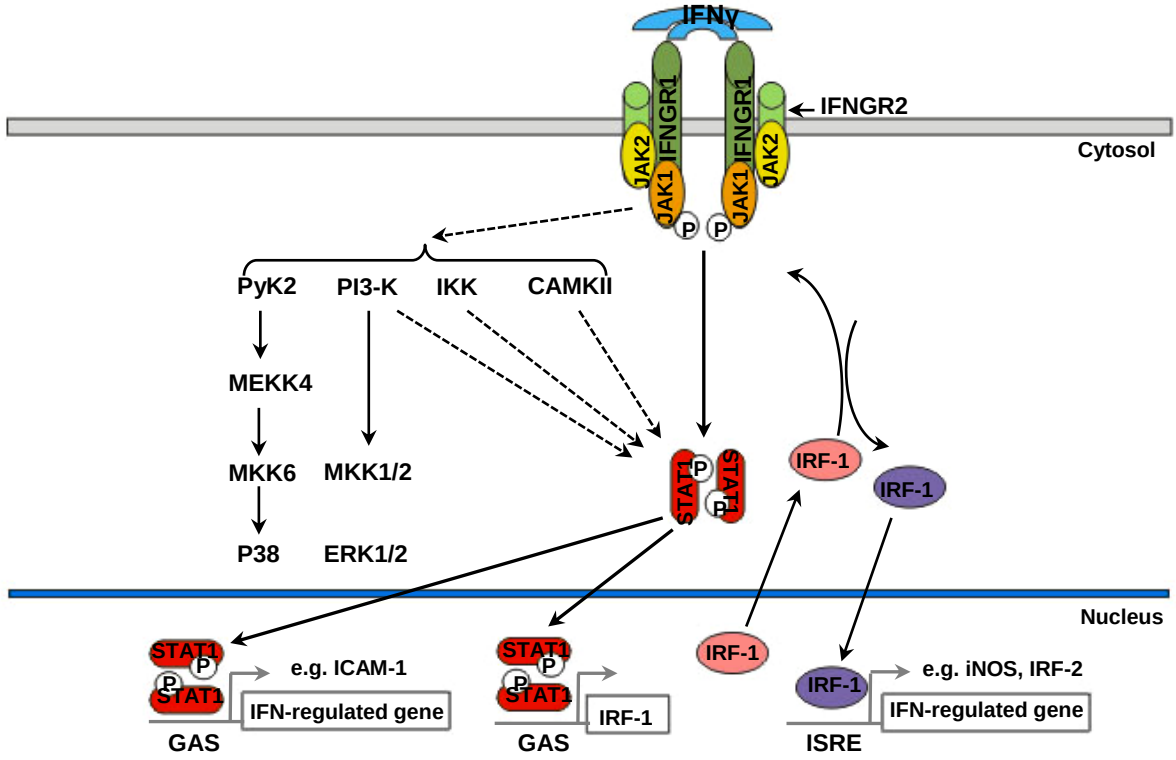

Figure 1. 5 IFNγ signaling. A conformational change occurs after ligand binding in IFNGR which allows the autophosphorylation and activation of JAK2. The activated JAK2 transphosphorylates and activates JAK1 which is responsible for the running of downstream signaling such as Stat1 activation. The phosphorylated and homodimerized Stat1 translocates into the nucleus and binds to IFNγ-activation site (GAS) to initiates/suppress the expression of IFN-regulated genes. IRF-1 as a transcription factor which is regulated by IFNγ drives the next wave of transcription such as iNOS and IRF-2. After activation by IFNGR, IRF-1 translocates into the nucleus and binds to IFN-stimulated response element (ISRE) and regulates the corresponding genes' transcription. The alternative pathways triggered by IFNγ include the activation of protein-tyrosine kinase (PyK) 2, Phosphatidylinositide 3-kinase (PI3-K), Inhibitor of κB kinase (IKK), and Ca^{2+}/calmodulin-dependent protein kinase (CAMK) II. The figure has been modified from (Schroder, Hertzog et al. 2004).

IFN-regulatory factor (IRF) family members are involved in IFNs signal cascades, of which IRF-1, IRF-2, and IRF-9 participate in IFNγ signaling (Sims, Cha et al. 1993; Harada, Takahashi et al. 1994). Stat1 and NF-κB dramatically increase IRF-1 transcription (Pine 1997). The activation of MEK1/ERK1/2 MAP kinase pahway (Hu, Roy et al. 2001; Gough, Sabapathy et al. 2007), and MKK6/p38 MAP kinase pathway by IFNγ have been reported (Sun and Ding 2006). Although the activation of JNK by IFNγ in macrophages has been observed (Valledor, Sanchez-Tillo et al. 2008) most of the reports show no activation of JNK by IFNγ (Platanias 2005; Gough, Sabapathy et al. 2007). The involvement of PI-3K and CamKII in IFNγ triggered signal transduction have also been reported (Nguyen, Ramana et al. 2001; Nair, DaFonseca et al. 2002).

The participation of IFNγ in β-cell dysfunction and death has been documented. Overxpression of IFNγ in a transgenic mice model leads to inflammatory destruction of islet β-cells (Sarvetnick, Liggitt et al. 1988). IL-1β, TNFα, and IFNγ alone did not induce lysis of islet cells but their combination resulted in β-cell dysfunction and death (Eizirik, Sandler et al. 1994; Suk, Kim et al. 2001; Liu, Cardozo et al. 2002; Thomas, Darwiche et al. 2002). Different pathways have been suggested for cooperative deleterious effect of these cytokines in β-cells. The combination of TNFα and IFNγ leads to β-cell death via up-regulation of Fas expression (Dudek, Thomas et al. 2006; McKenzie, Dudek et al. 2006). The expression of SERCA (sarcoplasmic/endoplasmic reticulum Ca^{2+} ATPase) 2 in β-cells is inhibited after treatment with IFNγ + IL-1β which leads to ER (endoplasmic reticulum) depletion of Ca^{2+} store, ER stress and finally β-cell death (Cardozo, Ortis et al. 2005). The combination of IL-1β, TNFα, and IFNγ induces the expression and phosphorylation of Stat1 in pancreatic islet cells. The expression of Stat1 has also been observed in pancreatic islet of diabetic NOD mice which is co-localized with apoptotic β-cells. In addition transfection with phosphorylation defective Stat1 protects β-cells from death induced by IFNγ + TNFα (Suk, Kim et al. 2001; Kutlu, Cardozo et al. 2003). On the other hand the absence of Stat1 prevents β-cells from death induced by IFNγ + IL-1β (Gysemans, Ladriere et al. 2005). Stat1 deficient NOD mice were also protected from insulitis and diabetes (Kim, Kim et al. 2007).

Despite the Jak-Stat signaling pathway, IRF transcriptional activity is also triggered by IFNγ which exhibits a protective effect in β-cells in contrast to Stat signaling (Gysemans, Pavlovic et al. 2001). Regarding these reports IFNγ might play a dual role in β-cell destruction and survival.

1.3 DLK

Dual leucine zipper-bearing kinase (DLK) is a member of mixed lineage kinase (MLK) family and known as a mitogen-activated protein kinase kinase kinase (MAPKKK) which is expressed in brain and the peripheral nervous system (Holzman, Merritt et al. 1994; Hirai, Kawaguchi et al. 2005). Its expression has been also reported in primary murine islets and the β-cell line HIT (Oetjen, Lechleiter et al. 2006).

The MLK family is composed of five distinct members, designated MLK1, MLK2, MLK3, DLK (also called MUK and ZPK), and LZK (Leucine zipper-binding kinase), which share two common structural features: A hybrid catalytic domain similar to serine/threonine and tyrosine kinases, and two leucine/isoleucine motifs separated by a short spacer and a proline-rich COOH-terminal domain (Dorow, Devereux et al. 1993; Hirai, Izawa et al. 1996; Sakuma, Ikeda et al. 1997; Rasmussen, Rusak et al. 1998).

According to their structure MLK1, MLK2, and MLK3 form one closely related subfamily whereas DLK and LZK form another distinct subfamily (Holzman, Merritt et al. 1994; Sakuma, Ikeda et al. 1997). The first subfamily shows a 70% sequence identity in highly conserved kinase catalytic and leucine zipper (LZ) domains and possess an SH3 (SRC homology 3) domain in their NH_2-terminal region. DLK and LZK show a sequence identity more than 90% in their kinase catalytic and dual LZ domains which are only 36% identical to those of MLK2 and MLK3. DLK and LZK lack the SH3 domain and have a structurally different region than of those of MLK2 and MLK3 close to COOH-terminal (Teramoto, Coso et al. 1996; Nagata, Puls et al. 1998) (Fig. 1.6). Regarding to distinct structural features, different subcellular localization and substrates have been proposed for these two subfamilies of MLKs, where both DLK and MLK3 utilize MKK7 as a substrate, but unlike MLK3, the involvement of DLK in phosphorylation and activation of MKK4 is not well clarified, yet (Merritt, Mata et al. 1999).

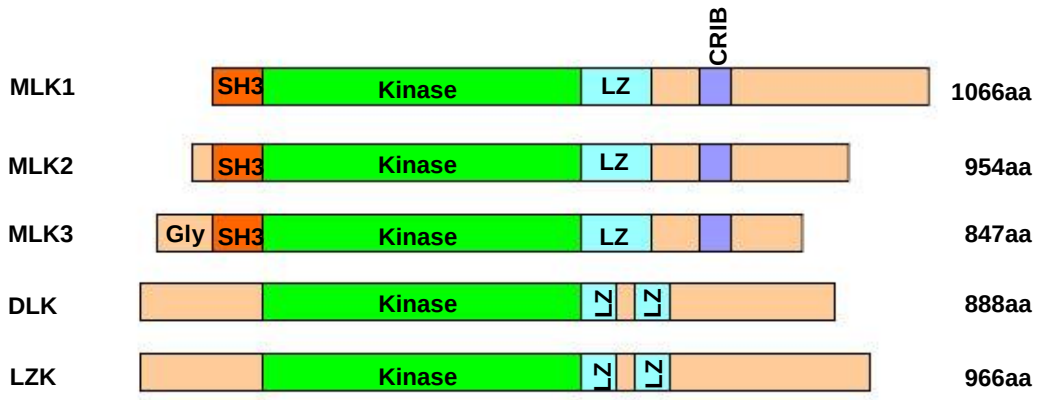

Figure 1. 6 Schematic structure of the MLK family members. The first subfamily including MLK1, MLK2, and MLK3 possess an SH3 domain in their N-terminal region, a catalytic kinase domain, one LZ domain, and a CRIB (Cdc2/Rac interactive binding) domain within the C- terminal of the peptide. The second subfamily including DLK and LZK lack the SH3 domain in their N-terminal and the CRIB domain within their C-terminal, and possess a dual LZ which is separated by a spacer sequence. The figure has been modified from (Gallo and Johnson 2002).

The regulatory role of DLK in cell proliferation, differentiation and survival has been studied. DLK expression is not ubiquitously distributed during mouse embryogenesis and is mostly restricted to central nervous system, epithelia of the skin, intestine, pancreas, and kidney, manifesting the areas undergoing terminal cell differentiation (Nadeau, Grondin et al. 1997). $DLK^{-/-}$ mice die perinataly probably due to the role of DLK in axonal

growth and neuronal migration of the developing cerebral cortex (Brancho, Ventura et al. 2005; Hirai, Cui de et al. 2006; Bisson, Tremblay et al. 2008). DLK also has been reported to be involved in tissue regeneration (Matsui, Sarkar et al. 1996; Douziech, Grondin et al. 1998). Overexpression of DLK was shown to inhibit cell growth in fibroblasts and primary human keratinocytes (Bergeron, Douziech et al. 1997; Germain, Fradette et al. 2000). In addition, DLK induces apoptosis in a neuronal cell line, a fibroblast cell line and HIT cells which is dependent on its enzymatic activity (Xu, Maroney et al. 2001; Parkash, Chaudhry et al. 2005; Rhodes 2005; Plaumann, Blume et al. 2008). On the other hand a recently reported study demonstrated the participation of DLK in the proliferation of WI-38 human fibroblast cell line by modulating the expression of cell cycle regulating proteins (Daviau, Couture et al. 2011). Oligomerization and homodimerization have been suggested as a mechanism for DLK activation. The calphostin activated transglutaminase triggered the oligomerization and activation of overexpressed DLK (Robitaille, Daviau et al. 2008). On the other hand, dephosphorylation of DLK by calcineurin, a calcium/calmodulin dependent phosphatase, might be a regulating mechanism of DLK activity, where inhibition of calcineurin by immunosuppressive drugs cyclosporin A (CsA) and tacrolimus enhanced DLK-induced phosphorylation of the substrate casein and DLK itself (Oetjen, Lechleiter et al. 2006; Plaumann, Blume et al. 2008).

CRE- (cAMP response element) binding protein (CREB) is a transcription factor that has been implicated in the survival and maintenance of β-cells (Oetjen, Diedrich et al. 1994; Oetjen, Grapentin et al. 2003). The transcriptional activity of CREB is induced by different signals such as cAMP, calcium, extracellular signal-regulated kinase (ERK1/2) and p38 MAPK (Habener, Miller et al. 1995; Mayr and Montminy 2001). Mice with β-cell specific inactivated CREB develops diabetes due to reduced proliferation and increased β-cell apoptosis (Jhala, Canettieri et al. 2003). The inhibitory effect of DLK on membrane depolarization-induced transcriptional activity of CREB has been reported in a β-cell line (Oetjen, Lechleiter et al. 2006) which might suggest a role for DLK in the pathogenesis of diabetes.

All members of MLK family including DLK have been proposed to act as a MAPK kinase kinase in the pathway leading to activation of JNK/SAPK (c-Jun N-terminal kinase/stress activated protein kinase) (Fan, Merritt et al. 1996; Hirai, Izawa et al. 1996; Rana, Gallo et al. 1996; Tibbles, Ing et al. 1996; Hirai, Katoh et al. 1997; Sakuma, Ikeda et al. 1997; Nagata, Puls et al. 1998). It is assumed that JNK triggers the dissociation of DLK from scaffold protein JIP (JNK interacting protein) which leads to DLK homodimerization, autophosphorylation and activation (Leung and Lassam 2001; Nihalani, Meyer et al. 2001; Nihalani, Wong et al. 2003). The JNK/SAPK is well known as

stress inducing protein and is activated as one of the three major MAPKs, which is induced by upstream MKK4 and MKK7. Different cellular stress stimuli trigger JNK pathway, including ultraviolet light, heat shock, osmotic shock, protein synthesis inhibitors and different kinds of cytokines such as TNFα and Fas (Hibi, Lin et al. 1993; Galcheva-Gargova, Derijard et al. 1994; Kyriakis, Banerjee et al. 1994; Toyoshima, Moriguchi et al. 1997).

1.4 The aim and objectives of the study

The hypothesis of this study is that DLK participates in the pathogenesis of type 2 diabetes. The regulation of DLK by prediabetic signals (pro-inflammatory cytokines TNFα, IL-1β, and IFNγ) was investigated employing a phosphorylation specific antibody against DLK.

The subcellular localization of DLK driven by prediabetic signals was studied through the interaction of DLKwt and mutant (NLS1, NLS2, PP) proteins with nuclear receptors, which are crucial for the nuclear translocation of proteins carrying NLS (nuclear localization signal), as well as in vitro experimentation (immunocytochemistry) in HIT cells.

The role of DLK in diet-induced diabetes was investigated in C57BL/6J wild-type and DLK-heterozygote mice under different diet.

Since the global DLK knock-out mice die perinataly, a targeting vector was designed and generated to produce β-cell specific DLK knock-out mice, using BAC (bacterial artificial chromosome)-recombineering and gap-repair strategy.

2. Materials and methods

2.1. Equipment

2.1.a. Apparatus

Autoclave	Bioclav, Schütt Labortechnik, *Goettingen, Germany*
	MediTech service GmbH, *Norderstedt*, *Germany*
AutoLumat luminometer	LB 953, E&G Berthold, *Bad Wildbach*, *Germany*
Balances	Sartorius AG, *Goettingen, Germany*
Cell culture hood	Herasafe - Heraeus, *Langenselbold, Germany*
Centrifuge rotors	JA-20/JA-17/JA-14, Ti 70, Beckmann GmbH, *Germany*
Centrifuges	Beckman GS-6–Beckman Coulter GmbH, *Krefeld, Germany*
	Beckman J2-21– Beckman Coulter GmbH, *Krefeld, Germany*
	Beckman L8-70M Ultracentrifuge, Beckman Coulter GmbH, *Krefeld, Germany*
	Eppendorf 5415D, Eppendorf GmbH, *Hamburg, Germany*
	Eppendorf 5424R, Eppendorf GmbH, *Hamburg, Germany*
	Rotina 35R, Andreas Hettich GmbH & Co. KG, *Tuttlingen, Germany*
Cell Disrupter	Branson Sonifyer® B15 – Heinemann Ultraschall- u. Labortechnik, *Schwäbisch Gmünd*, *Germany*
	Bandelin UW 2200, *Berlin, Germany*
DNA Sequencer	ABI PRISM 3100 Genetic Analyzer – Applied Biosystems, *Darmstadt, Germany*
	ABI PRISM 7900 HT Sequence Detection System – Applied Biosystems, *Darmstadt, Germany*
Electrophoresis power supplier	Biometra® Standard Power Pack P25 – Whatman Biometra, *Goettingen, Gemany*
	Bio-Rad Power PAC Basic, *Munich, Germany*
	Bio-Rad Power PAC HC, *Munich, Germany*
Electrophoresis chamber (DNA)	Carl Roth, *Karlsruhe, Germany*
	Mini-sub cell GT, Bio-Rad, and Wide mini-sub cell GT, Bio-Rad, *Munich, Germany*
Electrophoresis (proteins)	Electrophoresis chamber SE 600 – Hoefer Scientific Instruments, *San Francisco, USA*
	Mini-protein Tetra system, Bio-Rad, *Munich, Germany*
	Mighty Small SE 250/SE 260, Hoefer, *San Francisco, USA*

	Mighty Small SE245 Dual Gel Caster, glasses, spacer, combs – Hoefer Scientific Intsruments, *San Francisco, USA*
Electroporater	Micropulser, Bio-Rad, *Munich, Germany*
Electroporation Cuvettes	25×1mm gap, PeQLab Biotechnology, *Erlangen, Germany*
Fluorometer Fusion	Canberra-Packard, *Dreieich, Germany*
Gel Dryer	Gel Dryer Model 583, Bio-Rad, *Munich, Germany*
Immunoblot detection device	Chemi Genius - Bio Imaging System, SYNGENE, *Cambridge, UK* Versa doc Imaging System, Bio-Rad, *Munich, Germany*
Incubators	Bacteria Incubator - Heraeus , *Langenselbold, Germany* CO_2-Incubator BB15 - Heraeus, *Langenselbold, Germany*
Micro pipettes	Eppendorf, *Hamburg, Germany*
Microscope	Zeiss Axiovert 25 microscope – Carl Zeiss AG, *Oberkochen*, *Germany* Zeiss Axiovert 200m-Apotom – Carl Zeiss Ag, *Oberkochen, Germany*
PCR cycler	PCR cycler T-Gradient – Biometra, *Goettingen, Germany* PCR system 9700 - Applied Biosystems, *Darmstadt, Germany* PTC-200 Peltier Thermal Cycler – Biozym, Hess, *Oldendorf, Germany*
pH meter	pH 523, Schütt Labortechnik, *Goettingen, Germany* 766 calimatic Knick, *Berlin, Germany*
Rocking platform	Biometra, *Goettingen, Germany* Duomax 1030 – Heidolph Instruments GmbH & Co.KG, *Schwabach, Germany*
Rolling platform	TRM-V – IDL, *Nidderau, Germany*
Rotator	Rotator GFL 3025 – Gesellschaft für Labortechnik mbH, *Burgwedel, Germany*
Spectrophotometer	Eppendorf Biometer, Eppendorf, *Hamburg, Germany* Nanodrop spectrophotometer-ND1000, *Wilimington, USA*
Semi-dry transfer device	Bender & Hobein, *Zurich*, *Switzerland*
Shaking platform	Certomat®R shaking platform – Sartorius, *Goettingen, Germany* GFL - RM5 U-30 - CAT, GFL, *Burgwedel, Germany*
Thermomixer	Eppendorf Comfort, Eppendorf, *Hamburg, Germany*
Transilluminator	Biometra Ti1 - Biometra, *Goettingen, Germany*
Tube Sealer	Beckmann Tube Sealer – Beckmann GmbH, *Munich, Germany*

Vacuum Pump	KnF Laboport, *Neuberger*, *Germany*
Vacuum Chamber	Bachofer, *Reutlingen, Germany*
Waterbath	W. Krannich GmbH, *Goettingen, Germany*
	HAAKE DC3, *Goettingen, Germany*
	Circulating water bath, Julabo, *Seelbach, Germany*

2.1.b. Consumables

Plates & Cell culture dishes	10 cm agar plate, Sarstedt, *Nuembrecht, Germany*
	6 cm cell culture dishes, Sarstedt, *Nuembrecht, Germany*
	15 cm cell culture dishes, Sarstedt, *Nuembrecht , Germany*
	BD Falcon™ 15 cm cell culture dishes, Schuett24 GmbH, *Goettingen, Germany*
	6-well plate, Sarstedt, *Nuembrecht, Germany*
	6-well plate, Greiner Bio-One, *Frickenhausen, Germany*
	96-well Millipore plates, Millipore GmbH, *Schwalbach, Germany*
Coverslips	Marienfield-Superior, *Lauda-Koenigshofen, Germany*
Disposable cell scraper	Sarstedt, *Nuembrecht, Germany*
Dialysis tubes	*GIBCO BRL, Karlsruhe, Germany*
Glass pipettes	WU, *Mainz,Germany*
Gloves	Paul Hartmann AG, *Heidenheim, Germany*
	Meditrade Nitril-gloves, *Kiefersfelden, Germany*
Microscope slides 75x25mm	Karl Hecht*, Sondheim/Rhoen, Germany*
Nitrocellulose membrane (0.45µm)	Hybond™, ECL™, Amersham Biosciences, *Freiburg, Germany*
Parafilm	Parafilm® M – Brand GmbH & Co KG, *Wertheim, Germany*
Pasteur pipettes	Carl Roth, *Karlsruhe, Germany*
Pipette tips	Sarstedt, *Nuembrecht, Germany*
Quick Seal Tubes	Beckmann GmbH, *Munich, Germany*
Spectrophotometer cuvettes (plastic)	Sarstedt, *Nuembrecht, Germany*
Spectrophotometer cuvettes (quartz)	Sarstedt, *Nuembrecht, Germany*

Syringes	BD Discardit II, Beckton Dickinson, *Heidelberg, Germany*
Syringe filters	Sartorius, *Goettingen, Germany*
Syringe needles	Sterican, B/BRAUN, *Melsungen, Germany*
Tubes	15 ml red-cap tubes, Sarstedt, *Nuembrecht, Germany*
	50 ml red-cap tubes, Sarstedt, *Nuembrecht, Germany*
	0.5, 1, and 2 ml eppendorf tubes, Eppendorf, *Hamburg, Germany*
Ultracentrifuge tubes	Beckman Coulter GmbH, *Krefeld, Germany*
Whatman paper P81	Whatman, *Maidstone, UK*

2.2. Chemicals

2.2.a. Substances

37% formaldehyde – Carl Roth, *Karlsruhe, Germany*

99.5% glycerol – Carl Roth, *Karlsruhe, Germany*

Acetic acid – Sigma-Aldrich, *Seelze, Germany*

Acrylamide/Bis – Bio-Rad, *Munich, Germany*

Agar – Carl Roth, *Kralsruhe, Germany*

Agarose (electrophoresis grade) – Carl Roth, *Karlsruhe, Germany*

Ammoniumpersulphate (APS) – Carl Roth, *Karlsruhe, Germany*

Ampicillin – Sigma-Aldrich, *Seelze, Germany*

Amylose Resin – BioLabs, *Ipswich, USA*

Arabinose – Sigma-Aldrich, *Seelze, Germany*

ATP – Applichem, *Darmstadt, Germany*

β-Mercaptoethanol – Carl Roth, *Karlsruhe, Germany*

Boric acid – Carl Roth, *Karlsruhe, Germany*

Bovine serum albumin (BSA) – Applichem, *Darmstadt, Germany*

Bradford reagent – Bio-Rad, *Munich, Germany*

Bromophenol blue – Sigma-Aldrich, *Seelze, Germany*

BSA fatty acid free – PAA, *Coelbe, Germany*

Cesium chloride (CsCl) – Applichem, *Darmstadt, Germany*

Chloramphenicol – Carl Roth, *Karlsruhe, Germany*

Chloroform – Applichem, *Darmstadt, Germany*

Collagenase P – Roche, *Mannheim, Germany*

Coomassie brilliant blue – Sigma-Aldrich, *Seelze, Germany*

Cyclosprin A – Sigma-Aldrich, *Seelze, Germany*

DEAE-Dextran – Amersham*, Glattbrugg, Switzerland*

Dimethyl sulfoxide (DMSO) – Sigma-Aldrich*, Seelze, Germany*

Deoxynucleoside triphosphates (dNTPs) – Fermentas*, St. Leon-Rot, Germany*

Di-potassium hydrogen phosphate (K_2HPO_4) – Carl Roth*, Karlsruhe, Germany*

Di-sodium hydrogen phosphate (Na_2HPO_4) – Carl Roth*, Karlsruhe, Germany*

Dithiothreitol (DTT) – Applichem*, Darmstadt, Germany*

D-Luciferin – P.J.K., *Kleinbittersdorf, Germany*

D-Saccharose – Carl Roth*, Karlsruhe, Germany*

EDTA – Carl Roth*, Karlsruhe, Germany*

EGTA – Carl Roth*, Karlsruhe, Germany*

Ethanol – Carl Roth*, Karlsruhe, Germany*

Ethidium bromide – Applichem*, Darmstadt, Germany*

Fetal calf serum – Biochrom*, Berlin, Germany*

Forskolin – Sigma-Aldrich, *Seelze, Germany*

Glucose – Carl Roth*, Karlsruhe, Germany*

Glutathione agarose – Sigma-Aldrich, *Seelze, Germany*

Glycine – Carl Roth*, Karlsruhe, Germany*

Glycylglycine – Applichem, *Darmstadt, Germany*

HEPES – Carl Roth*, Karlsruhe, Germany*

His bind Resin – Novagen, *Darmstadt, Germany*

Horse serum – GIBCO BRL, *Karlsruhe, Germany*

Hydrochloric acid (HCl) – Carl Roth*, Karlsruhe, Germany*

Interferon gamma (IFNγ) – Biomol, *Hamburg, Germany*

Interleukin 1-betta (IL-1β) – Biomol, *Hamburg, Germany*

Isoamylalcohol – Applichem, *Darmstadt, Germany*

Isopropanol – Sigma-Aldrich*, Seelze, Germany*

Isopropyl-β-D-thiogalactoside (IPTG) – Applichem, *Darmstadt, Germany*

Kanamycin Sulfate – Carl Roth*, Karlsruhe, Germany*

L-Glutathione – Sigma-Aldrich, *Seelze, Germany*

Lysozyme – Sigma-Aldrich*, Seelze, Germany*

Magnesium chloride ($MgCl_2$) –Carl Roth, *Karlsruhe, Germany*

Magnesium sulphate ($MgSO_4$) – Carl Roth*, Karlsruhe, Germany*

Metafectene – Biontex, *Munich, Germany*

Methanol – Carl Roth*, Karlsruhe, Germany*

Milk Powder – Carl Roth*, Karlsruhe, Germany*

Nonidet-P40 – Applichem, *Darmstadt, Germany*

Oligofectamine – Invitrogen, *Karlsruhe, Germany*

Polyethylene glycol 6000 (PEG 6000) – Applichem, *Darmstadt, Germany*

Penicillin / Streptomycin – GIBCO BRL, *Karlsruhe, Germany*

Pepton from casein – Carl Roth*, Karlsruhe, Germany*

Phenol (Tris saturated) – Biomol, *Hamburg, Germany*

Phenylmethylsulfonylfluorid (PMSF) – Applichem, *Darmstadt, Germany*

Phosphatase Inhibitor (PhosStop) – Roche, *Mannheim, Germany*

Ponceau S solution – Applichem, *Darmstadt, Germany*

Potassium chloride (KCl) – Carl Roth*, Karlsruhe, Germany*

Potassium di-hydrogen phosphate (KH_2PO_4) – Carl Roth*, Karlsruhe, Germany*

Protease Inhibitor – Roche, *Mannheim, Germany*

Ribonuclease A – Applichem, *Darmstadt, Germany*

Sephadex G50 – Amersham Biosciences, *Freiburg, Germany*

Silver nitrate ($AgNO_3$) – Sigma-Aldrich, *Seelze, Germany*

Sodium acetate trihydrate (NaAc) – Carl Roth*, Karlsruhe, Germany*

Sodium carbonate (Na_2CO_3) – Carl Roth*, Karlsruhe, Germany*

Sodium chloride (NaCl) – Carl Roth*, Karlsruhe, Germany*

Sodium di-hydrogen phosphate (NaH_2PO_4) – Carl Roth*, Karlsruhe, Germany*

Sodium dodecylsulphate (SDS) – Carl Roth*, Karlsruhe, Germany*

Sodium hydroxide (NaOH) – Carl Roth*, Karlsruhe, Germany*

Sodium thiosulphate ($Na_2S_2O_3$) – Applichem, *Darmstadt, Germany*

Tetramethyethylenediamine (TEMED) – Merck*, Darmstadt, Germany*

Tris – Carl Roth*, Karlsruhe, Germany*

Triton X100 – Carl Roth*, Karlsruhe, Germany*

Trypsin / EDTA – Biochrom*, Berlin, Germany*

Tumor Necrosis Factor-α (TNFα) – Biomol, *Hamburg, Germany*

Tween 20 – Carl Roth*, Karlsruhe, Germany*

Yeast extract – Carl Roth*, Karlsruhe, Germany*

2.2.b. Stock solutions and buffers

2.2.b.I. Stocks

All stock solutions were prepared in double-destilled water, exceptions are mentioned.

Ampicillin*	10% (w/v)	1 g / 10 ml
APS**	10 % (w/v)	1 g / 10 ml
Chlorophorm / isoamylalcohol	1/24 (v/v)	1 ml / 24 ml
Chloramphenicol**	3.4% (w/v)	34 mg /ml 99% EtOH
Cyclosporin A***	830 µM	1 mg in 0.1 ml 99% EtOH, and 20 µl Tween 80
Dithiothreitol (DTT)**	1 M	1.542 g / 10 ml
EDTA pH 8.0	0.5 M	46.53 g / 250 ml
EGTA pH 8.0	180 mM	3.423 g / 50 ml
Ethidium Bromide	10 mg/ml	100 mg / 10 ml
Forskolin**	10 mM	1 mg / 243.6 µl DMSO
HEPES pH 7.5	1 M	59.58 g / 250 ml
Glucose	0.5 M	9 g / 100 ml
Glycine	1 M	7.507 g / 100 ml
Glycylglycine pH 7.8	0.5 M	3.303 g / 50 ml
Kanamycine**	5% (w/v)	0.5 g / 10 ml
KCl	2 M	2.98 g / 20 ml
K_2HPO_4	0.5 M	4.35 g / 50 ml
KH_2PO_4	100 mM	3.402 g / 250 ml
$MgCl_2$	1 M	5.08 g / 25 ml
$MgSO_4$	1 M	12.324 g / 50 ml
NaCl	0.5 M	0.292 g / 10 ml
Na_2HPO_4	75 mM	1.33 g / 100 ml
NaH_2PO_4	75 mM	1.33 g / 100 ml
NaOH	1 N	4 g / 100 ml
Penicillin/Streptomycin**	10,000 U/ml	10,000 µg/ml (ready to use solution)
PhosStop**	10x	according to the manufacturer's instruction
PMSF**	200 mM	348 mg / 10 ml 99%-ethanol
Protease inhibitor**	7x	according to the manufacturer's instruction
RNase**	0.01% (w/v)	0.1 mg/ml
Sodium dodecyl sulphate (SDS)	10% (w/v)	25g / 250 ml
Tris/HCl	1 M	60.57 g / 500 ml

Stock solutions were stored at room temperature.

***** Stored at -80°C

** Stored at -20°C

*** Stored at +4°C

Different pHs were adjusted for Tris-base and HEPES using HCl.

2.2.b.II. Buffers

Total volume for all buffers was adjusted by double-destilled water.

PBS pH 7.4	*1x*	*1 L*
NaCl	140 mM	8.00 g
KCl	2.5 mM	0.20 g
Na_2HPO_4	8.1 mM	1.44 g
KH_2PO_4	1.5 mM	0.24 g

pH was adjusted by HCl.

TBS	*1x*	*1L*
Tris/HCl (pH 8.0)	10 mM	10ml of 1M
NaCl	150 mM	30ml of 5M

TAE-buffer	*1x*	*1 l*
Tris	40 mM	4.84 g
EDTA	1 mM	2 ml of 0.5 M stock
Acetic acid	20 mM	1.14 ml

TBE-buffer	*1x*	*1L*
Tris	89 mM	10.8 g
Boric Acid	89 mM	5.5 g
EDTA (pH 8.0)	2 mM	4 ml of 0.5 M stock

The pH of the buffer will be approximately 8.3 and should not be adjusted.

2.2.c. Kits

Big Dye® Terminator v1.1 Cycle Sequencing Kit – Applied Biosystems, *Darmstadt, Germany*

Bradford Dye Reagent for Protein Assays – Biorad, *Munich, Germany*

Easy Pure® DNA purification kit – Biozym*, Hess.-Oldendorf, Germany*

Geno Pure plasmid maxi kit – Roche*, Mannheim, Germany*

High-pure plasmid isolation kit – Roche, *Mannheim, Germany*

Hi-pure plasmid maxiprep kit – Invitrogen*, Karlsruhe, Germany*

Hi-pure plasmid miniprep kit – Invitrogen, *Karlsruhe, Germany*

Lumi-light^{plus} Western Blotting Analysis System – Roche, *Mannheim, Germany*

NucleoBond® BAC 100 – Macherey-Nagel, *Dueren, Germany*

Vectashield® Mounting Medium with DAPI – Vector Laboratories*, Burlingame, USA*

2.3. Biological material

2.3.a. Bacterial strains

Chemically competent *Escherichia coli* strain DH5α and electro-competent *Escherichia coli* strain Top10 were used for plasmid amplification and expression of recombinant GST-fused proteins. Electro-competent *Escherichia coli* strain BL-21 was used for expression of recombinant His-tagged proteins. Electro-competent *Escherichia coli* strain K12Δ was used for expression of recombinant MBP-fused proteins.

Electro-competent *Escherichia coli* strains SW102, SW105, and SW106 were used for BAC recombineering experiments.

2.3.b. Eukaryotic cell line

Hamster insulinoma tumor cells, clone HIT-T15, are an insulin-producing beta-cell line established by simian virus 40 transformation of pancreatic islet cells from Syrian hamster (Santerre, Cook et al. 1981). HIT-T15 cells were used for all of the cell culture experiments.

2.3.c. Prokaryotic culture and media

LB medium		*1L*
NaCl	1% (w/v)	10 g
Pepton	1% (w/v)	10 g
Yeast extract	0.5% (w/v)	5 g
Antibiotic*		

***** Final concentration for Ampicillin is 50 µg/ml and for Kanamycin is 15 µg/ml

The LB medium was autoclaved and stored at room temperature. Antibiotic was added freshly before use.

Bacteria were cultured in LB-medium supplemented with appropriate antibiotic, using a shaking platform agitating at a range of 150-220 rpm, at 32°C or 37°C depending on the experiment.

LB-antibiotic agar plates were prepared by using LB medium containing 1.5% (w/v) agar. The solution was autoclaved for 20 min at 121°C. After cooling to 50°C the appropriate antibiotic was added and the LB-antibiotic agar was poured into 10 cm dishes. The agar plates were solidified at room temperature and stored at 4°C.

2.3.d. Eukaryotic culture and media

RPMI complete		*500 ml*
RPMI Medium		420 ml
fetal calf serum	10% (v/v)	50 ml
horse serum	5% (v/v)	25 ml
Penicillin / streptomycin	1% (v/v)	5 ml

The RPMI complete medium was stored at 4°C.

One patch of the frozen HIT-T15 cells was thawed at 37°C and cultured in RPMI complete medium. The cells were incubated at 37°C in a CO_2-incubator with 95% (v/v) humidity and 5% (v/v) CO_2. The cells were split once a week at full confluence into 15-cm dishes. After washing once with phosphate-buffered saline (PBS), the cells were trypsinized for 3-5 min with 3 mL trypsin / EDTA at 37°C. The reaction was stopped by addition of 7 mL RPMI complete medium. Cells were detached from the dish by tapping at the bottom and the wall, collected in the medium, centrifuged for 2 min at 800 rpm, and washed once with RPMI complete medium. The cells were seeded at a density of ~0.5 x 10^6 cells / cm^2. After three days the medium was renewed. The cells from a confluent dish

were collected in RMPI complete medium, transferred to the RMPI medium containing 50% FCS (fetal calf serum) and 10% DMSO (dimethyl sulfoxide), and frozen at -80°C for the later culture.

2.3.e. Plasmids and Oligonucleotides

2.3.e.I. Expression constructs

An overview of all expression vectors used in the present work is listed in Table 1.
All basic expression vectors for mammalian or bacterial expression are listed in Table 2.

Flag-DLK wild-type construct encodes the full length of mouse DLK. The coding sequence was cloned into pcDNA3.1 expression vector using *HindIII* and *XhoI* restriction enzymes. This construct encodes 888 amino acids of full length DLK (Holzman, Merritt et al. 1994). The Flag epitope (DYKDDDDK) was inserted between amino acids one and two of all constructs carrying the Flag epitope, using a modified primer (Holzman, Merritt et al. 1994).

Flag-DLK K185A construct encodes the full length of mouse DLK with a point mutation where Lysine-185 residue was replaced by Alanine. The coding sequence was cloned into pcDNA3.1 expression vector at the restriction sites of *HindIII* and *XhoI (Holzman, Merritt et al. 1994).*

Flag-DLK S298A construct encodes the full length of mouse DLK with a point mutation where Serine-298 residue was replaced by Alanine. The coding sequence was cloned into pcDNA3.1 expression vector at the restriction sites of *HindIII* and *XhoI* (this study).

Flag-DLK S302A construct encodes the full length of mouse DLK with a point mutation where Serine-302 residue was replaced by Alanine. The coding sequence was cloned into pcDNA3.1 expression vector at the restriction sites of *HindIII* and *XhoI* (this study).

Flag-DLK S298A/S302A construct encodes the full length of mouse DLK with two point mutations where Serine-298 and Serine-302 residues were replaced by Alanine. The coding sequence was cloned into pcDNA3.1 expression vector at the restriction sites of *HindIII* and *XhoI* (this study).

Flag-DLK PP construct encodes the full length of mouse DLK with two point mutations where Leucine-437 and -463 residues were replaced by Proline residues. The coding sequence was cloned into the expression vector pcDNA3.1 at the restriction sites of *HindIII* and *Xho*I (Nihalani, Merritt et al. 2000).

Flag-DLK NLS1 construct encodes the full length of mouse DLK with two point mutations where Lysine-186 and Arginine-188 residues were replaced by Alanine

residues. The coding sequence was cloned into the expression vector pcDNA3.1 at the restriction sites of *HindIII* and *Xho*I (Walbach M, medical thesis, Goettingen 2000).

Flag-DLK NLS2 construct encodes the full length of mouse DLK with three point mutations where Lysine-196, Arginine-199 and Lysine-200 were replaced by Alanine residues. The coding sequence was cloned into the expression vector pcDNA3.1 at the restriction sites *HindIII* and *Xho*I (Walbach M, medical thesis, Goettingen 2000).

hIP-DLK NLS2 construct encodes the full length of mouse DLK NLS2 mutant under the control of human insulin promoter (hIP). The coding sequence was cloned into expression vector pcDNA5/FRT at the restriction sites of *HindIII* and *XhoI*. The promoter was cloned upstream to the coding sequence at the restriction site of *HindIII*. hIP-DLK NLS2 fragment can be cut out of the vector by *XhoI* and *NheI* restriction digest (this study).

PGK-DLK NLS2 construct encodes the full length of mouse DLK NLS2 mutant under the control of ubiquitously expressed promoter PGK. The coding sequence was cloned into expression vector pcDNA5/FRT at the restriction sites of *HindIII* and *XhoI*. The promoter was cloned upstream to the coding sequence at the restriction sites of *HindIII* and *NheI* (this study).

pGEX-DLK NLS wild-type, 1, and 2 mutants constructs encode a truncated form of mouse DLK comprising amino acids 140-285, which is N-terminally fused to GST (glutathione s-transferase). The coding sequences were cloned into the bacterial expression vector pGEX-6p1 at the restriction sites of *SmaI* and *XhoI* (this study).

pET-DLK NLS wild-type, 1, and 2 mutants constructs encode a truncated form of mouse DLK comprising amino acids 140-285, which is N-terminally fused to 6xHis cassette (Histidine). The coding sequences were cloned into the bacterial expression vector pET 28a^{+} at the restriction sites of *BamHI* and *SalI* (this study).

pMAL-DLK NLS wild-type, 1, and 2 mutants constructs encode a truncated form of mouse DLK comprising amino acids 140-285, N-terminally fused to MBP (Maltose Binding Protein) (MBP-DLK). The coding sequences were cloned into the bacterial expression vector pMAL-c2x at the restriction sites of *BamHI* and *SalI* (this study).

pMAL-DLK KNLSLZ (consists of the catalytic region, NLS, and the leucine zipper region of DLK) wild-type, 1, and 2 mutants constructs encode a truncated form of mouse DLK comprising amino acids 140-517, which is N-terminally fused to MBP. The coding sequences were cloned into the bacterial expression vector pMAL-c2x at the restriction sites of *BamHI* and *SalI* (this study).

The expression construct GAL4-CBP encodes the full-length CBP fused C-terminally to the DNA-binding domain of GAL4 (Oetjen, Thoms et al. 2005).

G5E1B-Luc (Kruger, Schwaninger et al. 1997) expressing luciferase contains five repeats of the enhancer element, identified in yeast as binding site for the yeast transcription factor GAL4 (Webster, Jin et al. 1988), upstream to the viral E1B TATA box (Lillie and Green 1989; Liu and Green 1990).

CRE-Luc expresses luciferase reporter gene under the control of four copies of CRE of the rat somatostatin gene promoter (Oetjen, Diedrich et al. 1994).

pGFPtpz-cmv® vector (Caberra-Packard, Dreieich, Germany) was used as internal control for luciferase reporter-gene assays. This expression vector encodes the green fluorescent protein (GFP) variant topaz under the control of cytomegalovirus promoter.

Table 1. Expression Constructs

This table summarizes all constructs used in the present study. The providers of the constructs are mentioned in the footprint of the table.

Name	Source	Vector	Note
DLK wild-type[1]	Mus musculus	pcDNA3.1	Flag-tag full length
DLK K185A[1]	Mus musculus	pcDNA3.1	Flag-tag Lys185 →Ala
DLK S298A[2]	Mus musculus	pcDNA3.1	Flag-tag Ser298 →Ala
DLK S302A[2]	Mus musculus	pcDNA3.1	Flag-tag Ser302 →Ala
DLK S298A/S302A[2]	Mus musculus	pcDNA3.1	Flag-tag Ser298 →Ala Ser302 →Ala
DLK PP[4]	Mus musculus	pcDNA3.1	Flag-tag Leu437→Ala Leu463→Ala
DLK NLS1[3]	Mus musculus	pcDNA3.1	Flag-tag Lys186→Ala Arg188→Ala

DLK NLS2[3]	Mus musculus	pcDNA3.1	Flag-tag Lys196→Ala Arg199→Ala Lys200→Ala
hIP-DLK NLS2*	Mus musculus	pcDNA5/FRT	Flag-tag full length
PGK-DLK NLS2*	Mus musculus	pcDNA5/FRT	Flag-tag full length
GST-DLK NLS wt*	Mus musculus	pGEX-6p1	aa 140-285
GST-DLK NLS1*	Mus musculus	pGEX-6p1	aa 140-285
GST-DLK NLS2*	Mus musculus	pGEX-6p1	aa 140-285
His-DLK NLS wt*	Mus musculus	pET-28a$^+$	aa 140-285
His-DLK NLS1*	Mus musculus	pET-28a$^+$	aa 140-285
His-DLK NLS2*	Mus musculus	pET-28a$^+$	aa 140-285
MBP-DLK NLS wt*	Mus musculus	pMAL-c2x	aa 140-285
MBP-DLK NLS1*	Mus musculus	pMAL-c2x	aa 140-285
MBP-DLK NLS2*	Mus musculus	pMAL-c2x	aa 140-285
MBP-DLK KNLSLZwt*	Mus musculus	pMAL-c2x	aa 140-517
MBP-DLK KNLSLZ1*	Mus musculus	pMAL-c2x	aa 140-517
MBP-DLK KNLSLZ2*	Mus musculus	pMAL-c2x	aa 140-517
GAL4-CBP[2]			Full length
CRE-Luc[2]			

∗ Generated in this work

1. Generated by (Holzman, Merritt et al. 1994)
2. Generated by Elke Oetjen
3. Generated by Manuel Walbach
4. Generated by (Nihalani, Merritt et al. 2000)

pcDNA3.1, pcDNA5/FRT,and pBluescript$^+$ plasmids were used for DNA cloning and amplification. pGEX-6p1, pET28a$^+$, and pMAL-c2x plasmids were used for protein purification. PL253, PL451, and PL452 plasmids were used for BAC recombineering and gap-repair experiments. pBluescript$^+$ was used as control for cell transient transfection.

Table 2. Mammalian and bacterial expression vectors

Vectore	Provider
pcDNA3.1	Invitrogen, *Karlsruhe, Germany*
pcDNA5/FRT	Invitrogen, *Karlsruhe, Germany*
pGEX-6p1	GE Healthcare, *Freiburg, Germany*
pET28a^{+}	Novagen, *Darmstadt, Germany*
pMAL-c2x	NEB Biolab, *Ipswich, USA*
PL253*	Frederick National lab, *Frederick, USA*
PL451*	Frederick National lab, *Frederick, USA*
PL452*	Frederick National lab, *Frederick, USA*
pBluescript^{+}	Invitrogen, *Karlsruhe, Germany*

* Kindly given by Prof. Ahmed Mansouri, *Goettingen, Germany*

2.3.e.II. Oligonucleotides

Table 3 presents a list and the sequence of oligonucleotides used for all PCR cloning. Oligonucleotides used for sequencing of the constructs and the whole genome are listed in Table 4. (F) refers to forward primer and (R) refers to reverse primer.

Table 3. Oligonucleotides for cloning

Name	Direction	Sequence 5'-3'	Restriction site for
pGEX-DLK NLS	F	AAGC*CCCGGG*GTTCCACAGAACACAAG	*SmaI*
	R	AAT*CTCGAG*CTTCACCACATCGTC	*XhoI*
pET-DLK NLS	F	AAG*GGATCC*TCCACAGAACACAAG	*BamHI*
	R	AAGT*GTCGAC*CTTCACCACATCGTC	*SalI*
pMAL-DLK NLS	F	AAG*GGATCC*TCCACAGAACACAAG	*BamHI*
	R	AAGT*GTCGAC*CTTCACCACATCGTC	*SalI*
pMAL-KNLSLZ	F	AAG*GGATCC*TCCACAGAACACAAG	*BamHI*
	R	AAGT*GTCGAC*GTTTCCATGTAGGAGG	*SalI*
PGK-DLK NLS2	F	CGA*GCTAGC*ATAGGGCGAAT	*NheI*
	R	CCCATGTCGACATC*AAGCTT*	*HindIII*
5' Southernblot probe	F	CGTA*GAATTC*TACGGGCAGCAAAT	*EcoRI*
	R	TATT*GGATCC*GCTGTCATAGCCTA	*BamHI*
3' Southernblot probe	F	CCGC*GAATTC*ATGTAATTTTAACAATAC	*EcoRI*
	R	CGAA*GGATCC*GGTATTAAGCCAAACA	*BamHI*

Gap-repair A	F	ATAA*GCGGCCGC*AGCTAATGGCACCTT	*NotI*
Gap-repair B	R	GTC*AAGCTT*CTAATGGTTGCTGGG	*HindIII*
Gap-repair C	F	ATAA*GCGGCCGC*CTGTAGGTAGGAGG	*NotI*
Gap-repair D	R	GTC*GAATTCAGATCT*CAAGTGCTCTACAA AA	*EcoRI,BglII*
Gap-repair E	F	ATA*GGATCC*GCTAGGATGTGTAAAACC	*BamHI*
Gap-repair F	R	GTC*GTCGAC*AGATCCCTGTAAGAACA	*SalI*
Gap-repair G	F	ATAA*GCGGCCGC*AAGGTGGATTAGAA	*NotI*
Gap-repair H	R	GTC*GAATTC*AGCACTTGAGAGGCAGAG	*EcoRI*
Gap-repair I	F	ATA*GGATCC*GGAATTAAAGGCATGTGCC	*BamHI*
Gap-repair J	R	GTC*GTCGAC*GAACCTGTTACTGACATT	*SalI*
Gap-repair Y	F	GTC*AAGCTT*TCCTGTTTCTCTGCCCAAAC	*HindIII*
Gap-repair Z	R	TCT*ACTAGT*TGTAGAGCAGCTGGTGCATT	*SpeI*

Table 4. Oligonucloetides for sequencing

Name	Direction	Sequence 5'-3'
pET-DLK NLS	F	GCTTTGTTAGCAGCCGGATCT
	R	CAGCCATATGGCTAGCATGA
pMAL-DLK NLS	F	TTCGAGCTCGAACAACAACA
	R	TGCTGCAAGGCGATTAAGTT
hIP-DLK NLS	F	CCATCAAGCAGGTCTGTTCCAA
	R	GCACCTCATATAGCTGTCCT
PGK-DLK NLS	F	CGTCTCACTAGTCTCGTGCAGAT
	R	GGCACAACATCTCGAAGTACAC
BAC recombineering		
DNA retrieved from BAC	F1	GGCGATTAAGTTGGGTAA
	R1	GGTCAAGAGTGCTTACTGTT
	F2	GGAGGTCTCAAAACACCTAT
	R2	GTGTTCGAATTCGCCAATGA
First loxP inserted into the targeting vector	F1	GTGGCTTCCTTGAAGGTCTTT
	R1	GGGAGGATTGGGAAGACAAT
	F2	CGGTAGAATTTCGACGACCT
	R2	TGAGGGGAGTCCTATGTGTCA
Second loxP inserted into the	F	GGCTTGGAAGACACTATGT

targeting vector	R	CATCGCATTGTCTGAGTAGG
Final recombinant vector	F1	GGCGATTAAGTTGGGTAA
	R1	GATATAGCTCAGTTGGTAGG
	F2	GGAGATTGAACTCAAGGCCT
	R2	AACTCTCCCAATTTTTCAGG
	F3	CATGTGGCTGGAAGAATAGT
	R3	CAGGCAATAGAAATTCGTCC
	F4	GTCACATCCCACTTCCTCAA
	R4	TCGTGTAGTGGCATATACAC
	F5	CACTGTACAAACAATGCTGG
	R5	AGTTACTGCAAGAGCTCACG
	F6	GTACAGAGAGTTGACACTCA
	R6	TGGTCTTGTGAAAAGCTAGG
	F7	GTGGCTTCCTTGAAGGTCTTT
	R7	TGAGGGGAGTCCTATGTGTCA
	F8	GAAGCACCCCAACATCATCA
	R8	TCTCTCCAGTCAGTAGTTCC
	F9	CCCTTCCAAATGATGTTCCT
	R9	AAGTTATTAGGTGGATCCGG
	F10	GGCTTGGAAGACACTATGT
	R10	CGAAATGGACCCTGTTCTCT
	F11	GCTCAGGTATGTGCCTATTT
	R11	ACATCTTTCGGAGTAGAAGG
	F12	TTCAGCTTGGGATGCTTG
	R12	CACTTTTCAGTGTCTGGTGG
	F13	ACTTCAGAGGTGGTCCCTGA
	R13	CCTCCTCCCAAGTGCAAAAT
	F14	CTGTCTATCCCTGAACACTG
	R14	GTGTTCGAATTCGCCAATGA
Genomic DNA sequencing of DLK	F1	CTTGTGGTTCAGAGTGACAGGCGAA
	R1	ATCCTCAGAAACGGTCTGCAGCTCT
	F2	ACTGCCCTAAAAGTCGAGCAGGTGA
	R2	ACTCGTGGGGTTGCTTTGGGATACA
	F3	ACTGTATCCCAAAGCAACCCCACGA
	R3	GCACCGGAGAATTTCCTGCAAACGA

	F4	TGTGCTCTCTTCTCCCCTCTTGGA
	R4	CCGCACATGCTCCGTGTATTTCTCAG
	F5	TGAGAAATACACGGAGCATGTGCGG
	R5	GAGGCTATGGGAACGATGGAACCAGA
	F6	TGTCCATCTCTTCACCCCCTTAGCA
	R6	GCAATCCTGAGATATGGAGGGCTCA
	F7	TGAGCCCTCCATATCTCAGGATTGC
	R7	CACAAACTCATCAGCCCCGTTTGCT
	F8	CGGGGCTGATGAGTTTGTGTTTTGG
	R8	TACTCTCCTGGGAACGAACCACAGT
	F9	ATGCAGATCCCAAACAAACCCCGTC
	R9	TTCGTCCCAGTTTGTAGCTGTGTGC
	F10	GCACACAGCTACAAACTGGGACGAA
	R10	GCCTCTCCAGTGGGATGTGATCTTGT
	F11	ACCCCATTGGATAGTTCTGCCCTCA
	R11	CTTCCTCTTGGCTGTGCAGTTGTCA
	F12	GGGGTTAATGACAACTGCACAGCCA
	R12	TCATCATGCCCAGGTTTCATGCCCA
	F13	TGGGCATGAAACCTGGGCATGATGA
	R13	AAGCCAACCCCCAAAAGTGTTGTCC
	F14	TGCCTTGCACATGTTGAACGCTTTG
	R14	CCAGCTTTCGCATAGAAGCCTCACT
	F15	CCCTTCCTTTGGGGGCTTTGTGTCTA
	R15	CCCAAGTTCCTGGGTTCAGTTTCCT
	F16	TTGTGCTAGGAAACTGAACCCAGGA
	R16	TGATGTTGGGGTGCTTCAGCTTTCG
	F17	CGAAAGCTGAAGCACCCCAACATCA
	R17	AGGTGACCTACACGCACATCAGCTT
	F18	AGGATGCAAGCTGATGTGCGTGTAG
	R18	ACACCCCAGATGATGGCTGAGGAAT
	F19	TTGGGGTGGTGCTATGGGAACTACT
	R19	GGCCACACCTTTCCCCACAACTTTT
	F20	CCCCAAGGAAGGAAGACTGAACCTGT
	R20	TCTCCTGGGGTGTAGAGAGCACATCA
	F21	AGCAAACCACGAAATCGCCCATCAT

	R21	TCTCCGCATCACCAGTTCCTCTTCT
	F22	ACCGCCTAGAAGAGGAACTGGTGAT
	R22	GGATCCCTCCTGCAATGTCCTCATGT
	F23	CAGAAACTGTCGCCCCACAGCAAAA
	R23	GCTGATAGCAGGTCTGGGGATGATGA
	F24	TGTCATCATCATCCCCAGACCTGCT
	R24	AGTGGGGTTGGGGTATAGTTAGCACT
	F25	GGCTGCTGTGACTCGAAGTCAGGTAA
	R25	TACTGCCAACTTCTGGTGTGCCACT
	F26	TTCCCCAAGTGGCACACCAGAAGTT
	R26	GGAGCCTTGGGGACCCTTCTTTTACA
	F27	TGGTTCCGAGCATATAGTGCCTGATG
	R27	AGCTGCCAGTGTCCCCAGAACTTAT
	F28	AGTGAACGACGCCCCTGACCAATTA
	R28	ACCCCTACCAGGCACCAAGATAACA
	F29	GCATGTGATGGCTCAGGCTGAAGAA
	R29	AATTTGCCCTCAATCACCTCCCCCT
	F30	AGGGGGAGGTGATTGAGGGCAAAT
	R30	TCTGAACAGTCAGCGACTCCAGGTT
	F31	AACCTGGAGTCGCTGACTGTTCAGA
	R31	AGGCTCCCAACACAAAGTTCCTTCA
	F32	AGGCTTCAAGGAGTTGATCCTGTCG
	R32	AAGCTTGTGGTGTGGACCTGAGACA

2.3.f. Antibodies

All primary and secondary antibodies used in the present study are listed in Table 5.

Table 5. Primary and secondary antibodies.

Name	Source	Application	Dilution	Provider
DLK	rabbit	Immunoblot	1:2,500	Holzman *et al*,. 1994
phospho-DLK	rabbit	Immunoblot	1:1,000	This group
Cleaved caspase3	rabbit	Immunoblot	1:1,000	Cell signalling, *Frankfurt M, Germany*
anti-His	mouse	Immunoblot	1:5,000	Sigma-Aldrich, *Seelze, Germany*
GAPDH	mouse	Immunoblot	1:5,000	Santa Cruz, *Heidelberg, Germany*
FLAG M2	mouse	Immunocytochemistry	1:200	Sigma-Aldrich, *Seelze, Germany*
Rabbit IgG-HRP*	donkey	Immunoblot	1:10,000	GE Healthcare, *Freiburg, Germany*
Mouse IgG-HRP*	sheep	Immunoblot	1:10,000	GE Healthcare, *Freiburg, Germany*
Rabbit IgG-Alexa®*	goat	Immunocytochemistry	1:50	Eugene, *Oregon, USA*
anti-MBP	mouse	Immunoblot	1:5,000	NEB Biolabs, *Ipswich, USA*
Tubulin	rabbit	Immunoblot	1:1,000	Cell signalling, *Frankfurt M, Germany*

* Secondary antibodies

anti-DLK antibody detects the C-terminus of DLK protein. phospho-DLK antibody detects the phospho-serine 302 residue in DLK protein. Cleaved caspase3 antibody detects two bands of 17 and 19 kd of caspase3 peptide cleaved adjacent to Asp 175. anti-His antibody detects the 6xHis box tagged to the proteins of interest. GAPDH antibody detects the full-length of human glutaraldehyde-3-phosphate dehydrogenase between amino acids 1-335.

FLAG M2 antibody detects the Flag epitope (DYKDDDDK) which is inserted between amino acids 1 and 2 in the proteins of interest.

Rabbit IgG-HRP and mouse IgG-HRP are labelled with horseradish peroxidase and were used as secondary antibodies in immunoblot experiments.

Rabbit IgG-Alexa® is labelled with AlexaFlour®488 and was used as secondary antibody in immunocytochemistry experiments.

2.3.g. Enzymes and Markers

2.3.g.I. Restriction endonucleases

Endonuclease restriction enzymes used in the present study are listed in Table 6. The enzymes were used in combination with appropriate buffer according to the instruction of manufacturer.

Table 6. Restriction endonucleases

Name	Recognition site	Provider
BamHI	5'-G|GATCC-3'	Fermentas, *St. Leon-Rot, Germany*
DrdI	5'-GACNNNN|NNGTC-3'	Fermentas, *St. Leon-Rot, Germany*
EcoRI	5'-G|AATTC-3'	Fermentas, *St. Leon-Rot, Germany*
HincII	5'-GTY|RAC-3'	NEB Biolabs, *Ipswich, USA*
HindIII	5'-A|AGCTT-3'	Fermentas, *St. Leon-Rot, Germany*
NheI	5'-G|CTAGC-3'	NEB Biolabs, *Ipswich, USA*
NotI	5'-GC|GGCCGC-3'	NEB Biolabs, *Ipswich, USA*
SalI	5'-G|TCGAC-3'	Fermentas, *St. Leon-Rot, Germany*
SmaI	5'-CCC|GGG-3'	Fermentas, *St. Leon-Rot, Germany*
SpeI	5'-A|CTAGT-3'	NEB Biolabs, *Ipswich, USA*
XcmI	5'-CCANNNNN|NNNNTGG	NEB Biolabs, *Ipswich, USA*
XhoI	5'-C|TCGAG-3'	Fermentas, *St. Leon-Rot, Germany*

2.3.g.II. Modifying enzymes

Modifying enzymes listed in Table 7 were used in combination with appropriate buffers according to the instruction of manufacturer.

Table 7. Modifying enzymes

Name	Concentration	Provider
CiAP (calf intestine alkaline phosphatase)	1U/µl	Fermentas, *St. Leon-Rot, Germany*
Lysozyme	4,700U/mg	Sigma-Aldrich, *Seelze, Germany*
Pfu DNA polymerase	2.5U/µl	Fermentas, *St. Leon-Rot, Germany*
Prime-STAR DNA polymerase	2.5U/µl	Takara, *St-Germain-en-Laye, France*
RNase A		Applichem, *Darmstadt, Germany*
T4 DNA ligase	1U/µl	Fermentas, *St. Leon-Rot, Germany*

2.3.g.III. Molecular weight markers

Markers and ladders were provided by Fermentas Life Sciences (St. Leon-Rot, Germany). PFG (pulsed-field gel) markers are from NEB Biolabs.

DNA-ladders:

GeneRuler™ 100bp DNA Ladder

GeneRuler™ 100bp Plus DNA Ladder

GeneRuler™ 1kb DNA Ladder

GeneRuler™ 1kb plus DNA Ladder

Mid Range PFG Marker

Low Range PFG Marker

Protein ladder:

PageRuler™ Prestained Protein Ladder

2.4. DNA oriented experiments

2.4.a. Polymerase Chain Reaction (PCR)

PCR was used to amplify DNA *in vitro*. In this reaction a designed fragment of DNA is separated to single strand DNA by heating up to 95°C. Annealing of specific primer pairs occurs at the melting temperature of the primers. A thermostable DNA polymerase starts the elongation of the fragment from the annealed primers at 72°C. The time of elongation is dependent on the type of polymerase and the length of the fragment. The cycle is repeated up to 35 times. An overview of the reaction is shown below.

a typical PCR reagents:

DNA Template	Genomic DNA (1-10 ng), plasmid DNA (10-50 ng)
dNTPs	200 µM
Forward primer	30 pmol
Reverse primer	30 pmol
Reaction buffer+Mg^{++}	1x
Polymerase	1 U
ddH_2O	ad 50 µl

a typical PCR setup:

	Initial denaturation	3 min at 95°C
35 cycles	Cyclic denaturation	20sec at 95°C
	Primer annealing	20sec at 5°C lower than the melting temperature of the primers
	Elongation	Time depended on polymerase and the length of the fragment, at 72°C
	Final elongation	7 min at 72°C

dNTP mix was purchased from Fermentas as 10 mM stock solution. Primers were synthesized by MWG operon.

The PCR product was subjected to horizontal electrophoresis on an agarose gel and purified.

2.4.b. Agarose gel electrophoresis

Agarose gel electrophoresis was used for separation of DNA fragments. The size of the fragment determines the percentage of the agarose gel. The relation of these two factors is as follows:

Percentage of agarose	DNA fragment
0.3 %	5–60 kb
0.6 %	1-20 kb
0.7 %	0.8-10 kb
0.9 %	0.5-7 kb
1.2 %	0.4-6 kb
1.5 %	0.2-4 kb
2.0 %	0.1-3 kb

(Sambrook, Fritsch et al. 1989)

Because of the difficult handling of the lower percentage gels (0.3.0.6%), preparation of a bed gel in higher percentage (1%) is recommended. Agarose was melted in TAE-buffer and cooled down to 60°C. Ethidiumbromide (5% v/v) was added and mixed well. The gel was casted and solidified at room temperature. The gel was placed in a running chamber and covered by TAE-buffer. DNA samples were supplemented with 6x loading dye (Fermentas) and loaded into the slots. 5µl of the appropriate DNA ladder were loaded beside the samples. A constant electric field (90V) was applied. When the loading

dye was almost at the end of the gel the electric field was stopped and the separation of the fragments was observed at UV-light of 366 nm. Other analysis and photography was performed by Bio Imaging System device and software.

TAE-buffer	*1x*	*1 l*
Tris	40 mM	4.84 g
EDTA	1 mM	2 ml of 0.5 M stock
Acetic acid	20 mM	1.14 ml

2.4.c. DNA purification from agarose gel

Easy Pure® purification kit was used for DNA extraction from agarose gel. The desired band of DNA was cut out of the gel and melted at 55°C in 3 volume of the salt solution. Silica beads (5µl + 1 µl/µg of DNA) were added and mixed well by pipeting. After 5 min of incubation at room temperature the beads were pelleted and washed 2 times with washing solution. The pellet was dried and DNA was eluted with 20 µl of ddH_2O by 1 min centrifugation using a table centrifuge at high speed. All steps were done according to the instruction of the manufacturer.

2.4.d. Restriction digest

Sufficient amounts of plasmid DNA or PCR product were mixed with ddH_2O to a final volume of 50 µl. The corresponding buffer was added in a 1x dilution. The mixture was supplemented with 1U of restriction enzyme per µg of DNA. Digestion was carried out for 1-2 hrs for plasmid DNA and overnight for PCR products at 37°C. An exception in temperature should be considered for some enzymes. The samples were gel electrophoresed and gel purified as described above.

2.4.e. DNA ligation

T4 DNA ligase facilitates the joining of DNA strands by catalyzing the formation of a phosphodiester bond. One important point to have a successful ligation is to take a proper ratio of vector and insert. 0.03 pmol of vector and 0.1-0.3 pmol of insert is a good ratio. The molecular weight of DNA can be measured by molecular weight calculators or conventionally by this equation:

$$MW\ (g/mol) = DNA\ bp \times 608$$

According to this formula, a DNA fragment of 1kb has a molecular weight of 60.8 g/mol. 1µg of this fragment is equivalent to 1.65 pmol. The final calculation was corrected to the concentration of DNA which had been measured by Nanodrop.

The optimum temperature for T4 ligase activity is 25°C, with high temperature increase the chance of the homologous pairing of the sticky ends and the hydrogen bonding decreases. The optimum temperature for the ligation of 4 nucleotides overhang is between 12-16°C.

Regarding these rules, the fragments were mixed with ddH_2O in a total volume of 20 µl. 1x final concentration of ligation buffer was added and the mixture was supplemented with 1U of T4 DNA ligase and mixed well. The reaction was completed overnight at 16°C. The ligated DNA was amplified by transforming competent bacteria.

2.4.f. Bacterial transformation

2.4.f.I. Chemically competent E.coli

The bacteria were thawed on ice. 100 ng of plasmid DNA or 3 µl of ligated DNA were added to 30 µl of bacteria and immediately kept on ice for 30 min. Heat shock was applied by 90 sec incubation at 42°C, followed by 2 min incubation on ice. 500 µl of LB medium without antibiotic were added to the bacteria and incubated for 1hr at 37°C, 350 rpm in a thermomixer. 100 µl of the transformed bacteria was plated on a LB-agar plate containing the appropriate antibiotic and incubated overnight at 37°C.

2.4.f.II. Electro-competent E.Coli

To prepare electro-competent bacteria, chemically competent bacteria were cultured in 10ml LB medium without antibiotic, overnight at 37°C, 220rpm. Next day, 1 L of LB medium was inoculated with the overnight cultured bacteria, grown until the OD_{600} (optical density at 600 nm) reached 0.35-0.4, put immediately on ice and chilled for 30 min. The cells were pelleted using the already chilled centrifuge and washed 3-5 times with ice-cold ddH_2O. The white pellet was re-suspended in in 2 ml of ice-cold 10% glycerol. The final OD600 of the resuspended cells should be approximately 200 - 250. The aliquots were stored at -80°C. (Department of Molecular & Cell Biology, University of California, Berkeley).

The freshly prepared bacteria or thawed aliquots on ice were added to 2µl of ligated DNA or 10ng purified plasmid and mixed by tapping at the tube. The mixture was transferred to a electroporation cuvette and the electroporation was performed using the Micropulser electroporator. 1ml LB medium without antibiotic was added to transformed bacteria and incubated for 1hr at 37°C, 350 rpm in a thermomixer. 100µl of the

transformed bacteria was plated on a LB-agar plate containing appropriate antibiotic and incubated overnight at 37°C.

2.4.g. Mini preparation

High pure miniprep kits were used to extract plasmid DNA from bacteria. To screen the accuracy of the cloning conventional mini preparation (Sambrook, Fritsch et al. 1989) was employed as described below.

Buffer M1		*100 ml*
Tris/HCl pH 8.0	25 mM	2.5 ml of 1 M Tris/HCl pH 8.0 stock solution
Glucose	50 mM	10 ml of 0.5 M glucose stock solution
EDTA pH 8.0	10 mM	2 ml of 0.5 M EDTA pH 8.0 stock solution
add fresh before use:		
Lysozyme		2 mg / 1 ml buffer M1

Buffer M2		*5 ml*
NaOH	0.2 N	1 ml 1 N NaOH stock solution
SDS	1%	500 µl 10%-SDS stock solution
H_2O sterile		3.5 ml

Buffer M3		*20 ml*
Na acetate pH 4.8	3 M	8.165 g / 20 ml

The colony of interest was inoculated in 3 ml LB medium and incubated overnight at 37°C, 200rpm in a bacterial shaker. Next day, 1.5 ml of the overnight cultured cells were transferred into a 2 ml-eppendorf tube and pelleted at 6000 rpm using a table centrifuge for 2 min. The pellet was re-suspended in 150 µl of buffer M1 and kept on ice for 10 min. 200 µl of buffer M2 were added quickly and mixed by inversion (no vortexing) and kept on ice for 5 min. To stop the lysis, 150µl of buffer M3 were added and mixed by inverting the tube. After 10 min centrifugation at 14000 rpm, the supernatant was transferred into a new 1.5 ml eppendorf tube. To extract DNA in aqueous phase 200µl of phenol and 200µl of (24 chloroform-1 isoamylalcohol) mixture was added to the tube and mixed by vortexing. 5 min centrifugation at 14000 rpm is enough to separate the aqueous phase containing DNA from the lower organic phase (phenol) containing protein. The upper (aqueous) phase was transferred into new tube. 1/10 volume of buffer M3 was added and mixed. 2 volume of ice-cold 99% ethanol was added and mixed well. The sample was kept in -20°C

for 15 min and centrifuged for 30 min at 14000 rpm, 4°C. Supernatant was discarded carefully, 500 µl of 70% ethanol was added and centrifuged for 5 min at 14000 rpm, 4°C. Supernatant was discarded and the pellet was dried at 37°C for 10 min. Pellet was solved in 21 µl of RNase A (0.1mg/ml) for 30 min at 37°C. The concentration of DNA was measured by nanodrop.

2.4.h. Maxi preparation

To amplify large scale of plasmid DNA, High pure maxiprep kits were used beside the conventional maxi preparation (Sambrook, Fritsch et al. 1989) as described below.

STE buffer		*100 mL*
Tris/HCl pH 8.0	50 mM	5 mL of 1 M stock
Saccharose	25% (w/v)	25 g
EDTA pH 8.0	1 mM	0.2 mL of 0.5 M stock

Triton-mix		*100 mL*
Tris/HCl pH 8.0	50 mM	5 mL of 1 M stock
Triton X100	0.1% (v/v)	0.1 mL
EDTA pH 8.0	60 mM	12 mL of 0.5 M stock

PEG solution		*100 mL*
PEG 6000		30 g
NaCl	1.5 M	30 mL of 5 M stock

TNE buffer		*100 mL*
Tris/HCl pH 8.0	10 mM	1 mL of 1 M stock
NaCl	10 mM	0.2 mL of 5 M stock
EDTA pH 8.0	1 mM	0.2 mL of 0.5 M stock

TE buffer		*1 L*
Tris/HCl pH 8.0	10 mM	10 mL of 1 M stock
EDTA pH 8.0	1 mM	2 mL of 0.5 M stock

All buffers were stored at 4°C.

A single colony was inoculated in 30 ml LB medium with the appropriate antibiotic and cultured overnight at 37°C, 225 rpm in a bacterial shaker.

Next day, the overnight culture was transferred into 1 L LB medium with the appropriate antibiotic and grown up at 37°C, 225 rpm to reach the OD_{600} of 0.4 - 0.8. 200 mg of chloramphenicol were solved in ethanol, added to the culture, and the incubation was continued overnight.

The culture was pelleted in four 250 ml-centrifuge tubes at 4000 rpm for 15 min. Each pellet was re-suspended in 11.25 ml of ice-cold STE buffer and each 2 tubes were pooled in a one 50 ml centrifuge tube. 1.5 ml of lysozyme (60µg/ml of STE) was added to the re-suspended cells and incubated on ice for 20 min. 1.8 ml of 0.5 M EDTA (pH. 8) was added and incubated in ice for 5 min. 14.4 ml of Triton-mix was added and incubated in ice for 30 min. In this step it's important to shake the mixture every 5 minutes. After 1 hour centrifugation at 16000 rpm, 4°C, the supernatant was transferred into a 250 ml centrifuge tube. 40 ml of 30% PEG was added and incubated on ice for 1 hour. 10 min of centrifugation at 10000 rpm, 4°C, was applied, the supernatant was discarded and the pellet was dried using N_2 flow. The dried pellet was re-suspended in 10 ml of TNE buffer.

10.9 g CsCl plus 150 µl of 10 mg/ml ethidiumbromide were added to the solution and then transferred into ultracentrifuge Quick Seal tubes using a syringe and needle. The tubes were weighted. The difference between the filled tubes should not be more than 0.05g. The tubes were heat-sealed. After 20 hrs of ultracentrifugation at 60000 rpm, the red color band containing plasmid DNA was isolated and transferred to a 15ml tube.

Ethidiumbromide was extracted from the DNA by washing with the same volume of isoamylalcohol, until a colorless solution is obtained. During the washing plasmid DNA is always in the lower phase.

To remove CsCl from DNA, the sample was dialyzed twice, 12 hrs against TE buffer using a ¼ diameter dialysis tube at 4°C.

2.4.i. Measurement of DNA

After the dialysis was completed, the purity and the concentration of plasmid DNA were measured by a Nanodrop or other spectrophotometer. The OD260/OD280 ratio between 1.8 and 2 shows a good purity of DNA, but a ratio less than 1.8 represents bad purity of the extracted plasmid. The concentration of DNA can be calculated as follows:

$$DNA\ concentration = \frac{\mathrm{OD260}\times 50\times \mathrm{dilution\ rate}}{1000}\ \ (\mu g/\mu l)$$

The absorbance at 260 nm in a 1 cm quartz cuvette of a 50 µg/ml solution of double stranded DNA is equal to 1, since the number 50 is used as a factor for the DNA concentration calculation from the measured OD_{260} in the above mentioned equation.

2.4.j. Sequencing

Sequencing service of *Seqlab* and *MWG operon* was used to sequence the generated constructs. The chain-termination method (Sanger, Nicklen et al. 1977) was used for sequencing the genomic DNA. In this method the fragments are amplified by a PCR reaction using labeled dideoxynucleotides which are involved in Big Dye® Terminator v1.1 sequencing kit.

The reaction was prepared as follows:

DNA	300 ng
Primer	10 pmol
BigDye® mix	1.8 µl
ddH_2O	ad 20 µl

The PCR program was set up by following steps:

	Initial denaturation	2 min at 94°C
24 cycles	Cyclic denaturation	15 sec at 96°C
	Primer annealing	15 sec at 55°C
	Elongation	4 min at 60°C
	Final elongation	7 min at 72°C

The 96-well Millipore plate was filled by Sephadex resin and washed with ddH_2O. The PCR products were equalized to a final volume of 40µl by ddH_2O and loaded on prepared Sephadex. The samples were purified by 5 min centrifugation at 2000 rpm. The purified samples were applied to a capillary electrophoresis device and the results were analyzes using the ABI PRISM 3100 Genetic Analyzer.

2.4.k. Generation of targeting vector for DLK

In this experiment bMQ 317c09 has been used from bMQ BAC (Bacterial Artificial Chromosome) library. The vector carries sequences from 102.269.880-102.418.975 $^{+}$ strand on chromosome 15 (MAP3K12) of mouse SV129, inserted in BamHI restriction site.

2.4.k.I. Digestion pattern of bMQ 317c09

To check the accuracy of the made construct, the vector was cut by NotI overnight and run on agarose gel using a pulse field running system.

The setting of the system was as follows:

Time:	18 hrs	Final switch time (Sf):	25
Voltage:	6 V/cm	Angel:	120°
Initial switch time (Si):	1		

0.5x TBE buffer used for making 1% agarose gel and for electrophoresis. PFG (pulsed-field gel) middle range and low range markers from NEB were used as DNA ladder.

2.4.k.II. Gap-repair protocol

The gap-repair protocol describes how to generate a targeting vector for the generation of conditional cko (knock-out)-mouse model (Liu, Jenkins et al. 2003). A schematic figure of this protocol is depicted in Fig. 2.1 and Fig. 2.2.

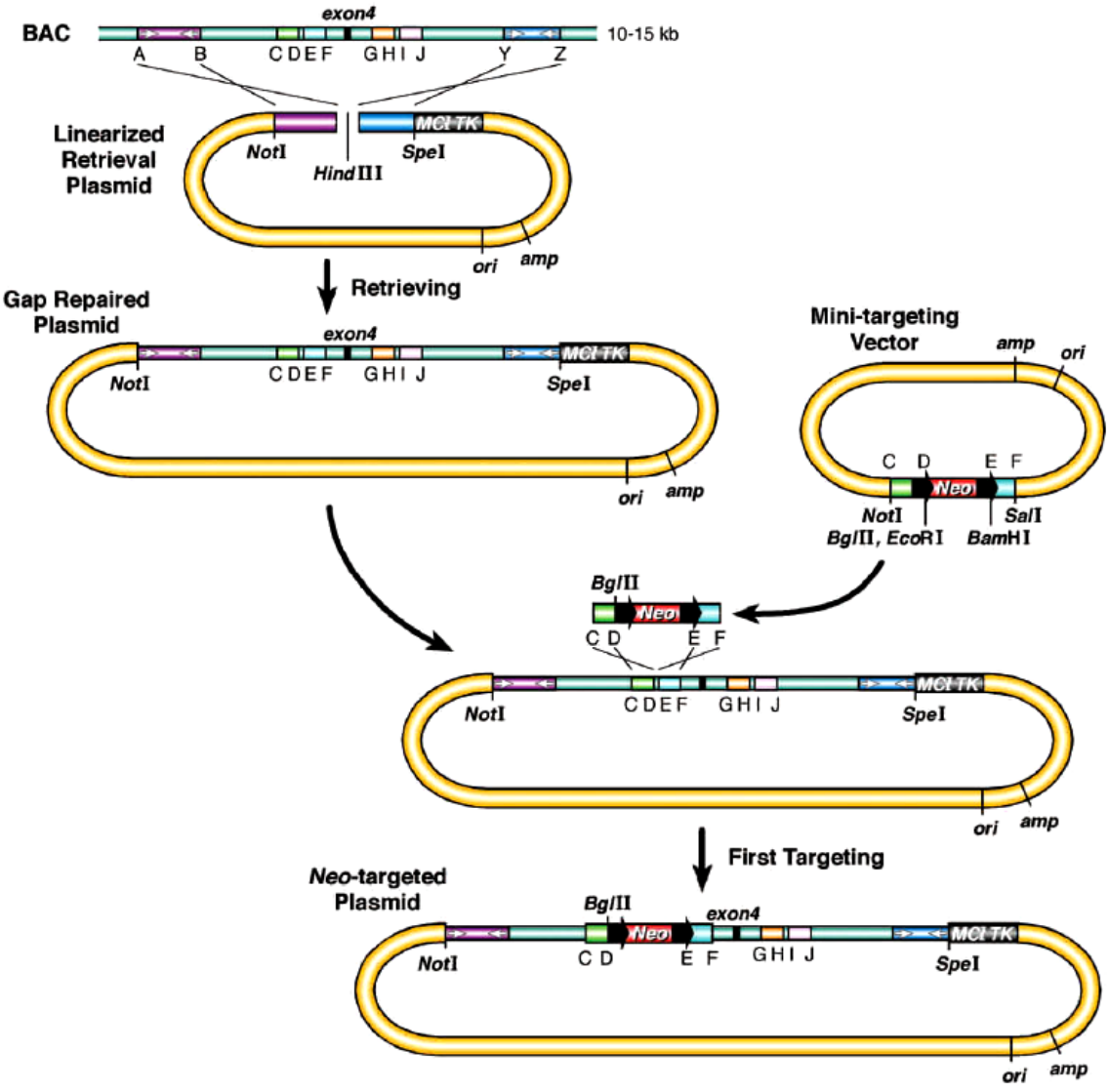

Figure 2. 1 Gap repair protocol for DNA recombineering. The DNA fragment which needs to be modified is subcloned from BAC plasmid to the targeting vector recruiting homologous recombination strategy. The neo cassette which is flanked by two loxP sites is introduced into the region of interest by homologous recombination (Liu, Jenkins et al. 2003).

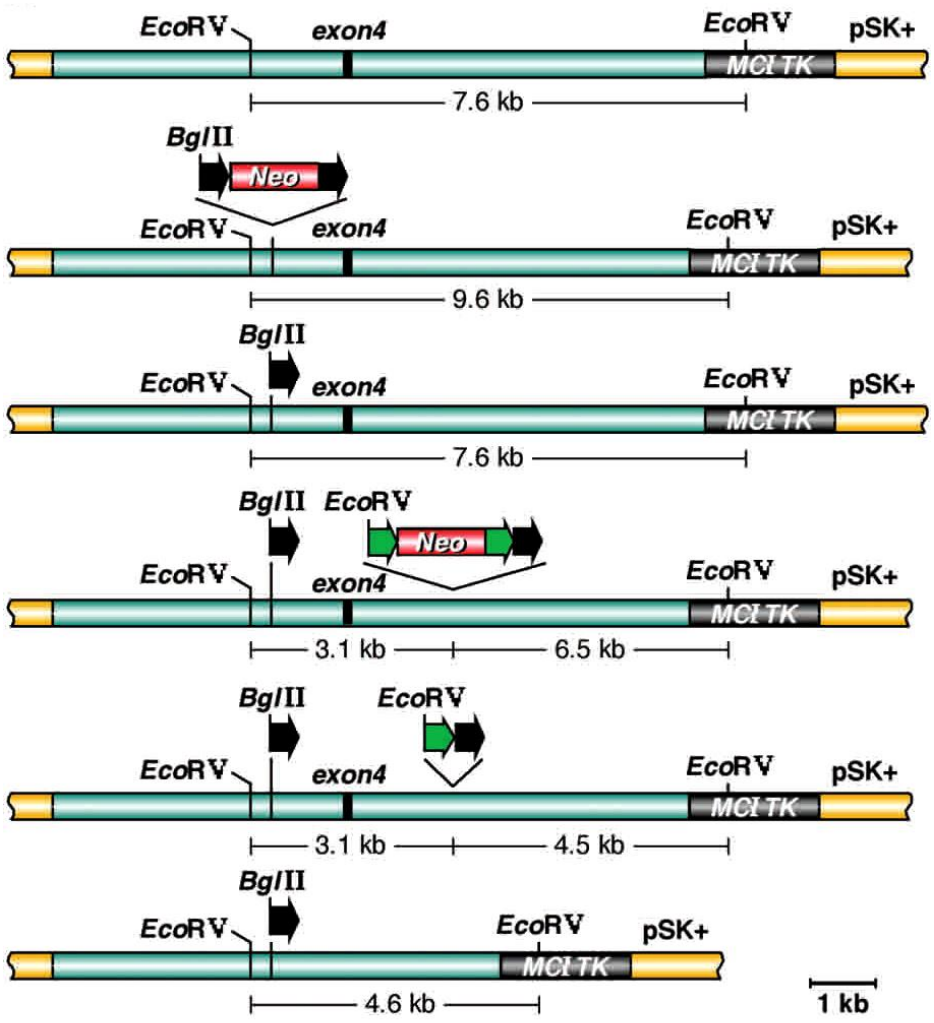

Figure 2. 2 Gap repair protocol for DNA recombineering. The neo cassette is excised by Cre-recombinase which left one of the two loxP sites on the vector backbone. The second loxP site is introduced through homologous recombination using a neo cassette flanked by two FRT (flippase recognition target) sequences, allowing the removal of the neo cassette by flippase (flpe) without the excision of the loxP site (Liu, Jenkins et al. 2003).

As illustrated, generation of a conditional cko-targeting vector consists of several steps:

1- Preparation of a restriction digest map
2- Generation of homology arms
3- Generation of retrieval plasmid
4- Retrieval of DNA from BAC into retrieval plasmid
5- Generation of mini-targeting vectors
6- Introduction of the first loxP site
7- Removal of the first neo cassette
8- Introduction of the second loxP site

2.4.k.II.1- Generation of homology arms and gap-repair plasmid

Two regions of about 500 bp of the BAC DNA were amplified using two sets of primers (A and B, and Y and Z). To apply a directional cloning of the PCR product into the pBluescript plasmid ($pBSK^+$) multiple cloning site, restriction sites of different enzymes were included in the primers as follows: HindIII in primers A and Y, NotI in primer B and SpeI in primer Z. The PCR products were purified using Biozym easy pure kit and digested with either NotI and HindIII or HindIII and SpeI. The digested fragments were purified again and ligated into the NotI and SpeI linearized PL253 plasmid. PL253 is a pBluescript-drived plasmid for retrieval of DNA from BAC. This plasmid contains a Mc1-driven thymidine kinase (TK) cassette for negative selection in ES cells. 2µl of ligated mix were electroporated into Top10 electro-competent cells. The positive colonies were selected by ampicillin resistance.

2.4.k.II.2- Retrieval of DNA from BAC

SW102 bacteria are DH10B bacterial strain which have been transformed by the defective λ prophage. The λ prophage contains the Red family (*exo*, and *bet*), and *gam* genes which are involved in recombination process. The expression of these genes is temperature inducible (section 4.3.b). SW102 cells were inoculated in LB medium overnight at 30°C. The next day a dilution of 1 to 50 from the overnight culture was grown at 30°C to reach the OD_{600} of 0.6. The cells were pelleted by centrifugation at 6000 rpm for 2 minutes. The pellet was washed 4-5 times with ice cold MQ autoclaved water to make fresh electro-competent cells. After washing, the pellet was re-suspended in 200 µl of ice cold MQ autoclaved water.

1 µl of BAC DNA was transferred into 40 µl of prepared SW102 cells by electroporation. The transformed cells were inoculated on a chloramphenicol agar plate (12.5 µg/ml chloramphenicol). DNA was extracted from positive colonies using miniprep protocol and

digested with NotI to compare with early digestion pattern (section 2.4.k.I). Colonies carrying the BAC were used for recombination experiment.

SW102 cells containing BAC was grownup overnight at 30°C. The next day a dilution of 1/50 was cultured in a total volume of 30 ml to reach the OD 600 of 0.6 (3-4 hrs). 15 ml of the culture were incubated at exactly 42°C for 15 minutes (to induce the Red recombination functions), and the rest 15 ml at 32°C as control. The cells were made electro-competent by washing several times with ice cold MQ autoclaved water, as described before.

Gap-repair plasmid which has AB and YZ homology arms was linearized with HindIII and purified from the gel. 1µl of linearized plasmid was transferred into 40µl of either induced or noninduced SW102 cells containing BAC DNA, by electroporation.

Transformed cells were grown on an ampicillin agar plate at 30 °C overnight. DNA was extracted from the ampicillin resistant colonies, which carry the targeting plasmid, and digested with EcoRI to compare with the prepared map(Fig. 3.13.A). DNA of interest was kept for the next step.

2.4.k.II.3- Generation of the first mini targeting vector

This mini vector permits the insertion of the loxP site into the desired DNA sequences by homology recombination and neo positive selection. Two regions of homology arms, up and down to the stretch where loxP site will be introduced, were amplified using two sets of primers (CD and EF) in which the NotI and EcoRI, BamHI and SalI recognition sites were included, respectively. The PCR products were digested by the appropriate enzymes and purified with Biozym easy pure kit. The loxP flanked neo cassette was cut out of PL452 plasmid with BamHI and EcoRI restriction enzymes and purified from the gel. $pBSK^+$ plasmid was linearized with NotI and SalI and purified from the gel. The purified homology arms and the purified loxP flanked neo cassette were ligated into the linearized $pBSK^+$ plasmid. The positive colonies were selected on kanamycin (15µg/ml) agar plate. DNA was extracted by miniprep and the accuracy was controlled by restriction digestion and sequencing.

2.4.k.II.4- Introduction of the first loxP site

The loxP flanked neo gene, together with the homology arms, was excised from $pBSK^+$ by NotI and SalI digestion, and gel-purified.

Red recombination functions were induced in SW102 cells by growing them at 42°C for 15 min. The cells were made electro-competent as described before. 150ng of purified fragment co-electroporated along with 10 ng of purified gap-repaired subcloned DNA into

already induced electro-cmpetent cells. Transformants were selected on kanamycin plates. The restriction digestion patterns were used along with sequencing to ensure the accurate recombination.

2.4.k.II.5- Excision of the first neo cassette

A single colony of SW106 cells was cultured in 5 ml LB medium at 32 °C, overnight. Next day 1 ml of overnight culture was inoculated in 10 ml LB medium at 32°C for 3 hrs (OD600= 0.5). Cre expression was induced in SW106 cells by growing in arabinose-containing media. 100µl of 10% arabinose added to the culture and incubated on bacterial shaker at 32°C for 1 hour. The cells were made electro-competent by washing several times (4-5 times) with ice cold MQ autoclaved water and transformed with gap-repaired plasmid containing loxP flanked neo cassette by electroporation. The electroporated cells were plated on either ampicillin (100µg/ml) or kanamycin (15µg/ml) plates. With a successful Cre-mediated recombination no colonies will grow on kanamycin plate. Colonies growing on ampicillin plate were checked for their kanamycin sensitivity by plating on kanamycin agar plate. Restriction digestion pattern was used besides sequencing to control that the neo cassette has been excised properly.

2.4.k.II.6- Introduction of the second loxp site

The FRT (flippase recognition target) flanked Neo+loxP fragment was cut out from PL451 plasmid by BamHI and EcoRI and gel purified. The homologous arms GH and IJ were digested by NotI and EcoRI, and BamHI and SalI, respectively. The homologous arms and the Neo cassette were ligated into the $pBSK^{+}$ vector which had been already linearized by NotI and SalI. The constructed vector was transferred into TOP10 cells by electroporation and the positive colonies were selected on Kanamycin agar plate. After DNA extraction from positive colonies, which carrying the neo cassette integrated into the targeting vector, and sequencing the cloned fragment was cut out from mini vector by NotI and SalI restriction enzymes and gel purified.

The purified fragment was co-electroporated with the targeting vector from the previous step into SW102 competent cells which had been induced before at 42°C for 15 min. The transformed colonies were selected on Kanamycin agar plate. DNA of the colonies was extracted and digested by EcoRI and the digestion pattern was compared to the prepared map (Fig. 3.19).

Since pBluescript is a high-copy plasmid the cell might carry the targeted and nontargeted plasmids after recombination carried out. In this case both positive and negative digestion pattern is observed for the same extracted DNA. To overcome this

problem 1ng of the targeted vector was electroporated into TOP10 cells and the colonies were selected on Kanamycin agar plate. After digestion of the extracted DNA with EcoRI the positive clones can be distinguished from the negative ones by comparing to the prepared map. Sequencing proved the accuracy of the cloning.

To functionally test the loxP and FRT sites in the targeting vector, the cko-targeting vector was transferred into arabinose-induced SW106 and SW105, respectively, by electropoation. SW106 cells have a Cre recombinase gene under the control of an arabinose-inducible promoter, whereas SW105 cells have Flpe recombinase under the control of an arabinose-inducible promoter. Cells were plated on ampicillin plates for the selection of the transformed cells which are expected to be ampicillin resistant. Plasmid DNA was prepared and digested with EcoRI to confirm the expected recombination. Sequencing was done to control the accuracy of the digestion pattern.

2.5. Protein oriented experiments

2.5.a. Bradford assay

The Bradford assay was performed to measure the concentration of extracted proteins. The Dye Reagent containing the Coomassie Brilliant Blue G-250 has different colours in different pH. At pH less than 1 the colour is red with absorption maximally at 470 nm. The colour changes to green when the pH is 1≥<2 with maximum absorption at 620 nm, and the dye is bright blue when the pH is above 2 with maximum absorption at 595 nm (Chial HJ 1993). Binding to proteins, changes the colour of the reagent to blue. The intensity of the blue colour correlates with the amount of proteins in solution (Bradford, 1976). The reagent was diluted 1:5 in H_2O. Different concentrations of BSA were used to generate a standard curve ranging from 0.1 µg/ml to 30 µg/ml in coomassie reagent. The spectrophotometer measures the OD_{595} of different concentrations and generates a standard curve. (Biometer, Eppendorf). 1µl of protein sample was added to 1 ml of diluted reagent, mixed well and kept at room temperature for 5 min. The optical density of the samples was measured at 595 nm. The spectrophotometer calculates the concentration of the protein according to the previously generated standard curve. When the OD_{595} of the sample is in the range of the standard curve the corresponding concentration in the standard curve is reported for the sample.

2.5.b. SDS-PAGE electrophoresis

Buffers used for SDS-PAGE electrophoresis are listed below.

Stacking gel buffer		200 mL
Tris/HCl pH 6.8	0.5 M	12.144 g
SDS	0.4% (w/v)	8 mL of 10% SDS

Separating gel buffer		200 mL
Tris/HCl pH 8.8	1.5 M	36.342 g
SDS	0.4% (w/v)	8 mL of 10% SDS

Running buffer		1 L
Tris	25 mM	3.03 g
Glycine	192 mM	14.41 g
SDS	0.1% (w/v)	10 mL of 10% SDS

Laemmli-loading buffer	2x	100 mL
Tris/HCl pH 6.8	160 mM	16 mL of 1 M stock
SDS	4 % (w/v)	4 g
Glycerol	10 % (v/v)	10 mL 99.5% Glycerol
Bromophenolblue	0.05 % (w/v)	50 mg
β-Mercaptoethanol	10 % (v/v)	10 mL

Laemmli-loading buffer was stored in aliquots at -20°C

The gel caster components, including glass plates with 1.0 mm spacer and short glass plates were set up according to the manufacturer's instructions (Bio-Rad). Separating gel in the desired concentration of acrylamide-mix were prepared and poured into the set plate.

% of acrylamide	Molecular weight (kDa)
8	50-130
10	30-100
12	20-70
15	≤40

Ingredients for a sample stacking and separating gel:

Stacking gel 4%	5 ml
ddH_2O	3 ml
Stacking gel buffer	1.25 ml
Acrylamide-mix	670 µl
10% APS	50 µl
TEMED	5 µl

Separating gel 10%	8 ml
ddH_2O	3.2 ml
Separating gel buffer	2 ml
Acrylamide-mix	2.67 ml
10% APS	80 µl
TEMED	8 µl

TEMED was added when the solution was mixed very well and the gel was poured immediately. 5 ml of prepared separating gel mixture was poured into the set plate. 200 µl of Isopropanol were added at the top of the gel to make the surface even. After polymerizing, isopropanol was carefully removed. The stacking gel was poured into the plate, the appropriate comb was inserted immediately, and the gel was left at room temperature to polymerize (30-60min).

The gel was fixed in the running chamber according to the instruction of the manufacturer, and the chamber was filled up with the running buffer. The comb was removed carefully and the slots were washed with the running buffer using a micropipette and long tip.

The samples were supplemented with the same volume of 2x laemmli-loading buffer and boiled for 10 min at 95°C. The droplets were collected from the wall by a short spinning down using the table centrifuge. The same amount of protein was loaded into each slot of the gel. 5 µl of prestained PageRuler was loaded as molecular weight marker. An electricity field of 80V was applied to start the electrophoresis. When the loading dye passed through the border between the stacking gel and separating gel, the electrical field was raised up to 110V. The run was stopped when the loading dye left the bottom of the gel. The gel was segregated from the unit and transferred to a new dish containing ddH_2O.

2.5.c. Coomassie blue staining

Proteins can be detected on SDS-PAGE by staining with coomassie brilliant blue. The staining and destaining solutions were prepared as follows:

Staining solution	1 L	
Coomassie brilliant blue	0.25 % (w/v)	2.5 g
Methanol	40 % (v/v)	400 mL
Acetic acid	10 % (v/v)	100 mL

Destaining solution		1 L
Isopropanol	25 % (v/v)	250 mL
Acetic acid	10 % (v/v)	100 mL
Methanol	10 % (v/v)	100 mL

Proteins were electrophoresed. The gel was washed with ddH_2O for 10 min and transferred to the staining solution. After 20 min shaking on a rocking platform the staining solution was removed and the stained gel was washed first by ddH_2O to wash out the remnants of the dye and then with destaining solution on a rocking platform. The destaining solution was changed repeatedly to decrease the washing time and gain a more transparent gel. The gel was dried in cellophane using a gel dryer according to the instruction of the manufacturer.

2.5.d. Immunoblot

Immunoblot was used for qualitative and quantitative analysis of proteins using specific antibodies for the detection of specific proteins. Buffers and solutions used for immunoblotting are listed below.

Transfer buffer	1x	2L
Glycine	192 mM	28.8 g
Tris base	25 mM	6.04 g
Methanol	10%v/v	200 ml
ddH_2O		ad 2 L

TBS-T		1 L
Tween	0.1% (v/v)	1 ml
TBS		ad 1 L

Blocking solution		50 ml
Milk powder	5% (w/v)	2.5 g
TBS-T		ad 50 ml

Antibody solution		10 ml
Milk powder	1% (w/v)	100 mg
TBS-T		ad 10 ml

Blocking and antibody solutions were prepared freshly before use.

After SDS-PAGE, the gel was washed with ddH_2O for 5 min on a rocking platform, and then equilibrated to transfer buffer for 5 min on a rocking platform. Whatman paper and nitrocellulose membrane were soaked in the transfer buffer. A Wet/Tank blotting system was used to transfer proteins from the gel to the membrane. The blotting sandwich was packed in a way that the gel faced to the negative pole and the membrane faced to the positive pole (Fig. 2.3). Three layers of Whatman paper were placed on the sponge in the black side of the sandwich. The gel lay down on the paper and the membrane lay down on the gel. Three more layers of Whatman paper were put on the membrane and the sandwich was packed with another sponge. The package was placed in the chamber filled with transfer buffer. An ice box was used to cool the system down. An electricity current of 400 mA applied to run the transfer for 1hr.

The membrane was soaked in Ponceau solution for 15 min on a rocking platform to control a successful transfer. The membrane was destained by TBS-T and incubated with blocking solution for 1hr at room temperature on a rocking platform. The blocking solution was replaced by the antibody solution containing the primary antibody and incubated overnight on a rocking platform at 4°C. The next day the membrane was washed 3 times with TBS-T, 10 min each time and incubated with the antibody solution containing the secondary antibody for 1hr at room temperature. Afterward the membrane was washed 3 times with TBS-T, 10 min each time.

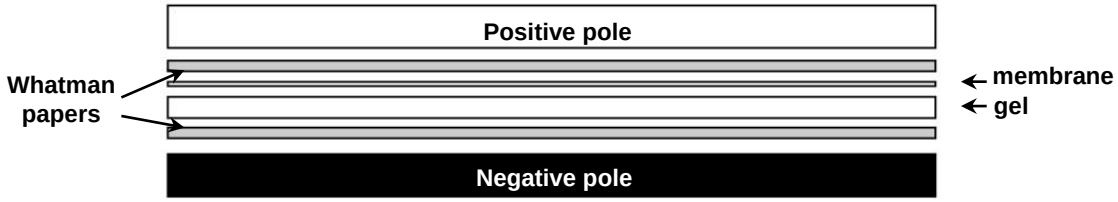

Figure 2. 3 The blotting package. The gel is faced to the negative pole and the membrane is faced to the positive pole. The electrical current from the negative pole to the positive pole in the blotting chamber facilitates the transfer of proteins from the gel to the membrane.

The Lumi-light^{plus} kit was used for immunodetection according to the instruction of the manufacturer. The detection was performed using a Chemi Genius or Versa doc imaging system. Quantity-one software was used for the evaluation of the optical density of the protein representing bands.

2.5.e. Protein purification

Affinity chromatography was used for the purification of the proteins from the bacterial extract. In this method the protein is fused to an agent which has a specific binding substrate. Binding to the substrate pools out the fused protein from the solution, allowing the purification of the protein of interest. The chromatography column is filled with the chromatography resins which are covered by the specific substrate. By running the solution containing the proteins through the column, the fused proteins bind to the substrate and the rest of the proteins pass through the column. By adding a high concentration of the binding substrate, the proteins can be refine from the resins. In this study, three fusion systems were used for the purification of proteins. The GST (glutathion S-transferase)-fusion system with glutathion as binding substrate, the His-tagged protein system with imidazole as binding substrate, and the MBP (maltose binding protein)-fusion system with maltose as binding substrate.

2.5.e.I. GST-fusion protein

DLK NLS was subcloned into the multiple cloning site of the pGEX-6p1 vector, directed by restriction enzymes. The coding sequence of DLK NLS containing the amino acids 140-285 was fused to GST. The expression of GST and the polypeptide fused to it is under the control of *lac* operon. In the absence of Lactose the *lac* repressors inhibit the expression. Lactose and similar molecules like IPTG (isopropyl-beta-D-thiogalactopyranoside) bind and inactivate the *lac* repressors and thereby inducing the expression of fusion protein on the expression vector.

2.5.e.I.1- Screening

The screening was performed to select the colonies in which the expression of the fused protein is well induced by IPTG for the large scale purification. DH5α chemically competent cells were transformed with the construct and plated on ampicillin agar plate. 7 growing colonies were picked and inoculated in 2 ml of LB containing 50 µg/ml ampicillin, shaking overnight at 37°C in a bacterial incubator. Next day, 100 µl of the each culture were inoculated in 2 ml of the LB containing ampicillin and cultured for 1hr at 37°C, 220 rpm.

500 µl of each tube was saved as control and the rest was supplemented with 1mM IPTG to induce protein expression and cultured for another 2 hrs at 37°C, 220 rpm. 500 µl of induced cultures were transferred to 1.5 ml eppendorf tubes. All control and induced samples were pelleted by centrifugation at 6000 rpm for 2 min using a table centrifuge. 20 µl of Laemmli-loading dye was added to each sample and boiled for 10 min at 95°C. The

samples were spun down and applied on a SDS-PAGE. The gel was stained with coomassie blue and the inducible samples were chosen for large scale purification.

2.5.e.I.2- large scale purification

10 ml of overnight culture of inducible sample was inoculated in 1 L of the LB containing ampicillin to reach the OD 600 of 0.6. In this state bacteria have a logarithmic growth, 500µl of bacteria was kept as control and 238 mg IPTG (1 mM final concentration) was added to the rest to induce expression at 37°C for 3 hrs. 500 µl of induced bacteria was taken and the rest was harvested by 10 min centrifugation at 4000 rpm using a Beckmann J2.21 centrifuge. The pellet was re-suspended in 30 ml of extraction buffer and kept in -80°C overnight.

Sufficient amounts of glutathione agarose beads were swollen overnight in 10 ml of PBS at 4°C. The next day, the beads were washed 3 times with 5 ml of the extraction buffer and finally a 50% slurry suspension of the beads in extraction buffer was prepared and kept on ice.

Extraction buffer	50 ml
PBS	ad 50 ml
DTT	1 mM
PMSF	1 mM

The extraction buffer was prepared freshly before use.

Elution buffer	Final concentration	10 ml
Tris pH 8.0	50 mM	0.5 ml of 1 M stock
Glutathione	10 mM	30.7 mg
ddH_2O		ad 10 ml

The elution buffer was prepared freshly before use and the pH was adjusted to 7.4

The sample was thawed on ice and the lysis was completed by 3 times sonication using Bandelin Sonopuls sonicator. The setting of the sonicator was as follows:

Time	2 min
Cycle	30%
Power	40%

To avoid the denaturation of the proteins the sample was kept in an ice-water-methanol bath during the sonication. The sonicated solution was pelleted by centrifugation at 4000

rpm for 30 min at 4°C. The supernatant was transferred into a 50 ml tube. 10 µl of the crude extract were kept for control. A tiny piece of the pellet was re-suspended in 50 µl extraction buffer and 10 µl of it was kept for control. 1 ml of the prepared GSH-agarose bead was added to the crude extract and incubated on an up and down rotator at 4°C for 2hrs. The beads were spun down for 10 min at 1200 rpm. 10 µl of the supernatant was kept for control. The beads were washed 3 times with 5 ml of extraction buffer. The protein was sequentially eluted from the beads by 600 µl of elution buffer in a 2 ml-eppendorf tube, shaking at 1000 rpm using a thermomixer for 10 min at room temperature. The eluted solution was collected by 1 min centrifugation at high speed using a table centrifuge.

Elution fractions were assessed by mini-bradford assay and the highest concentration fractions were selected. The eluted protein was dialyzed 2 times against 1 L of the extraction buffer for 2 hrs at 4°C. 5 µl of the sample was taken for control and the rest was supplemented with 10% glycerol and kept at -80°C. The preserved samples for control from all steps were supplemented with laemmlie-loading dye applied to SDS-PAGE. Coomassie staining was used to screen the expression and the step by step purification.

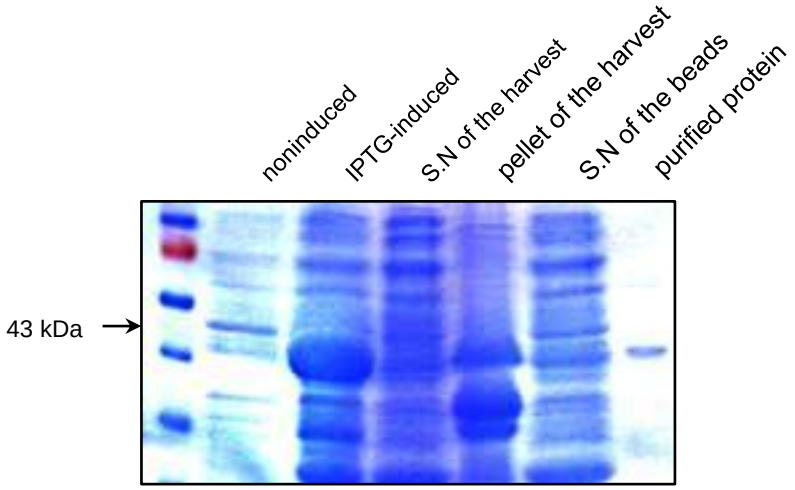

Figure 2. 4 Coomassie staining of GST-fusion protein. The preserved samples for control during the purification steps were subjected to SDS-PAGE. The gel was stained with coomassie dye. The GST-fusion DLK NLS is presented at 43 kDa.

2.5.e.II. His-tagged protein

DLK NLS was subcloned into the multiple cloning site of the pET28a^{+} vector. The coding sequence of DLK NLS containing the amino acids 140-285 is fused to a poly-Histidine epitope box. The expression of the tagged protein is under the control of *lac* operon. The BL21 competent bacteria were transformed by the expression plasmid. The screening

step was performed as described in section (2.5.e.I.1). The buffers used in this experiment are listed below.

Lysis Buffer pH 7-8	1x
Tris-HCl	50 mM
Glycerol	5%
NaCl	50 mM

Binding buffer pH 7-8	1x
Tris-HCl	20 mM
NaCl	0.5 M
Imidazole	5 mM

Washing buffer pH 7-8	1x
Tris-HCl	20 mM
NaCl	0.5 M
Imidazole	60 mM

Elution buffer pH 7-8	1x
Tris-HCl	20 mM
NaCl	0.5 M
Imidazole	1 M

10 ml of the overnight culture of inducible sample was inoculated in 1 L of the LB containing ampicillin and grown to an OD_{600} of 0.6. 500 µl of the bacteria were kept as control and 238 mg IPTG (1mM final concentration) were added to the rest to induce expression at 37°C for 3 hrs. 500 µl of induced bacteria was taken and the rest was harvested by 10 min centrifugation at 4000 rpm using a Beckmann J2.21 centrifuge. The pellet was re-suspended in 30 ml of lysis buffer and kept in -80°C overnight. The next day, the pellet was thawed on ice. 100 kU of lysozyme was added and incubated on a rocking platform for 20 min at room temperature. Sonication was performed as described in section (2.5.e.I.2). The sonicated solution was pelleted by centrifugation at 4000 rpm for 30 min at 4°C. The supernatant was transferred into a 50 ml tube. 10 µl of the crude extract were kept for control. A tiny piece of the pellet was re-suspended in 50 µl of lysis buffer and 10 µl of it was kept for control.

His Bind Resin was gently mixed and suspended. The 50% slurry resin is covered and charged by Ni^{2+} cations which bind to the His-tag epitope sequence. 1.5 ml of slurry

suspension was transferred into a 2 ml tube and washed 2 times with binding buffer. The resin was added to the crude extract and incubated on an overhead rotator at 4°C for 2hrs. The beads were spun down for 10 min at 1200 rpm. 10 µl of the supernatant was kept for control. The beads were washed 3 times with 1 ml binding buffer and 3 times with 1 ml washing buffer in a 2 ml-eppendorf tube. The protein was sequentially eluted from the beads by 600 µl of elution buffer in a 2 ml-eppendorf tube, shaking at 1000 rpm using a thermomixer for 10 min at room temperature. The eluted protein was collected by 1 min centrifugation at high speed using a table centrifuge.

Elution fractions were assessed by mini-bradford assay and the highest concentration fractions were selected. The eluted protein was dialyzed 2 times against 1 L of PBS+1 mM DTT for 2hrs at 4°C. 5 µl of the sample was taken for control and the rest was supplemented with 10% glycerol and kept at -80°C. The preserved samples for screening from all steps were supplemented with laemmlie-loading dye applied to SDS-PAGE. Coomassie staining was used to screen the expression and step by step purification.

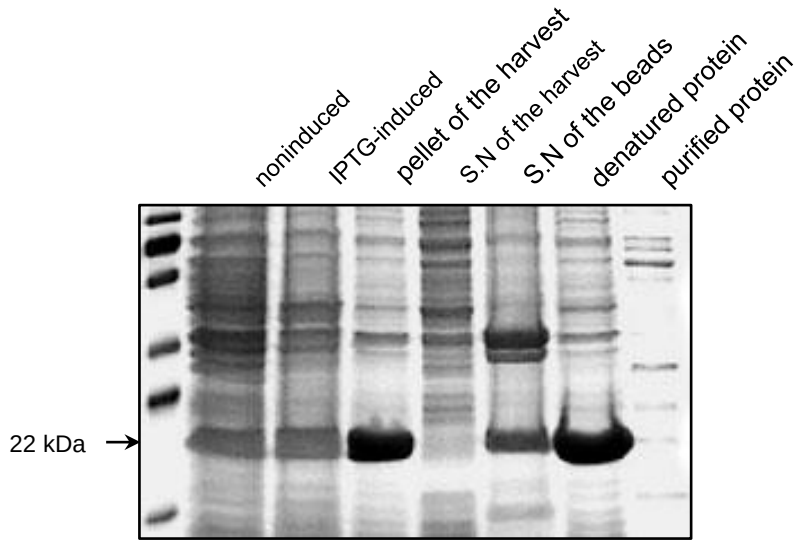

Figure 2. 5 Coomassie staining of His-tagged protein. The preserved samples for control during the purification steps were subjected to SDS-PAGE. The gel was stained with coomassie dye. The His-tagged DLK NLS is presented at 22 kDa.

2.5.e.III. MBP-fusion protein

DLK KNLSLZ was subcloned into the multiple cloning site of the pMAL-c2x vector. The coding sequence of DLK KNLSLZ containing the amino acids 140-517 is fused to MBP. The expression of the fusion protein is under the control of *lac* operon and is induced by IPTG. The K12Δ competent bacteria were transformed by the expression vector. All steps are similar to section (2.5.e.I), except: the column buffer was used instead of the

extraction buffer, the elution buffer contained maltose instead of glutathion, dialysis was performed against the extraction buffer (2.5.e.I), and amylose resin was used instead of glutathion-agarose bead. The amylose resins are covered by amylose which has a binding affinity to MBP. The bond MBP-fusion proteins can be refined by maltose (Fig. 2.6).

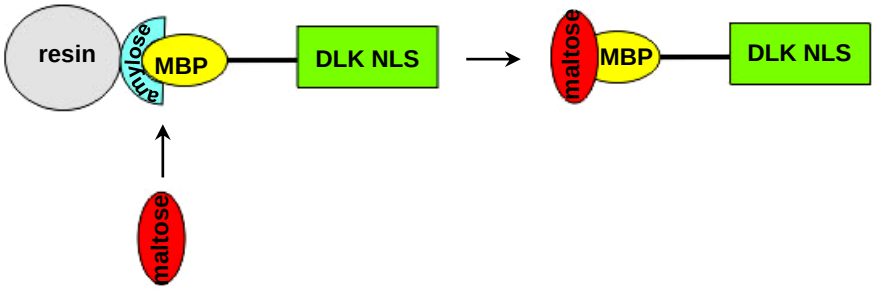

Figure 2. 6 Schematic figure of affinity chromatography protein purification. The amylose resin is covered by amylose molecules which bind to MBP sequences. The MBP-fusion protein is refined from the cell extract solution by the binding affinity of MBP to amylose. The fusion protein is retained from the resin by adding a high concentration of maltose which binds competitively to MBP.

Column buffer	1x
Tris-HCl	20 mM
NaCl	200 mM
EDTA*	1 mM
DTT*	1 mM
PMSF*	1 mM

* added freshly before use.

Elution buffer	1x
Column buffer	1x
Maltose	10 mM

2.5.f. Protein-protein interaction assay

Protein-protein interaction assay was performed to investigate the interaction between DLK NLS wild-type and mutants and some of the import proteins. MBP-DLK KNLSLZ and His-tagged importins (α, β, and transportin) were used in this experiment (Fig. 2.7).

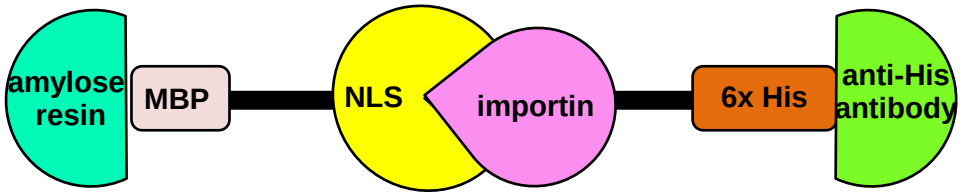

Figure 2. 7 Schematic figure for protein-protein interaction. The MBP-fusion proteins are immobilized to amylose resins. The interaction is performed between the MBP-fusion proteins and the His-tagged proteins, and can be detected by immunoblot using an anti-His antibody.

TPB buffer is a modified buffer for this experiment.

TPB buffer	1x
KoAc	110 mM
HEPES pH 7.4	20 mM
MgoAc	2 mM
DTT	1 mM
Protease inhibitor	1x

Blocking buffer	1x
TPB buffer	1x
Fatty acid free BSA	10 mg/ml

The buffers were prepared freshly and kept on ice.

500 µl of the slurry amylose resin were washed 3 times with TPB buffer and incubated with blocking buffer for 30 min on an overhead rotator at 4°C.

The resin was split into three 2 ml eppendorf tubes. 15 µg of each MBP fused proteins (DLK KNLSLZ wt, 1, and 2 mutants) was added to the tubes and labeled. The tubes were incubated for1hr at 4°C on a rotator. Meanwhile the importins were prepared in labeled 1.5 ml tubes according to the table below and kept on ice.

	DLK KNLSLZ wt	DLK KNLSLZ1	DLK KNLSLZ2
Importin α	2 µg	2 µg	2 µg
Importin β	2 µg	2 µg	2 µg
Transportin	2 µg	2 µg	2 µg
Blocking buffer	ad 380 µl	ad 380 µl	ad 380 µl

The resin was washed 3 times with 1 ml blocking buffer, spun down at 500 rpm for 1 min using a table centrifuge, and re-suspended in 200 µl blocking buffer. 20 µl of resin was added to each labeled tube containing importins and incubated for 2 hrs at 4°C on a rotator.

The resins were washed 3 times with 1 ml TPB buffer and spun down at 500 rpm for 1 min. The supernatant was discarded; 20 µl of laemmli-loading dye was added and boiled at 95°C for 5 min. The samples were analyzed by SDS-PAGE and immunoblotting using an anti-His antibody. 5% of the importin input (5% of 2 µg=0.1 µg) was loaded beside the samples to observe the interaction efficiency.

2.5.g. Preparation of cell lysates for immunoblotting

The lysis buffer used in this method was as follows:

Lysis buffer	1x
HEPES pH 7.5	50 mM
NaCl	150 mM
$MgCl_2$	1.5 mM
EGTA	1 mM
Triton X-100	1%

Protease and phosphotase inhibitors were added freshly before use.

The medium was removed and the cells were washed with PBS and kept on ice. The cells were detached from the dish using a cell scraper and collected in 50-150 µl of lysis buffer (depending on the number of cells). Lysis was completed by three freeze-thaw cycle in liquid nitrogen and 37°C water bath, respectively. Intensive vortexing was applied in each cycle of freezing and thawing. The extracted proteins were collected in the supernatant by 10 min centrifugation at 14,000 rpm, 4°C. The total amount of protein was measured by bradford assay. The samples were kept frozen at -20°C until running SDS-PAGE.

2.6. Working with HIT-T15 cells

2.6.a. Transient transfection using DEAE-Dextran

The complex formation of DNA with DEAE-Dextran facilitates the endocytosis of DNA through cell membrane. This method was used for the analysis of reporter gene activity. TD-buffer was used for cell and DNA preparation. DEAE-Dextran was prepared at

the concentration of 60mg/ml in ddH_2O, filtered by a 0.45 µm syringe filter and stored at 4°C.

TD-buffer

Tris-HCl pH 7.4	25 mM
NaCl	140 mM
KCl	5 mM
K_2HPO_4	0.7 mM

The buffer was autoclaved for 20 min at 121°C and stored at room temperature.

One 15-cm-confluent dish of HIT-T15 cells was used to split to twelve 6-cm-dishes. After detaching the cells from dish by trypsin/EDTA, the cells were collected in 7 ml of pure RMPI medium and washed once with 10 ml of TD-buffer. The cells were re-suspended in 1 ml/dish TD-buffer and supplemented with 5 µl DEAE-Dextran per dish. 2 µg/dish of plasmid DNA was prepared in 2 ml of TD-buffer and added to the cells. In the case of cotransfection of plasmids the final amount of DNA was equilibrated by pBluescript vector. The cells' suspension was incubated at room temperature for 15 min. The cell were pelleted by centrifugation at 800 rpm for 2 min, washed with RPMI complete medium, and re-suspended in 5 ml/dish RMPI complete medium and seeded into 6-cm-dishes. After 48 hrs incubation at 37°C, the cells were treated with additional agents and harvested for the measurement of reporter gene activity.

2.6.b. Transient transfection by metafectene

This method was used for the analysis of overexpressed proteins in HIT-T15 cells. One 15-cm-dish was split to eight 6-cm-dishes. Transfection was performed according to the instruction of manufacturer. 2 µg DNA was added to 200 µl RPMI per dish. 4 µl Metafectene prepared in 200 µl RPMI per dish, keeping a 1 to 2 ratio between DNA and metafectene. The prepared solutions were mixed together and incubated at room temperature for 15 min. The mixture was added to the cells during the first hour of seeding. 48 hrs after incubation, the cells were used for the next experiment.

2.6.c. Transient transfection by Oligofectamine

This method was used for the down-regulation of endogenous DLK by small interfering RNA (siRNA). 300.000 cells per well were seeded in 6-well plate and incubated for 24 hrs at 37°C. The next day, the cells were washed with pure RPMI to remove the sera which are included in complete medium, and supplemented with 800 µl OptiMEM® medium, a modified EMEM (Eagle's Minimum Essential Media) medium which is suitable

for lipid transfection. The cells were put back to the incubator. Oligofectamine and the siRNA were prepared according to the manufacturer's instruction.

Per 2 wells	Per 2 wells
5 µl siRNA (50 pmol/well)	8 µl Oligofectamine
ad 370 µl OptiMEM®	22 µl OptiMEM®

The solutions were incubated at room temperature for 5 min and subsequently mixed together and incubated for another 15 min at room temperature. 200 µl of the mixture was added to each dish and incubated for 4 hrs at 37°C. 500 µl of 3x RPMI (3 times concentrated for FCS, HS, and pen/strep) were added to the wells and incubated for 24 hrs.

2.6.d. Cell harvesting for reporter gene assay

The buffer used are listed below.

Scraping buffer	1x
Tris-HCl pH 7.5	40 mM
EDTA	1 mM
NaCl	150 mM

KPi buffer pH 7.8		540 ml
K_2HPO_4	100 mM	500 ml
KH_2PO_4	100 mM	ad 540 ml

The pH of basic K_2HPO_4 was adjusted to 7.8 by acidic KH_2PO_4. The buffers were stored at room temperature.

The medium was removed and the cells were washed with PBS. The cells were mechanically detached from the dish using a cell scraper and collected in 1.5 ml scraping buffer. The cells were pelleted by 4 min centrifugation at 5000 rpm, at 4°C. The supernatant was discarded and the pellet was re-suspended in 150 µl of KPi buffer, freshly supplemented with 1 mM DTT. The samples underwent three freeze-thaw cycles in liquid nitrogen and 37°C water bath, respectively. Intensive vortexing was applied in each cycle. The samples were centrifuged at high speed for 10 min at 4°C using a table centrifuge. The supernatant was kept frozen at -80°C until measurement.

2.6.e. Immunocytochemistry

The subcellular localization of DLK wild-type and DLK PP mutant (mutation in leucine zipper) was analyzed by immunocytochemistry. 300.000 HIT-T15 cells were seeded on a coverslip in 6-well plate. The cells were transfected by the expression vectors for DLK wild-type and PP mutant by the Metafectene method. 48 hrs later the cells were treated with 10 ng/ml TNFα for 1 hr. Coverslips were transferred to new 6-well plate and washed 5 min with PBS agitating on a rocking platform at room temperature. The cells were fixed by 4ml methanol (-20°C) for 10 min and then washed 3 times with PBS for 5 min each. To prevent nonspecific binding of antibodies the samples were blocked with blocking buffer for 45 min at room temperature and then washed once with PBS. The appropriate dilution of the primary anti-flag antibody was prepared and incubated with the samples overnight at 4°C. The next day, the samples were rinsed in PBS 3 times for 5 min each, and incubated with the secondary fluorescent labeled antibody for 30 min in a dark place. After rinsing 3 times in PBS for 5 min each, one droplet of Vectashield® mounting medium containing DAPI (4',6-diamino-2-phenylindole) was dropped on a glass slide and the coverslip lain down on it. The slides were left in a dark place for fixation. The imaging was performed using a Zeiss Axiovert 200M with Apo Tome Microscope and Axiovert 4.7 software.

The buffers were prepared in PBS as follows:

Blocking buffer

BSA	1% (w/v)
Horse serum	10%(v/v)

Antibody-dilution buffer

BSA	1% (w/v)

The buffers were prepared freshly before use.

2.7. Luciferase assay

The buffers and solutions used are listed below.

Glycylglycine buffer

Glycylglycine pH 7.8	25 mM
$MgSO_4$	15 mM
EGTA	4 mM

This buffer was stored at 4°C.

Luciferin stock		180 ml
DTT	10 mM	275 mg
Luciferin	1 mM	50 mg
Glycylglycine buffer		178.5 ml

The stock was stored as aliquots at -80°C.

Luciferase-assay mix		For 25 samples
Glycylglycine buffer		7.5 ml
KPi buffer	16.5 mM	1.5 ml
ATP	2 mM	100 µl of 200 mM ATP
DTT	1 mM	10 µl of 1 M DTT

This buffer was prepared freshly before use.

Luciferin solution		For 25 samples
Glycylglycine buffer		5.6 ml
DTT	10 mM	56 µl of 1 M DTT
luciferin	250 µM	1.4 ml of Luciferin stock

This solution was prepared freshly before use.

Luciferase refers to a class of oxidative enzymes participating in bioluminescence. Firefly luciferase from firefly *photinus pyralis* is a well-known member of this class of enzymes (Gould and Subramani 1988). The recombinant form of this enzyme is commercially available. Luciferin is the substrate of the enzyme. Luciferase catalyzes the reaction in two steps:

1. Luciferin + ATP $\dashrightarrow$ Luciferyladenylate + PP_i
2. Luciferyladenylate + O_2 $\dashrightarrow$ Oxyluciferin + AMP + photon of light

Oxyluciferin is electronically excited and emits a photon of light when turning back to its ground state.

50 µL of cell extract were mixed with 368 µL of luciferase-assay mix in a luminometer tube. Luciferase-assay mix was used as blank. 200 µL of the luciferin solution were injected automatically by the luminometer to the samples and the light emission was measured at 560 nm for 20 sec per sample.

2.8. GFPtpz fluorescence

The transfection efficiency values for luciferase reporter-gene assay was corrected to cotransfected pGFPtpz-CMV® vector. GFPtpz (GFP topz) contains 4 point mutations which shift emission spectrum from 504 nm to 527 nm (green to yellow) (Tsien 1998).

50µl of cell extract from each sample were used to measure the GFP fluorescence in a 96-well microplate using a fluorometer (Fusion). Excitation wavelength was at 485 nm and the emission wavelength was measured at 530 nm. The data were analyzed by the software supplied with the device (Fusion InstrumentControl Application version 3.50, Canberra-Packard).

2.9. Statistics

The raw data were analyzed by one-way analysis of variance (ANOVA), Student's *t*-test, and χ^2 test using the software SPSS V.17. The P value was set at $p \leq 0.05$.

3. Results

3.1. Regulation of DLK

3.1.a. Potential phosphorylation sites in DLK

According to a report (Leung and Lassam 2001) for MLK-3 (mixed Lineage Kinase-3), MLK family members have two putative autophosphorylation sites. The corresponding autophosphorylation sites for DLK are Serin-298 and Serin-302 residues. The mutant constructs of DLK coding sequence have been generated using a point mutation strategy for Serin-298 and Serin-302 residues (Fig. 3.1.A).

To investigate the expression level of the mutant constructs, HIT-T15 cells were transiently transfected with the constructs using Metafectene (chapter 2.6.b). The expression vector for DLKwt (wild-type) was used as positive control and the pBluescript vector was used as negative control.

48 hrs after transfection, the cells were harvested and the protein lysates were subjected to SDS-PAGE (sodium dodecyl sulfate - polyacrylamide gel electrophoresis) and immunoblotting. An antibody against the C-terminal of DLK protein was used to detect the expression of the protein (Fig. 3.1.B). An equally expression level of DLKwt and mutant proteins was observed, suggesting that the mutations had no effect on the expression of the proteins.

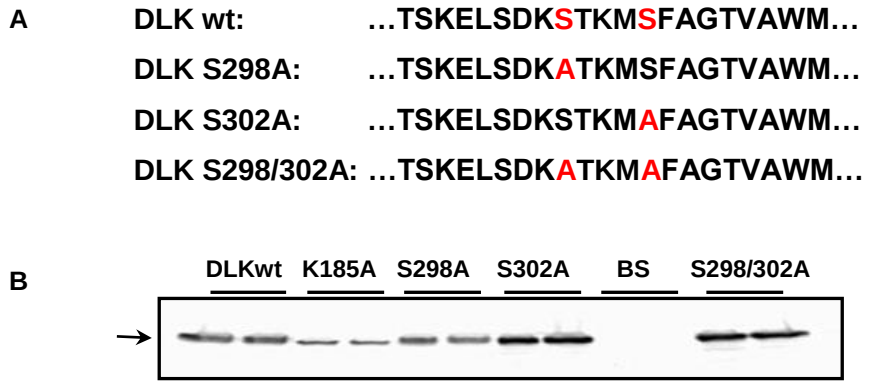

Figure 3. 1 Overexpression of DLK and its mutants in HIT-T15 cells. A. using the point mutation method, Serin-298 and Serin-302 residues of DLK were replaced by Alanine. **B.** HIT cells were transiently transfected with 2 µg of the expression vectors. DLK was detected using an anti-DLK antibody which detects the C-terminus of DLK peptide (Holzman *et al*,. 1994). The blot presents an equally expression level for DLKwt and the mutants. The migration on the gel is slightly affected by the mutation in K185 and S302 residues.
BS: pBluescript vector.

3.1.b. DLK and the regulation of gene transcription

3.1.b.I. DLK and CRE-directed gene transcription

DLK inhibits CRE (cAMP response element) -directed gene transcription in HIT-T15 cells, whereas its kinase dead mutant (K185A) does not (Oetjen, Lechleiter et al. 2006). To investigate the effect of the mutation of DLK in Serin-298 and Serin-302 residues on CRE-directed gene transcription, 0.6 µg of DLKwt and its mutant constructs were cotransfected with 2 µg of p4xSomCRELuc plasmid, using DEAE-Dextran method into HIT-T15 cells. The cells were treated with KCl (40 mmol/L) 6 hrs before harvesting. The cell lysates were extracted and the luciferase activity was measured (chapters 2.6.d and 2.7). DLKwt and DLK S298A mutant decreased CRE-dependent gene transcription stimulated by KCl. DLK K185A, S302A, and S298/302A mutants had no effect on CRE-dependent gene transcription.

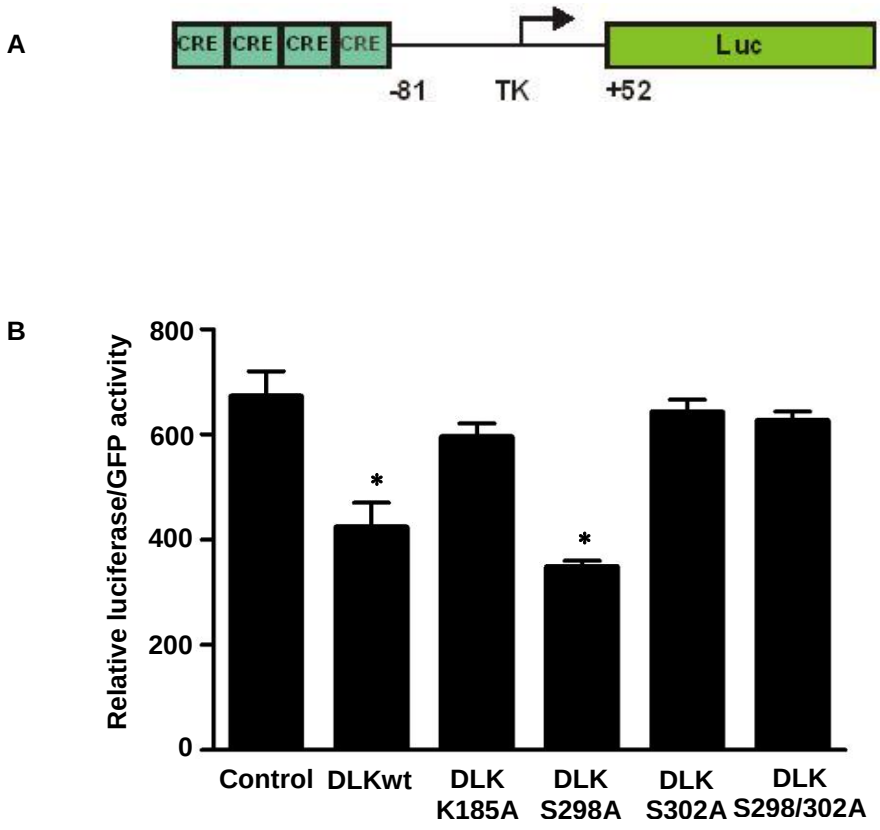

Figure 3. 2 Regulation of CRE-directed gene transcription by DLK. A. Schematic figure of CRE-luciferase construct. **B.** The luciferase activity is relative to the stimulated control cells with no DLK transfection. Values are mean ± SEM of three independent experiments, each done in duplicate. ∗p≤0.05 vs control.

3.1.b.II. DLK and CBP-dependent gene transcription

DLK inhibits the membrane-depolarization induced transcriptional activity of the β-cell protective factor CREB (cAMP response element binding transcription factor) and its coactivator CBP (CREB binding protein) in HIT-T15 cells, whereas DLK kinase dead mutant does not (Oetjen, Lechleiter et al. 2006). To examine the role of phosphorylation sites of DLK in its inhibitory effect on CBP-dependent gene transcription in HIT-T15 cells, 0.6 µg of DLK and its mutants were cotransfected along with 2 µg of 5xGal4E1BLuc plasmid, 2 µg of Gal4-CBP plasmid and 0.75 µg of GFPtpz as internal control for transfection efficiency using DEAE-Dextran. The cell lysates were extracted and the luciferase activity was measured (chapters 2.6.d and 2.7). DLKwt and DLK S298A mutant decreased CBP-dependent transcription, whereas DLK K185A, S302A, and S298/302A mutant had no effect.

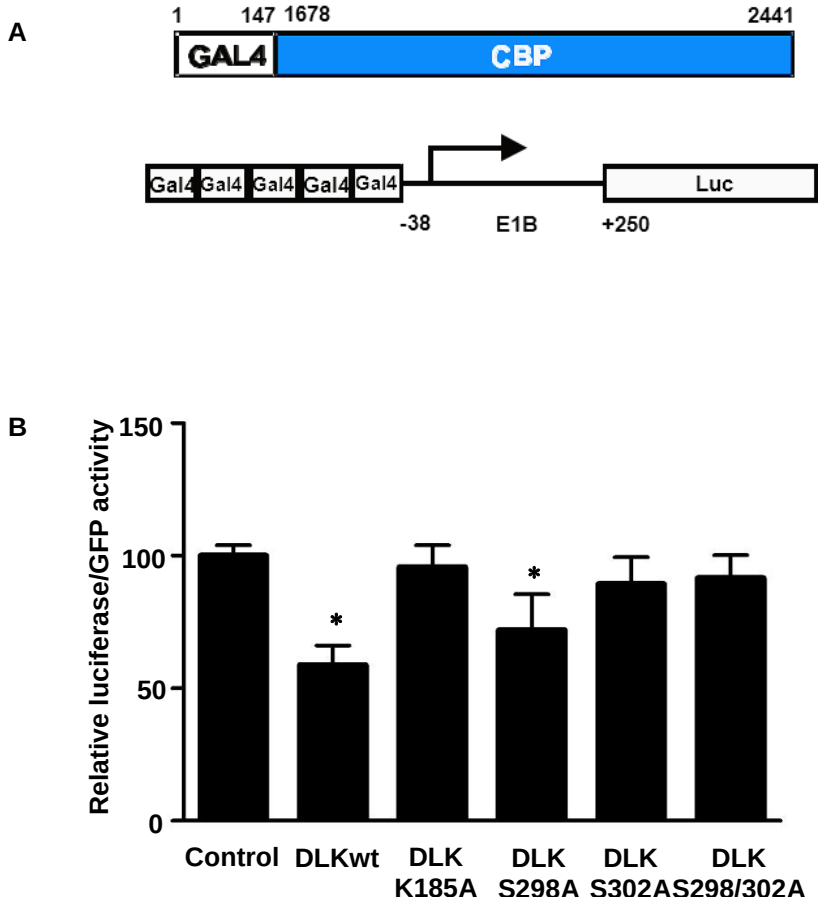

Figure 3. 3 Regulation of CBP-dependent gene transcription by DLK. A. Schematic figure of GAL4-CBP and 5xGal4E1BLuc constructs. **B.** Luciferase activity is corrected to GFP values in each experiment and is relative to control with no DLK transfection. Values are mean ± SEM of three independent experiments, each done in duplicate. ∗p≤0.05 vs control.

3.1.c. Phosphorylation of JNK by DLK

The stress activated protein kinase JNK is activated by different stress signals like pro-inflammatory cytokine TNFα. Like other members of MLK family DLK phosphorylates and activates JNK (chapter 1.3). In this study the role of putative phosphorylation sites of DLK in the phosphorylation of JNK was investigated. HIT cells were transiently transfected with DLKwt and mutant vectors. The antibiotic Anisomycin was used as positive control which phosphorylates JNK. Forty eight hours after transfection the cell lysates were extracted and subjected to SDS-PAGE. The phosphorylation level of JNK was measured with an antibody against phosphorylated JNK. DLKwt increased the phosphorylation of JNK. Mutation in K185 and S302 residues diminished the phosphorylation of JNK by DLK. Mutation in S298 residue had no effect on the activation of JNK by DLK.

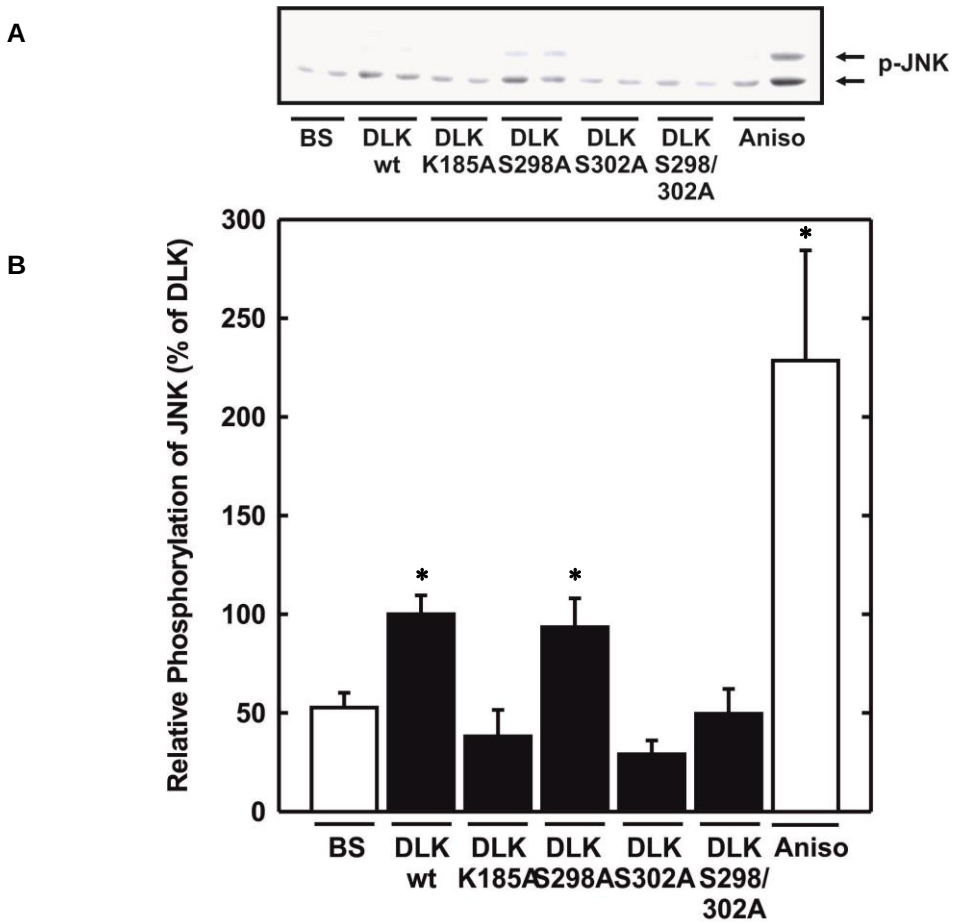

Figure 3. 4 Phosphorylation of JNK by DLK. A. A typical immunoblot picture detected by an antibody against phosphorylated JNK. HIT cells were transiently transfected with DLKwt and mutant vectors. The cells were harvested 48 hrs after transfection and the proteins were subjected to SDS_PAGE. BS: pBluescript, Aniso: Anisomycin. **B.** The optical density of p-JNK is corrected to the optical density of GAPDH for each experiment and is relative to DLKwt. Anisomycin as a potential activator of JNK caused high level of JNK phosphorylation. Values are mean ± SEM of three independent experiments, each done in duplicate. *p≤0.05, one way ANOVA.

3.1.d. Phosphorylation specific anti-DLK antibody

A phosphorylation specific antibody was produced which detects the phosphorylation of DLK at Serin-302 residue. HIT-cells were transiently transfected with expression vectors (chapter. 2.6.b). Forty eight hours after transfection the cell lysates were extracted and subjected to SDS-PAGE. The phosphorylation of DLK at Serin-302 residue was detected by the phosphorylation specific antibody. DLK K185A is unable to bind to ATP. This expression vector was used as a negative control for autophosphorylation of DLK. The expression vectors carrying the K185A and S302A mutations showed no phosphorylation.

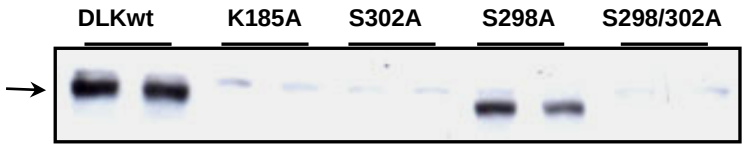

Figure 3. 5 Phosphorylation of DLK at Serin-302 residue. The cells were transfected with each expression vectors. 48 hrs after transfection the cell lysates were subjected to SDS-PAGE. The phosphorylation of DLK was detected using the antibody which recognizes the phosphorylated Serin-302 residue specifically. The phosphorylation was detected for DLKwt and the S298A mutant.

3.1.e. Regulation of DLK by proinflammatory cytokines

A variety of cytokines is involved in the pathogenesis of type 2 diabetes. TNFα and IL-1β play a role in inducing β-cell apoptosis in type 2 diabetes (Maedler, Fontana et al. 2002; Donath, Storling et al. 2003). To examine the role of proinflammatory cytokines TNFα and IL-1β in phosphorylation and subsequently activation of DLK, HIT-T15 cells were treated with TNFα (30 ng/ml) and IL-1β (10 ng/ml) for 60 min. The effect of forskolin (10µM, 30 min before harvesting), as an activator of adenylate cyclase, on the phosphorylation of DLK was also tested. The immunosuppressive drug cyclosporine A (5µM, 30 min before harvesting) was used as a positive control for DLK phosphorylation (Oetjen, Lechleiter et al. 2006; Plaumann, Blume et al. 2008). After harvesting, the total protein amount was measured by Bradford assay and 150 µg proteins were subjected to SDS-PAGE and immunoblotting. The expression level and the phosphorylation of DLK were detected with antibody against DLK and phospho-DLK, respectively. The optical density of the corresponding bands was measured and used for statistical analysis. No differences were observed in protein level of DLK in any experiments (Fig. 3.6). The amount of phosphorylated DLK at Serin-302 was increased by CsA, TNFα, and forskolin (Fig. 3.7).

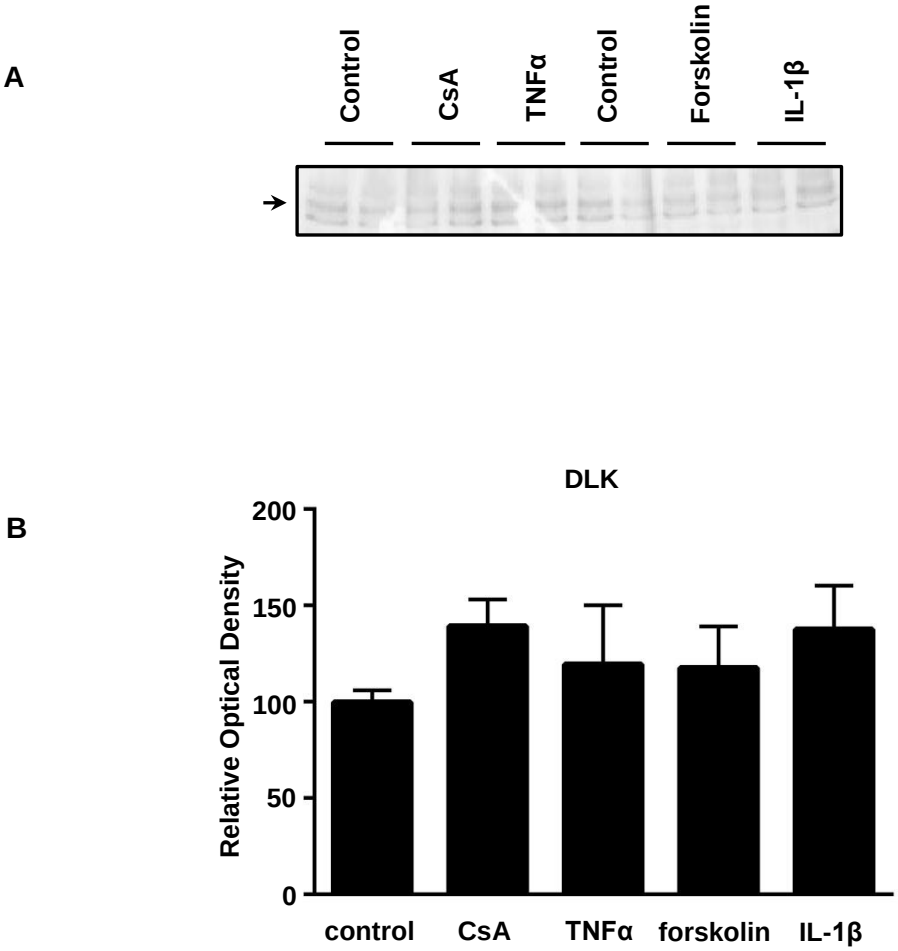

Figure 3. 6 Proinflammatory cytokines and the expression of DLK. A. A typical immunoblot picture detected by an anti-DLK C-terminus antibody. The arrow shows the corresponding band for DLK. **B.** The optical density of DLK is corrected to the optical density of GAPDH for each experiment and is relative to control. Values are mean ± SEM of three independent experiments, each done in duplicate.

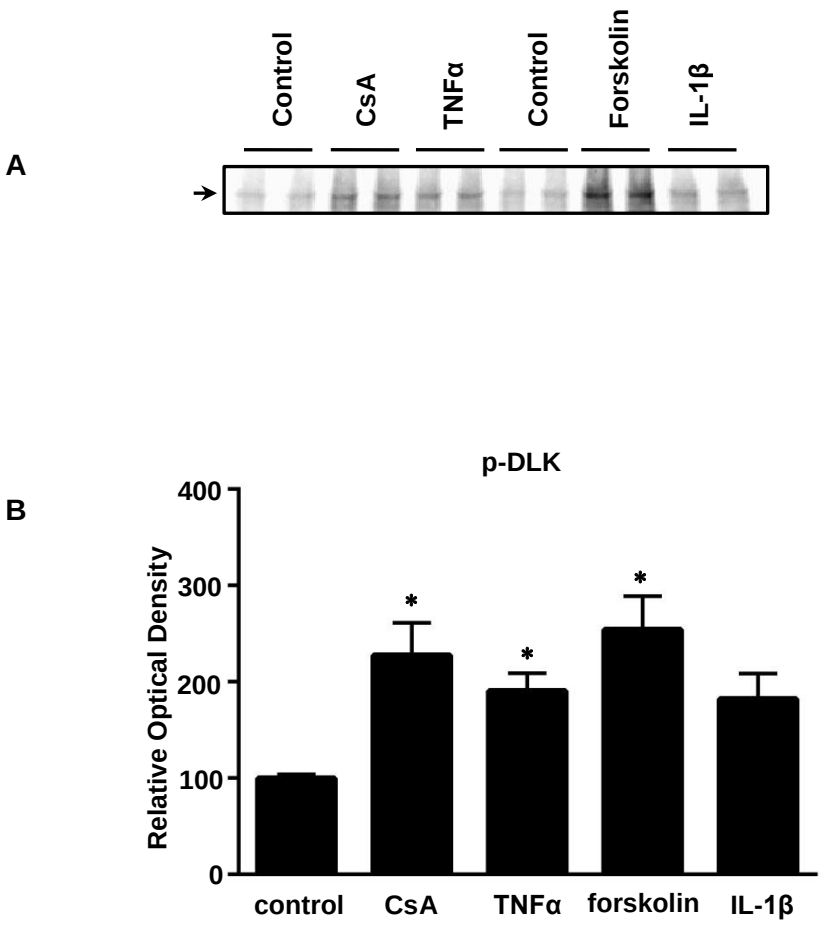

Figure 3. 7 Phosphorylation of DLK. A. A typical immunoblot picture detected by an antibody against phosphorylated DLK at Serin-302 residue. The arrow shows the corresponding bands for phosphorylated DLK. **B.** The optical density of phosphorylated DLK is corrected to the optical density of GAPDH for each experiment and is relative to control. Values are mean ± SEM of three independent experiments, each done in duplicate. ∗p≤0.05, One-way ANOVA.

3.1.f. Interaction of DLK with importins

Karyopherins are responsible for transportation of protein molecules between cytoplasm and nucleoplasm as import and export which occurs through nuclear pore. Importin is a member of karyopherins which transport protein molecule from cytoplasm into the nucleus by binding to a specific recognition sequence in the protein molecules, called nuclear localization signal (NLS). Previous work of our group introduced two putative NLS in DLK whose mutation prevents DLK nuclear localization driven by pro-inflammatory cytokines (Fig. 3.8.A).

To investigate whether DLK interacts with karyopherins, required for nuclear translocation, a protein-protein interaction assay was performed. The putative interaction between DLK-NLS and three different members of importin (importin α, importin β, and transportin) was examined. DLK protein was purified and immobilized on amylose resin (chapter 2.5.e.III). The interaction was performed with purified importins (chapter 2.5.f), and the resin carrying DLK interacted with importin was subjected to SDS-PAGE and immunoblotting. Since the importins were His-tagged purified proteins, the interaction efficiency was detected using an anti-His antibody. Ponceau staining was used to detect the equal amount of immobilized DLK proteins. DLKwt interacts with importin α, but neither with importin β nor with transportin. DLK NLS1 mutant showed a faint interaction with importin α. No interaction is observed between DLK-NLS2 and none of the importins (Fig. 3.8 C). DLK-PP interacts with importin α (Fig. 3.8 D).

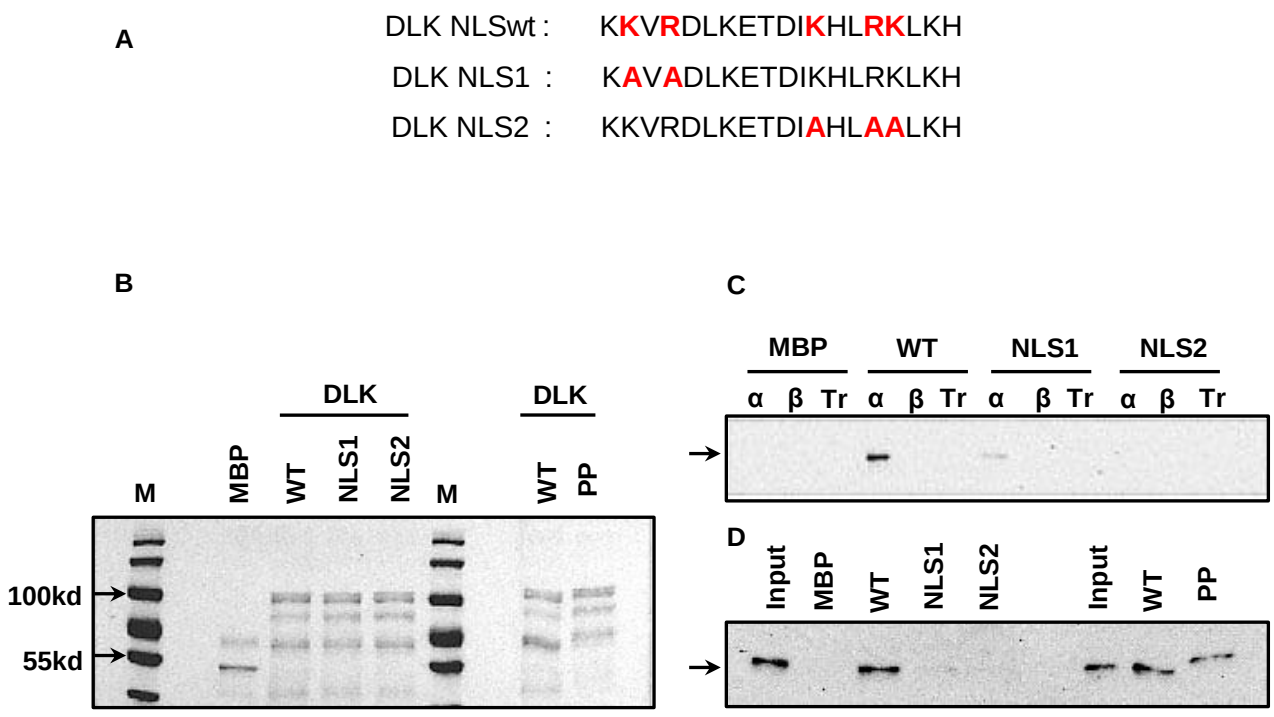

Figure 3. 8 Interaction of DLK with three members of importins. A. The amino acid sequence of DLK NLS. The key residues constructing the bipartite NLS, and the relative mutations are shown in red. **B.** Equal amount of immobilized proteins was detected by ponceau staining. The band corresponded to MBP was detected at 50 kDa and the bands of MBP-fused DLK proteins are at 92 kDa. The M letter labels the molecular weight ruler. **C.** The interaction between MBP-fused DLK proteins and three different importins was detected using an anti-His antibody. MBP was used as negative control. **D.** The interaction between MBP-fused DLK proteins and importin α was detected by anti-His antibody. 5% of total amount of importin α used for interaction (0.1 µg), was loaded as input. PP refers to DLK-PP mutant which has two point mutations in leucine zipper sequence. WT: DLKwt, NLS1: DLK NLS1, NLS2: DLK NLS2, MBP: maltose binding protein, α: importin α, β: importin β, Tr: transportin.

3.1.g. Nuclear localization of DLK wild-type and DLK-PP mutant

Two point mutations in leucine zipper part of DLK-PP (leucine-437 and leucine-463 were replaced by proline) make it unable to homodimerize. The aim of this experiment was to investigate the effect of homodimerization of DLK on its nuclear localization. HIT cells were transiently transfected with DLKwt or DLK-PP mutant, which contain a FLAG-epitope, using metafectene method (chapter 2.6.b). The cells were treated with TNFα (10 ng/ml) for 60 min. The cells were prepared for immunostaining and stained with DAPI and anti-flag antibody (chapter 2.6.e). Microscopy was performed by Zeiss Axiovert Apo Tome microscope (Fig. 3.9). TNFα treatment led to increase in nuclear localization of DLKwt. Nuclear localization of DLK-PP was increased by TNFα compared to control, but was significantly less than DLKwt treated by TNFα.

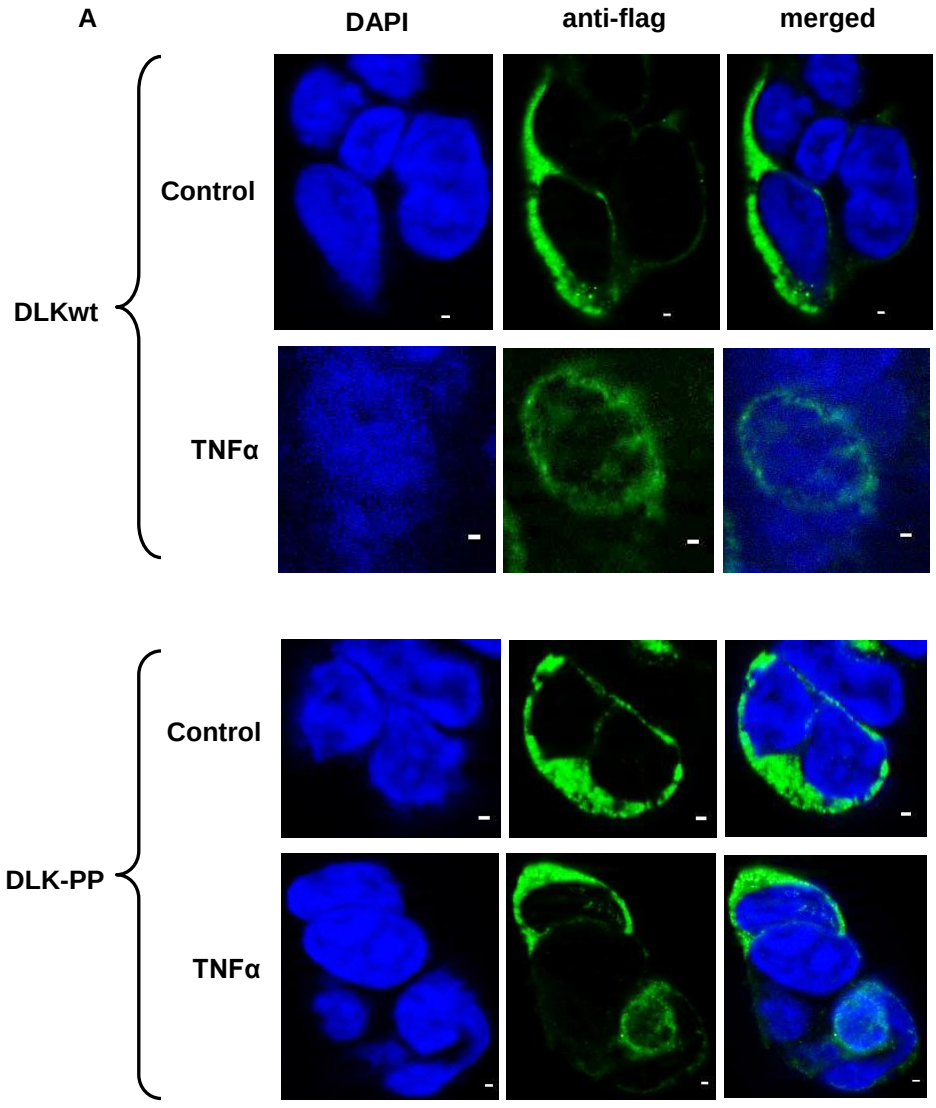

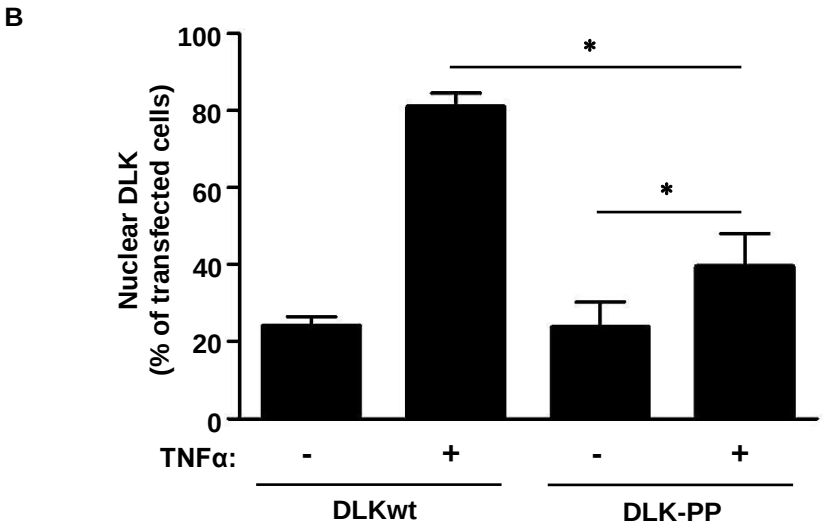

Figure 3. 9 Subcellular localization of DLKwt and DLK-PP mutant. A. Typical pictures of subcellular DLK. The blue color represents the nucleus stained by DAPI and the green color depicts DLK recognized by anti-flag antibody. The scale bar represents 1µm. **B.** HIT-cells were transfected with expression vectors and incubated for 47 hrs. The cells were treated with TNFα (10 ng/ml) for one hour. The control was kept nontreated. The values show the percentage of nuclear localized DLK divided to total transfected cells from three independent experiments. ∗p≤0.05, Pearson χ^2 test.

3.2 Effects of DLK on cell apoptosis

3.2.a. Activation of caspase-3 by proinflammatory cytokines in HIT cells

It has been reported before that TNFα, alone or in combination with IL-1β and IFNγ , induces β-cell apoptosis (Ishizuka, Yagui et al. 1999; Bonny, Oberson et al. 2000; Haefliger, Tawadros et al. 2003; Jambal, Masterson et al. 2003). Overexpression of DLK results in cell apoptosis (Plaumann, Blume et al. 2008). To investigate whether DLK mediates the apoptosis induced by proinflammatory cytokines in β-cells the cleavage of caspase-3 was studied by immunoblot analysis. 24 hrs after seeding the cells were treated with TNFα (1000U/ml), IL-1β (10U/ml), IFNγ (100U/ml), the combination of IL-1β and IFNγ, and the combination of TNFα and IFNγ, for the next 24 hrs. The cells were harvested and the total amount of protein was determined by Bradford assay. 100 µg of protein was subjected to SDS-PAGE and immunoblotting. The cleavage of caspase-3 was detected using an antibody against caspase-3 which detects the large fragment (17/19 kDa) of activated caspase-3 resulting from cleavage adjacent to Asp175. Treatment with TNFα alone and in combination with IFNγ increased the cleavage of caspase 3.

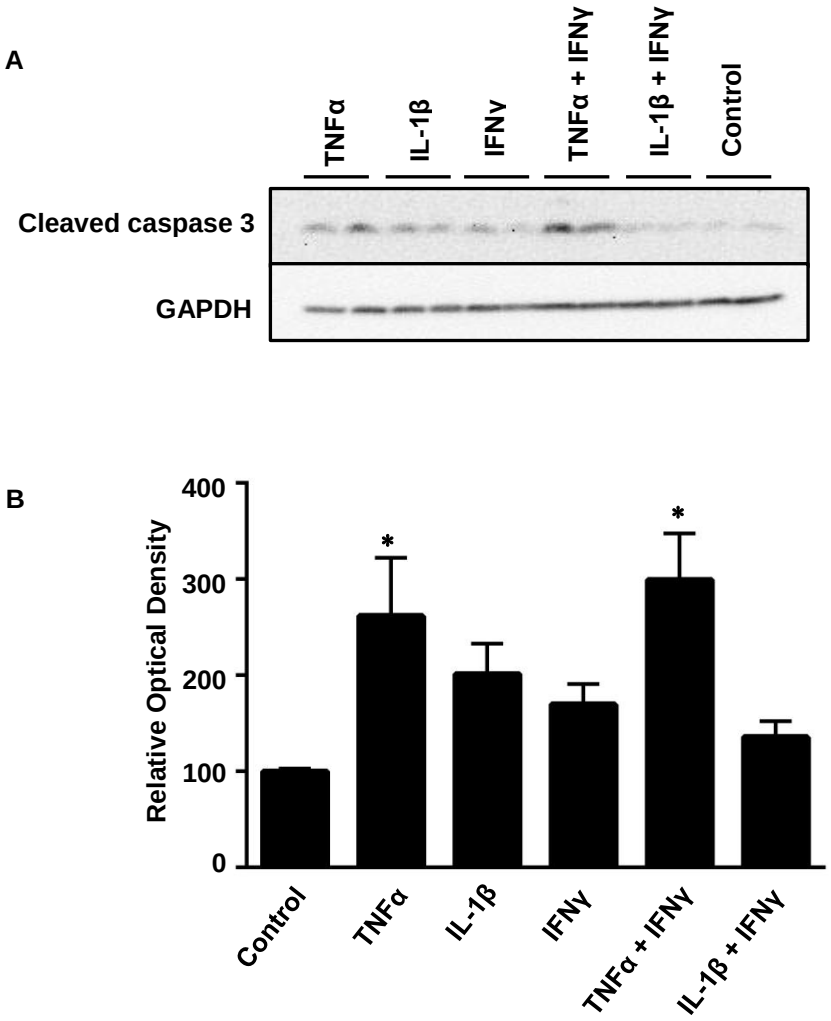

Figure 3. 10 The activation of caspase-3 by proinflammatory cytokines. A. A typical immunoblot picture detected by an antibody against activated caspase-3 which has been cleaved adjacent to Asp 175 residue. **B.** The optical density is corrected to GAPDH for each experiment and is relative to control. Values are mean ± SEM of three independent experiments, each done in duplicate. ∗p≤0.05, One-way ANOVA.

3.2.b. Intermediary role of DLK in the activation of capase 3 by proinflammatory cytokines

To study whether DLK is involved in β-cell apoptosis induced by proinflammatory cytokines, endogenous DLK was downregulated by small interfering RNA (chapter 2.6.c). 24hrs later, the cells were treated with TNFα (1000 U/ml) and TNFα in combination with IFNγ (100 U/ml), for the next 24 hrs. The cells were harvested and the total amount of protein was measured by Bradford assay. 80 µg of protein was subjected to SDS-PAGE and immunoblotting. No efficient down regulation of DLK is observed in HIT cells by DLK-specific siRNA (Fig. 3.11 B). TNFα increased the amount of cleaved caspase 3 in both nonspecific and DLK-specific siRNA transfected cells (Fig. 3.11 C).

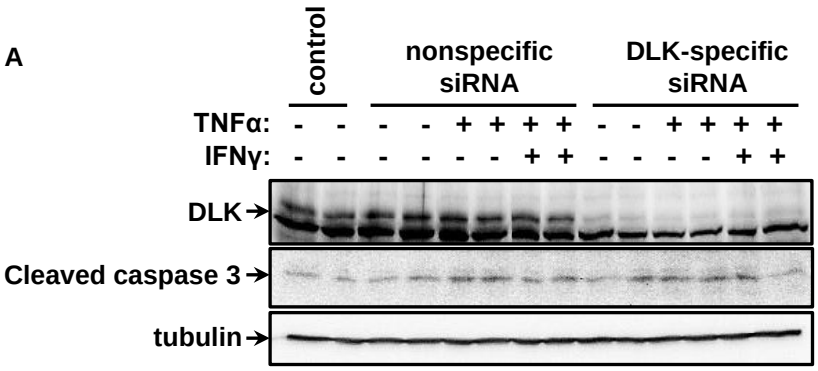
A
control
nonspecific siRNA
DLK-specific siRNA
TNFα: - - - - + + + + - - + + + +
IFNγ: - - - - - - + + - - - - + +
DLK
Cleaved caspase 3
tubulin

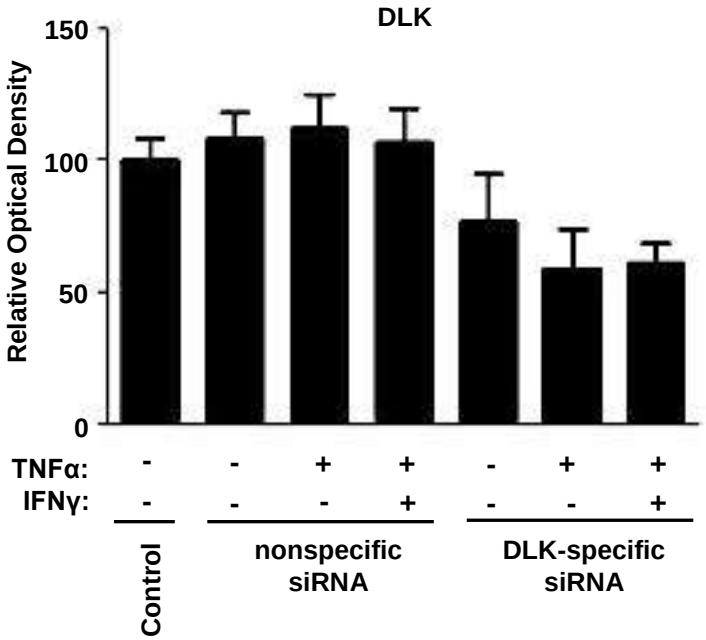
B
DLK
Relative Optical Density
150
100
50
0
TNFα: - - + + - + +
IFNγ: - - - + - - +
Control
nonspecific siRNA
DLK-specific siRNA

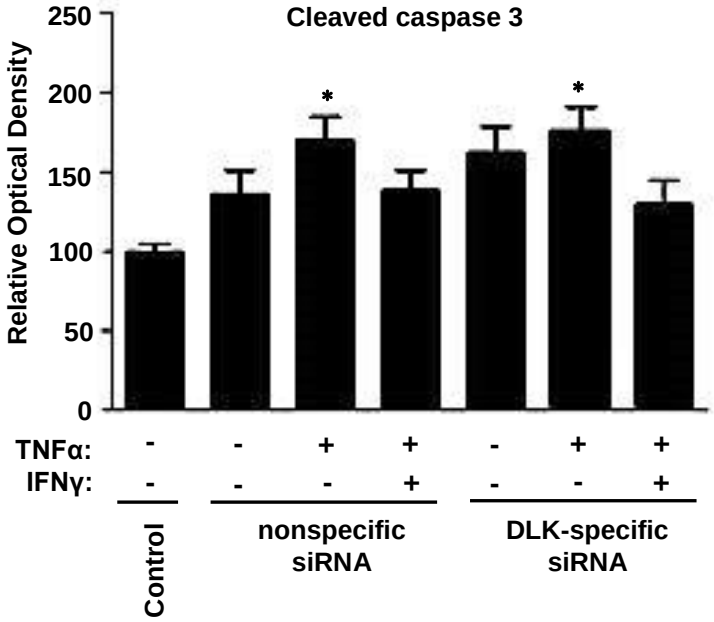
C
Cleaved caspase 3
Relative Optical Density
250
200
150
100
50
0
*
*
TNFα: - - + + - + +
IFNγ: - - - + - - +
Control
nonspecific siRNA
DLK-specific siRNA

Figure 3. 11 Role of DLK in β-cell apoptosis induced by proinflammatory cytokines. A. Typical immunoblot membrane detected by anti-DLK C-terminus, anti-cleaved caspase-3, and anti-tubulin antibodies. **B.** Downregulation of DLK by anti-DLK siRNA. Values are mean ± SEM of four independent experiments, each done in duplicate. **C.** Cleavage of caspase 3. The optical density is corrected to α-tubulin for each experiment and is relative to control. Values are mean ± SEM of four independent experiments, each done in duplicate. ∗p≤0.05, One-way ANOVA.

3.3 Animal experimentation; role of DLK in diet-induced diabetes

The role of DLK in diet-induced diabetes was investigated in C57BL/6J DLK-heterozygote mice and their wild-type littermates. The mice were divided into 3 groups of feeding, normal diet (ND), carbohydrate rich diet (CRD), and high fat diet (HFD). HFD contains 30% fat. The feeding was started at the age of 8 weeks and continued for 16 weeks. The mice were weighted at the beginning of experiment and also every other week until the end of the experiments. The blood glucose was measured at the beginning of the experiment (day 0) and every four weeks until the end of experiments. The plasma level of glycated hemoglobin (HbA1c) was measured at the end of experiment. No significant increase was observed in the body weight of different genotype and different diet (Fig. 3.12 A). No significant increase in blood glucose was observed in different genotypes and different diet (Fig. 3.12 B). Plasma level of HbA1c was increased in heterozygote mice under HFD compared to ND at the end of experiment (Fig. 3.12 D). No difference was observed in HbA1c between wild-type and heterozygote mice under HFD (Fig. 3.12 E).

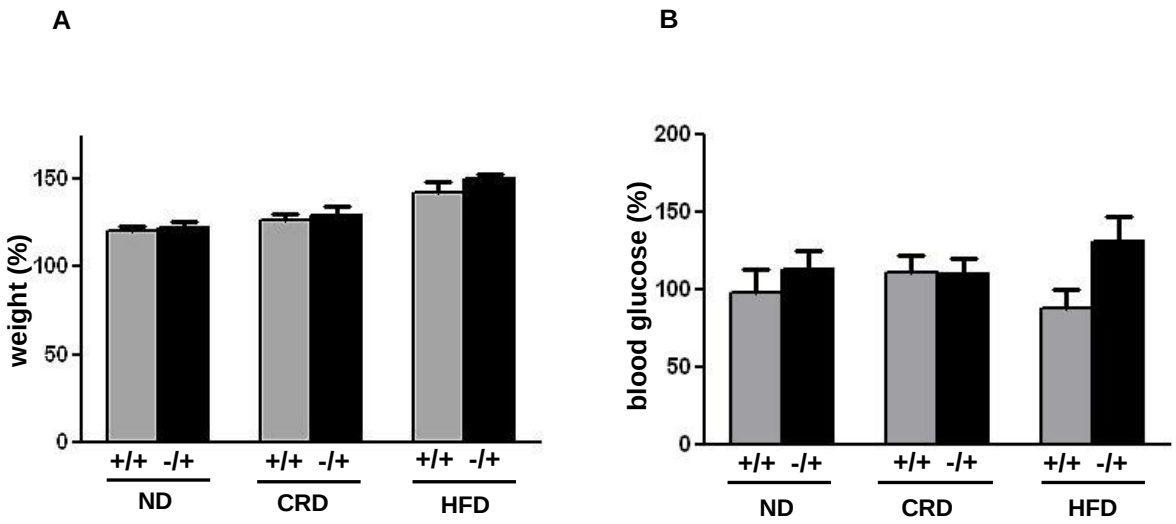

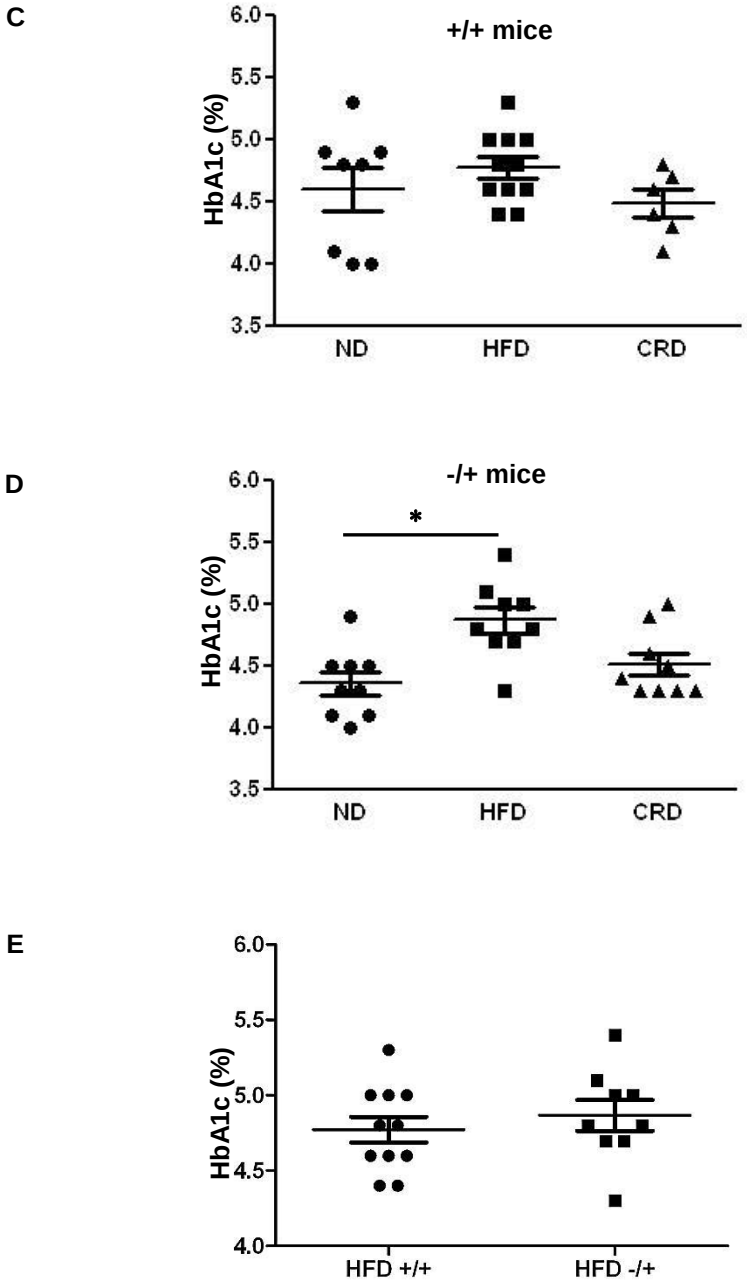

Figure 3. 12 Role of DLK in diet-induced diabetes. A. wild-type (+/+) and heterozygote (-/+) mice (10 per each group) were fed with different diets for 16 weeks. Values represent the increase of weight after 16 weeks of diet and are relative to the weight of each mouse at the beginning of diet. p≤0.05, student t-test. **B.** The values are mean ± SEM of blood glucose at week 16 relative to blood glucose of each mouse at the beginning of the experiment. p≤0.05, student t-test. **C.** The plasma level of HbA1c (glycated hemoglobin) was measured at the end of experiment. No significant difference in plasma level of HbA1c was detected in wild-type mice with different diet at the end of experiment. p≤0.05, student t-test. **D.** Plasma level of HbA1c was increased in heterozygote mice under HFD compared to ND at the end of experiment. ∗p≤0.05, student t-test. **E.** No difference was observed in HbA1c between wild-type and heterozygote mice under HFD. p≤0.05, student t-test.

3.4 Generation of a targeting knock-out vector for DLK

3.4.a. Sequencing of genomic DLK in 129Sv mouse strain

129Sv-derived embryonic stem (ES) cell lines are considered to be more reliable in colonizing than ES cells derived from other strains. 32 pairs of PCR primers were designed to amplify the full length sequence of DLK from a genomic DNA extracted from 129Sv strain. The primers were designed in a way that each amplified fragment overlaps at least 50 bp of the downstream fragment. The sequencing was performed according to chain-termination method (chapter 2.4.j). The resulted sequence was compared to the sequence of C57BL/6J strain which is available electronically in Ensembl Genome Browser. No mismatches were observed in DLK sequences between C57BL/6J and 129Sv strains.

Figure 3. 13 A typical picture of DLK sequence, comparing between 129Sv and C57BL/6J strains. The upper sequence labeled DLK.txt is referring to DLK in C57BL/6J strain. 21f_F01 is a part of the sequence of the fragment 21, and 22r_H01 is a part of the sequence of fragment 22 amplified from 129Sv strain. The overlapping nucleotides between two fragments guarantied the continues sequencing of all amplified fragments.

3.4.b. Digestion pattern of bMQ317c09

Bacterial artificial chromosome (BAC) is widely used for sequencing the genome in genome projects, as well as generating the genetically modified animal models. The benefits of these plasmids are that they are able to carry an insert of 150-350 kb nucleotide, and to distribute evenly after bacterial cell division. The BAC plasmid bMQ317c09 containing the genomic sequence of DLK from 129Sv mouse strain was used to generate the targeting knock-out vector for DLK. Before retrieving the DNA from BAC plasmid into the targeting vector the BAC DNA was digested with NotI restriction enzyme and the digestion pattern was compared to the prepared map. Three different fragments are expected from digestion after running the agarose gel using a pulsed-field system

(80.2 kb, 71.77 kb, and 8.73 kb) (Fig. 3.14 A and B). The expected fragments after digestion are shown by the arrows (Fig. 3.14 B).

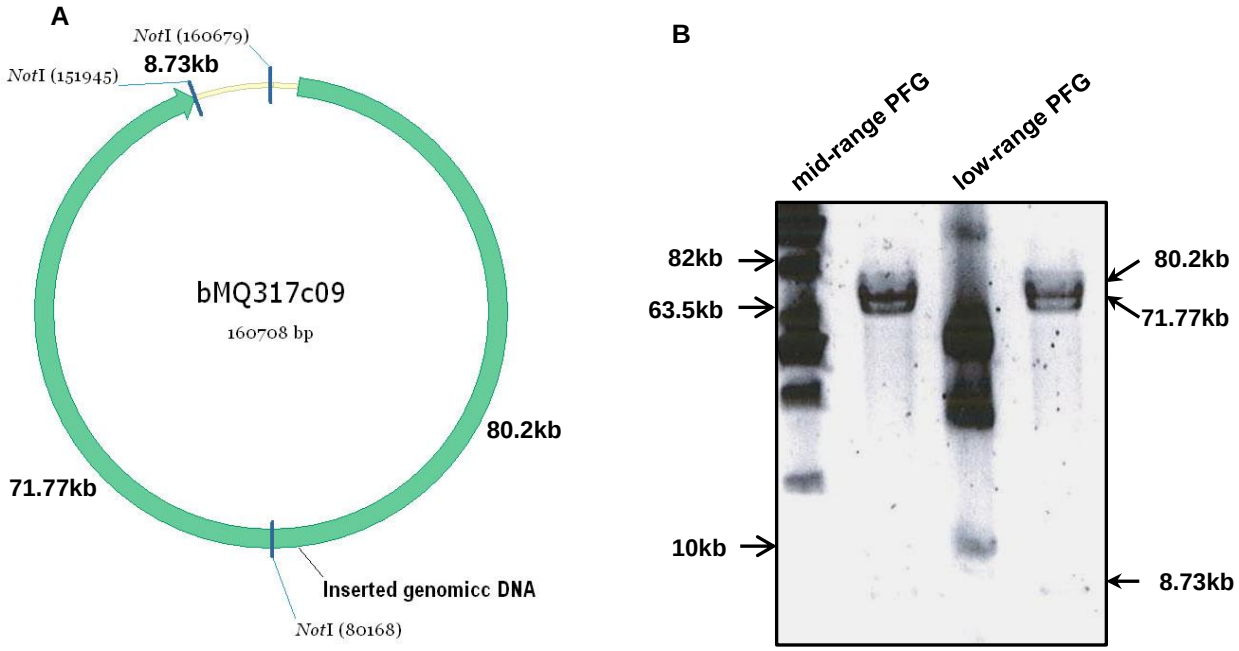

Figure 3. 14 Digestion pattern and map of bMQ317c09 plasmid. A. The map of bMQ317c09 and the restriction digestion sites of NotI and the corresponding fragments' size. **B.** Typical picture of a TBE gel used to run the digested DNA on a pulsed-field system. The arrows on the right show the expected fragments after digestion. The mid-range and low-range pulsed-field gel (PFG) markers were used to mark the digested fragments.

3.4.c. Generation of homology arms and the retrieval plasmid

To retrieve the sequence of interest from BAC plasmid into the targeting vector two homology arms was generated up- and downstream of the sequence of interest, by PCR amplification using two pairs of primers. The first homology arm is located in the sequences between 63627130-63627580bp and the second one is between 63616689-63617174bp on chromosome 15 of C57BL/6J mouse strain. The homology arms were amplified by PCR reaction, digested with restriction enzymes (NotI, HindIII, and SpeI), purified and inserted into the PL253 plasmid which had been linearized by NotI and SpeI. Nine out of ten colonies contained the retrieval plasmid (Fig. 3.15).

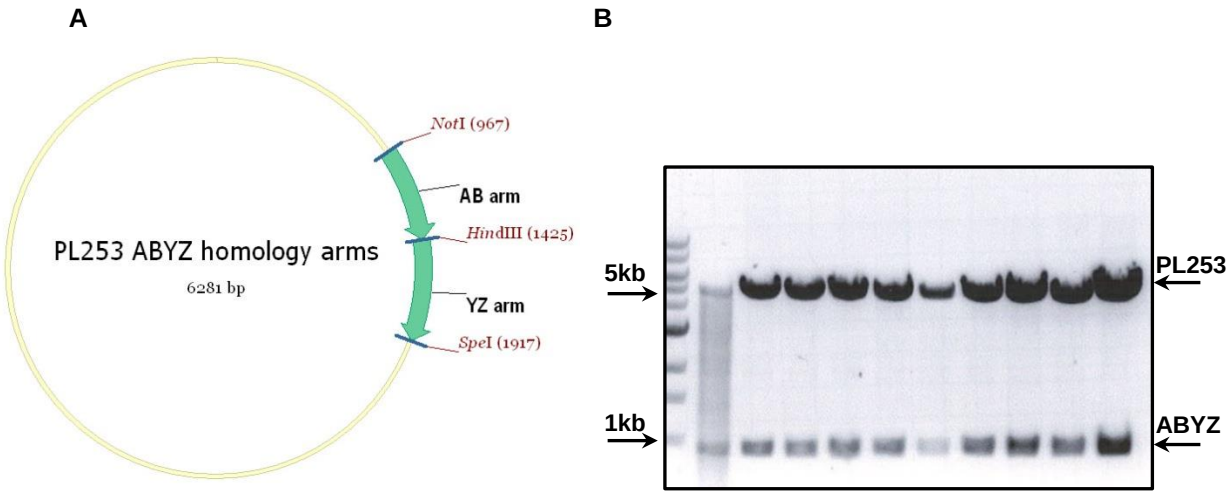

Figure 3. 15 Retrieval plasmid contains homology arms. A. The map of retrieval plasmid with the homology arms inserted. **B.** Digestion pattern of the retrieval plasmid after digestion with NotI and SpeI restriction enzymes. 10 positive colonies were picked and the DNA was extracted. The colonies carrying the retrieval plasmid were defined by digestion with NotI and SpeI.

3.4.d. Retrieval of DNA from BAC

SW102 cells were transformed with the BAC DNA. The positive colonies containing a chloramphenicol resistance made by BAC plasmid were selected on a chloramphenicol agar plate. DNA was extracted and digested with NotI restriction enzyme to prove the accuracy of the plasmid. The digestion pattern was compared to the pattern described in section 3.4.a.

The positive bacteria were induced for Red recombination function (chapter 2.4.k.II.2). The retrieval plasmid from the previous step was linearized with HindIII and gel purified. The induced bacteria were transformed with linearized plasmid and the positive recombinant cells were selected on an Amp^+ agar plate. The DNA was extracted and digested with EcoRI and compared to the prepared map. One colony showed successful recombination, thereby retrieval of DNA from BAC plasmid into the targeting vector (Fig. 3.16).

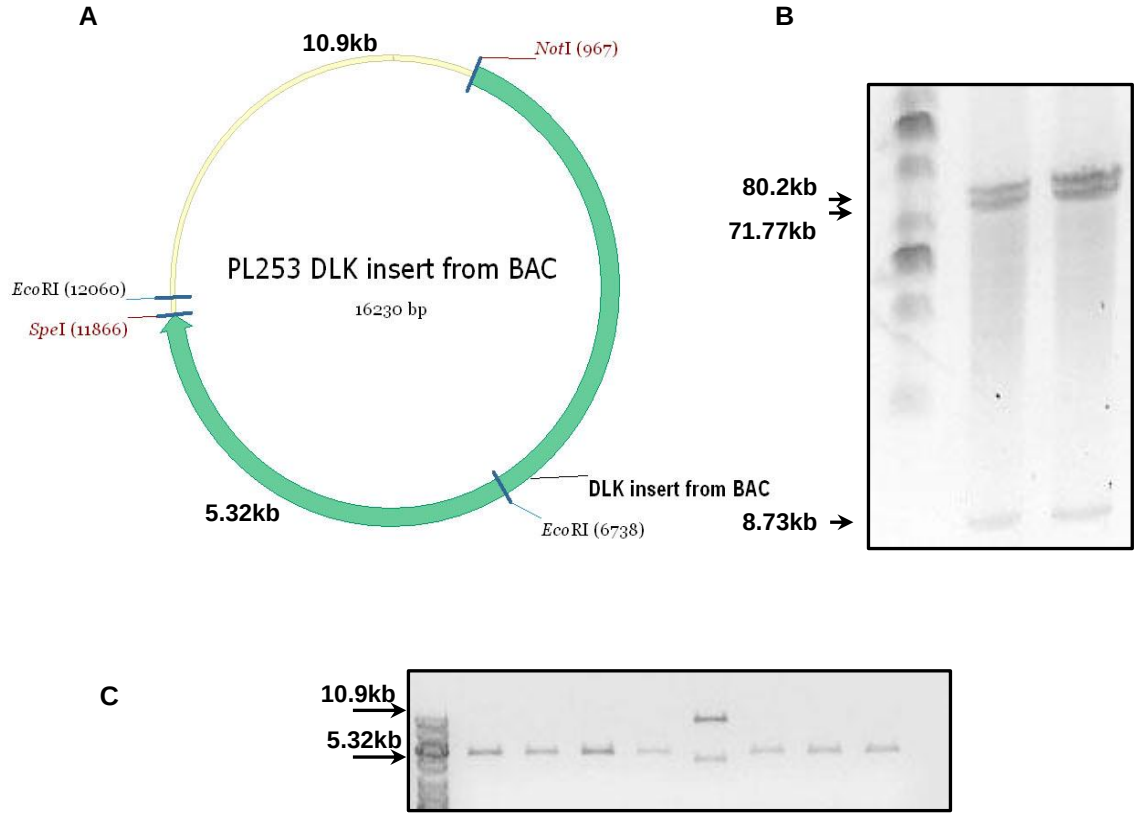

Figure 3. 16 Retrieving of DNA from BAC plasmid. A. The map of targeting vector after DNA retrieved from BAC plasmid. The restriction digestion sites for EcoRI and the resulted fragments are depicted. **B.** The DNA extracted from SW102 transformed with BAC plasmid was digested with NotI and run on a TBE gel using a pulsed-field system. The pattern is the same as the digestion pattern of the BAC plasmid before transformation. **C.** The DNA extracted after homologous recombination retrieval of DNA from BAC plasmid into targeting vector was restriction digested with EcoRI and the positive recombinant colony was selected according to the map.

3.4.e. Generation of mini-targeting vectors

To introduce the loxP sites in the targeting vector two pairs of PCR primers were designed to amplify two homology arms up- and downstream to the point of loxP insertion point. The homology arms were amplified using a PCR reaction and the bMQ317c09 DNA as template. The homology arms CD and EF are located on chromosome 15 of C57BL/6J mouse strain between 63622426-63622204bp and 63622632-63622427bp, respectively. The homology arms GH and IJ are located on chromosome 15 of C57BL/6J mouse strain between 63620524-63620317bp and 63620718-63620525bp, respectively. To generate the first mini-targeting vector the neo cassette flanked by loxP was cut out of the PL452 plasmid and ligated along with the CD and EF homology arms into the pBluescript^{+} vector (Fig. 3.17 A). The homology

arms GH and IJ were ligated along with the neo cassette plus loxP flanked by FRT, which had been cut out of the PL451 plasmid, into pBluescript plasmid (Fig. 3.17 B). Four out of five colonies were positive with generated mini-targeting vector. The successful ligated fragments were cut out of the plasmid and purified for the homologous recombination insertion of loxP site into the targeting vector. (Fig. 3.17 C).

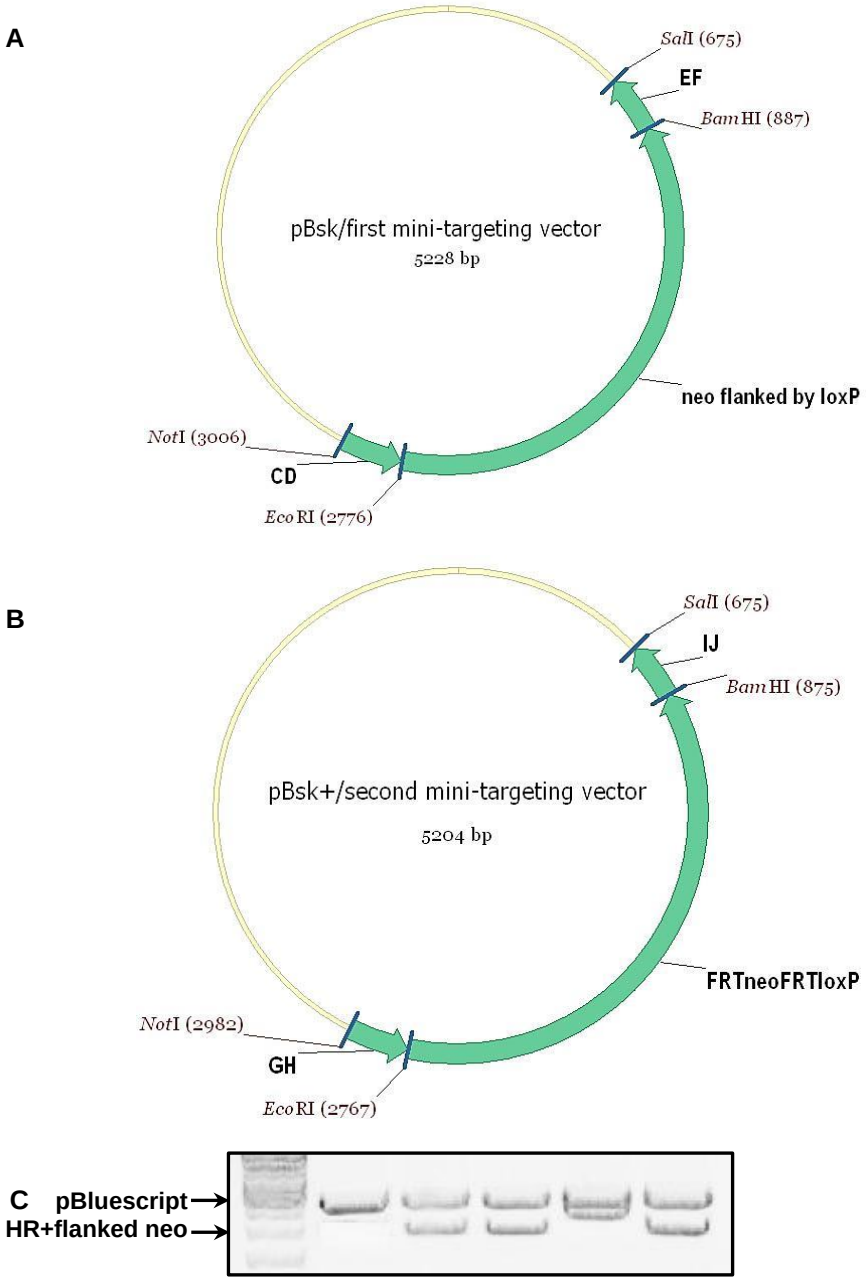

Figure 3. 17 Generation of mini-targeting vector. A. The map of the first mini-targeting vector which was used to insert the loxP site upstream to the exon 3 of DLK in targeting vector. **B.** The map of the second mini-targeting vector which was used to insert the second loxP site downstream to the exon 6 of DLK in targeting vector. **C.** Four out of five colonies were positive with generated mini-targeting vector. The homology arms (HR) and the neo cassette flanked by loxP sites were cut out together from the mini-targeting vector by NotI and SalI restriction digestion, and purified from the gel, first lane in the left.

3.4.f. Introduction of the first loxP site

To introduce the first loxP site into the targeting vector (3.4.c) SW102 cells carrying the targeting vector were induced for Red recombination function as described before. The induced cells were transformed with the loxP containing fragment (Fig. 3.17.A, C). The successfully recombinant cells were selected on a kanamycin agar plate, since the recombinant vector contains the neo cassette. The recombinant DNA was extracted and subjected to a restriction digest with EcoRI. The digestion pattern was compared to the prepared map and the positive colonies were selected for the next step. The digestion pattern defines the successful recombination, thereby the integration of the flanked neo cassette by loxP sites into the targeting vector. (Fig. 3.18).

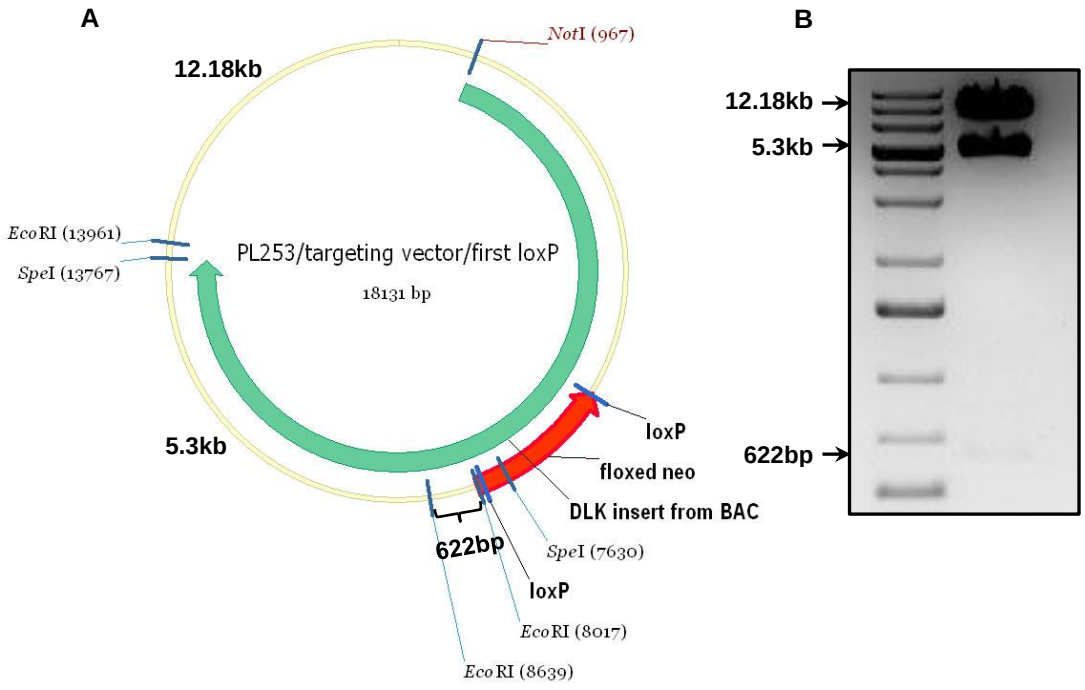

Figure 3. 18 Introduction of the first loxP site into the targeting vector. A. The map of the targeting vector with the neo cassette flanked by loxP sites inserted upstream to the exon 3 of DLK. **B.** The extracted vector was digested with EcoRI and the three expected fragments was compared to the map.

3.4.g. Excision of the neo cassette

Before introducing the second loxP sites, which will be selected also by kanamycin resistance, the existing neo cassette should be removed. This can be done by the

recombination activity of Cre-recombinase which recognizes the loxP sites and cuts out one of the loxP sites and the sequences flanked between the two loxPs. SW106 bacteria in which Cre-recombinase is already induced (chapter 2.4.k.II.5) were transformed with the targeting vector containing neo cassette flnaked by two loxP sites. The successful Cre-recombinase activity resulted in neo cassette excision, which can be selected on ampicillin agar plates and negative selection on kanamycin agar plates. The DNA was extracted from the cells and digested with SpeI. The digestion pattern was compared to the map, showing the successful remove of neo cassette from the targeting vector (Fig. 3.19).

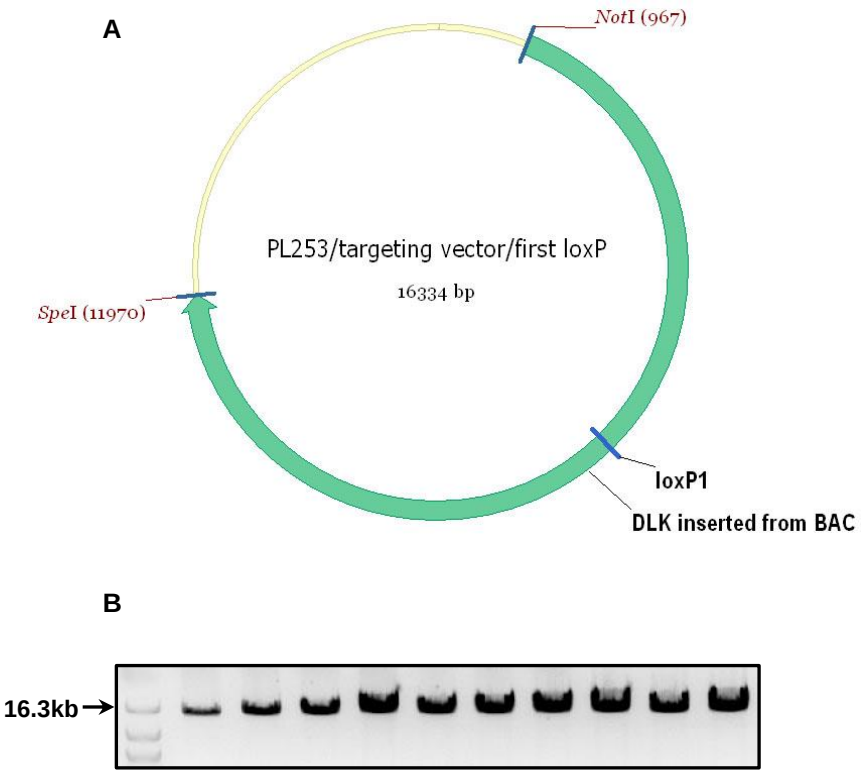

Figure 3. 19 Excision of the neo cassette. A. The map of the targeting vector after excision of the neo cassette. Cre-recombinase cut one loxP site and the neo cassette. **B.** The extracted DNA from ampicillin resistant colonies was digested with SpeI.

3.4.h. Introduction of the second loxP site

SW102 bacteria were transformed with targeting vector which contains one loxP site and induced for Red recombination function as described before. The induced cells were transformed with the purified fragment from second mini-targeting vector (Fig. 3.17. B and C). The successful recombinant cells were selected on a kanamycin agar plate. DNA was

extracted and digested with EcoRI and the digestion pattern was compared to the map. Both selected colonies which are kanamycin resistant, carrying the neo cassette flanked by loxP and FRT sites (Fig. 3.20).

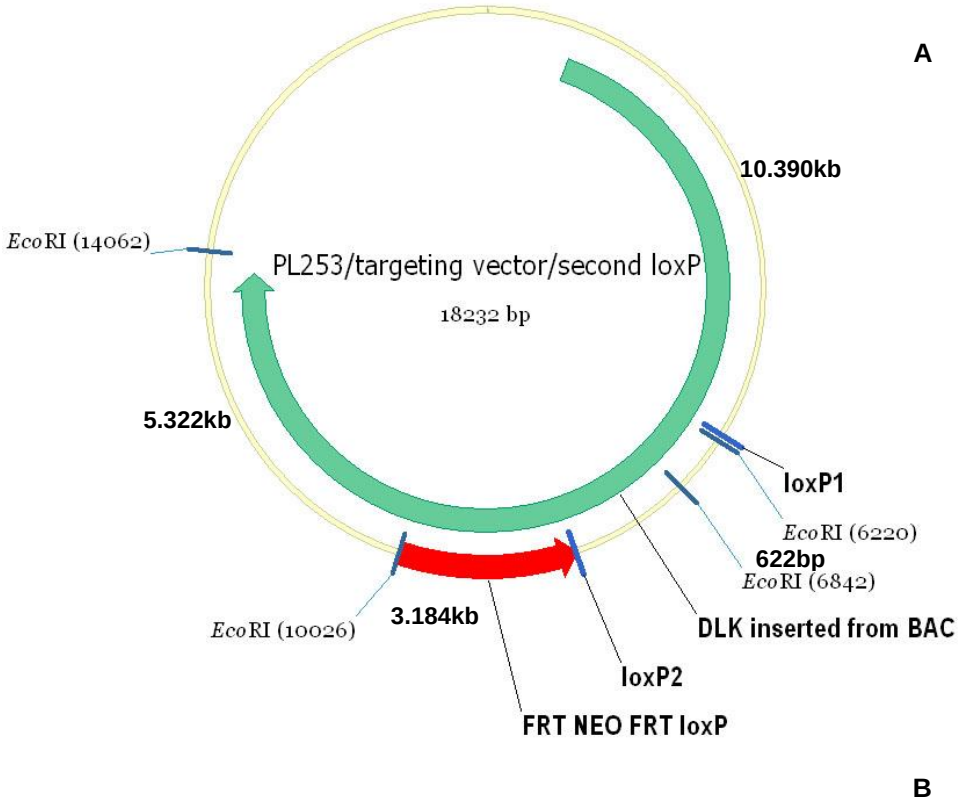

Figure 3. 20 Introduction of the second loxP. A. The map of the targeting vector with the second loxP site inserted. The neo cassette is flanked by two FRT sites which can be removed by flippase (flpe). **B.** DNA was digested with EcoRI and the digestion pattern was compared to the map.

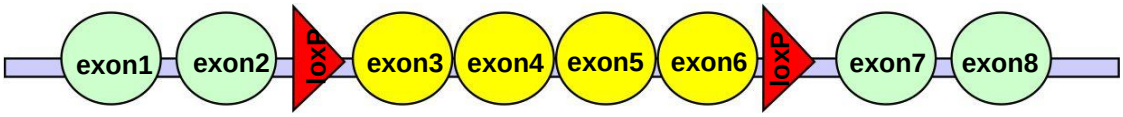

Figure 3. 21 Schematic figure of the generated targeting knock-out vector for DLK. Exons 3, 4, 5, and 6 are flanked by two loxP sites. The Cre-recombinase cut the flanked exons out by recognizing the loxP sites. This vector can be used to generate a conditional knock-out mice model for DLK, specifically in exons 3-6.

4. Discussion

4.1 Regulation of DLK by prediabetic signals

4.1.a. Enhancement of kinase activity of DLK

DLK was identified as a member of MLK family and known as a MAPKKK, expressed in the brain and peripheral nervous system as well as primary murine islets and the β-cell line HIT. Its activity resulted in the activation of downstream MAPKKs and consequently the activation of specific MAPKs (Holzman, Merritt et al. 1994; Oetjen, Grapentin et al. 2003; Hirai, Kawaguchi et al. 2005). Later on, an ATP-binding site was identified in DLK protein whose mutation led to catalytic disability of the kinase (Mata, Merritt et al. 1996). The putative autophosphorylation sites in MLK family members have been identified (Fig. 1.6) (Leung and Lassam 2001). The potential autophosphorylation sites, Serin-298 and Serin-302, in DLK were studied by generation of point mutations in these residues, in our research group (Fig. 3.1A). In this study the expression of DLKwt and the mutants were examined in HIT cells (Fig. 3.1B). Using an anti-DLK antibody it was identified that the mutations in autophosphorylation sites and the ATP-binding site do not affect the expression of the DLK protein in HIT cells. In addition a slightly faster migration was observed for the kinase dead mutant (K185A) and the Serin-302 (S302A) mutant on the immunoblott membrane, which might be because of the disability of these mutants to autophosphorylate (Fig. 3.1).

The glucose oxidation in pancreatic β-cells induces the membrane depolarization via closure of K_{ATP} channels, leading to calcium entry through voltage-sensitive L-type calcium channels, and consequently the phosphorylation and activation of the transcription factor CREB (Docherty and Clark 1994; Schwaninger, Blume et al. 1995; Jhala, Canettieri et al. 2003), an essential factor for β-cell function and survival (Eggers, Siemann et al. 1998; Jambal, Masterson et al. 2003; Jhala, Canettieri et al. 2003; Eliseev, Vanwinkle et al. 2004; Hsieh, Chen et al. 2005). CREB is a transcription factor which binds to and mediates the membrane depolarization responsiveness of the CRE in the regulation of insulin gene transcription (Oetjen, Diedrich et al. 1994; Eggers, Siemann et al. 1998; Oetjen, Grapentin et al. 2003). The overexpression of CREB in MIN6 β-cells prevented the cytokines-induced apoptosis (Jambal, Masterson et al. 2003) while the β-cell specific overexpression of a dominant-negative CREB mutant in mice caused β-cell apoptosis and diabetes (Jhala, Canettieri et al. 2003). In addition the disruption of the CRE-mediated transcription by overexpression of inducible cAMP early repressor (ICER)

in mice led to reduced expression of the insulin and the cyclin A genes, β-cell decline and severe diabetes (Inada, Hamamoto et al. 2004).

In the physiological state in β-cells, ATP produced from glucose metabolism induces the closure of the ATP-sensitive potassium (K_{ATP}) channels. The L-type voltage-dependent calcium channels ($VDCC_L$) sense the membrane depolarization followed by the closure of K_{ATP} channels and open (Drews, Krippeit-Drews et al. 2010). The increased Ca^{2+} influx triggers the downstream Ca^{2+}-dependent cascades like CamK which activates CREB (Ban, Yamada et al. 2000). The signals which induce protein kinase C (PKC) has also been shown to activate CREB (Brindle and Montminy 1992; Mayr, Canettieri et al. 2001). DLK was shown to inhibit the membrane depolarization-induced transcriptional activity of CREB in a β-cell line (Oetjen, Lechleiter et al. 2006). The activation of DLK by immunosuppressive drug cyclosporin A leads to β-cell apoptosis and β-cell mass decline (Plaumann, Blume et al. 2008). Cyclosporin A has been reported also to inhibit glucose-induced insulin gene transcription and CREB transcriptional activity through inhibition of calcineurin, which might participate in post-transplant diabetes under immunosuppressive drug therapy (Oetjen, Grapentin et al. 2003). CRTC (CREB regulating transcriptional coactivator) is a coactivator of CREB which interacts with CREB and participates in CREB-dependent gene transcription (Screaton, Conkright et al. 2004). The phosphatase calcineurin which is activated by elevated intracellular calcium, dephosphorylates CRTC thereby leading to its nuclear translocation, where CRTC interacts with CREB (Jansson, Ng et al. 2008).It has been reported that DLK inhibits CRTC function by phosphorylation on its inhibitory sites (Phu do, Wallbach et al. 2011). Then it could be proposed that glucose-induced membrane depolarization in one hand triggers the CRE-directed gene transcription, and in the other hand induces the Ca^{2+}-dependent phosphatase calcineurin which might dephosphorylate and deactivate DLK and dephosphorylate and activate CRTC (Fig. 4.1).

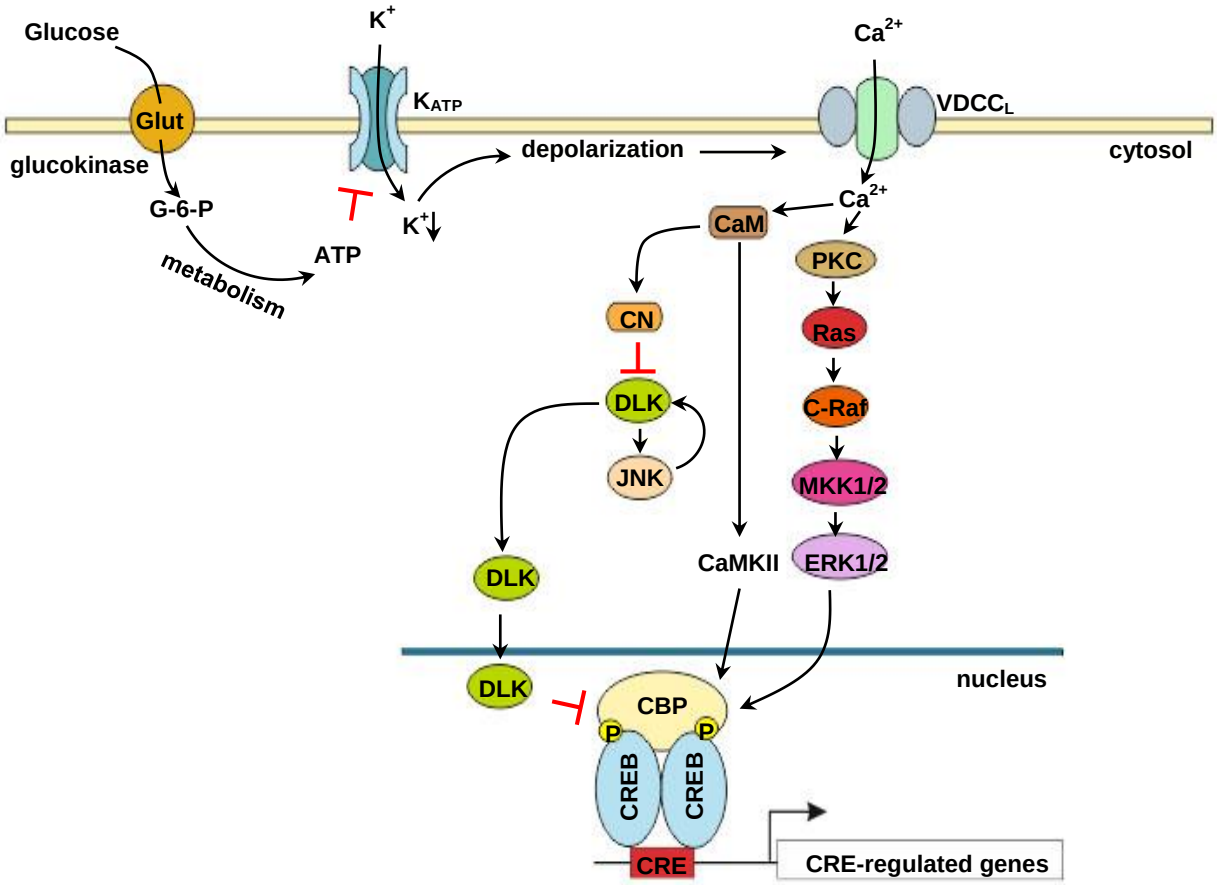

Figure 4. 1 CRE-directed gene transcription in β-cells. ATP produced from the oxidation of glucose blocks the ATP-sensitive potassium channels (K_{ATP}) leading to membrane depolarization and the opening of L-type voltage-dependent calcium channels ($VDCC_L$), resulting in calcium (Ca^{2+}) influx. Ca^{2+} activates the Ca^{2+}-dependent protein kinase (PKC), and the Ca^{2+}-modulated protein calmodulin (CaM). PKC triggers downstream cascade which finally leads to the activation of extracellular signal-regulated kinase (ERK) 1/2 and consequently the activation of CREB/CRE-dependent gene transcription. Ca^{2+}/CaM activates the Ca^{2+}/CaM-dependent phosphatase calcineurin (CN) which might dephosphorylate and deactivate DLK. When CN is inhibited DLK phosphorylates and activates JNK which does in return release DLK from JIP (JNK interacting protein). The released homodimerized DLK might translocate into the nucleus and inhibits the CREB/CRE-dependent gene transcription. Glut; glucose transporter, CBP; CREB binding protein.

In this study the role of the putative phosphorylation sites of DLK in the regulation of CRE-directed gene transcription was investigated (Fig. 3.2). DLKwt inhibited the CRE-directed gene transcription, while the kinase dead mutant DLK K185A showed no inhibitory effect which is in accordance to the previous report (Oetjen, Lechleiter et al. 2006). DLK S298A mutant showed a potential inhibitory effect on CRE-directed gene

transcription, while the DLK S302A mutant and the DLK S302/298A double mutant were unable in such an inhibitory effect. These data clarify that the Serin-302 is an important residue for the phosphorylation and activation of DLK.

As previously reported DLK inhibits the transcriptional activity of the CREB coactivator CBP triggered by membrane depolarization, while the DLK K185A mutant does not (Oetjen, Lechleiter et al. 2006). DLK might directly phosphorylate CBP on the inhibitory sites which disrupts its interaction to the CREB (Xu, Maroney et al. 2001). In this study the role of the putative phosphorylation sites in the regulation of CBP-dependent gene transcription was investigated (Fig. 3.3). DLKwt inhibited the CBP-dependent gene transcription, whereas the DLK K185A mutant did not. This result proves the previous report for the inhibitory effect of DLK on CBP-dependent gene transcription (Oetjen, Lechleiter et al. 2006). While DLK S298A mutant also inhibited the CBP-dependent gene transcription DLKS302A and DLK S302/298A mutants showed no inhibitory effect.

JNK is a member of the MAPK family that is activated by different stimuli, including cytokines, reactive oxygen species (ROS), and MAPKKKs. MAPKKKs activate JNK through MKK4 and MKK7 by phosphorylation of JNK at threonine (Thr) and tyrosine (Tyr) residues in its activation loop (Kallunki, Deng et al. 1996). MKK7 mediates the cytokine-induced JNK activation by phosphorylation of the Thr residue (Haeusgen, Herdegen et al. 2011). The initial activation of JNK by TNFα is transient and leads to cell proliferation through AP-1 (activator protein-1), but sustained activation of JNK leads to cell apoptosis (Karin and Lin 2002; Micheau and Tschopp 2003; Ventura, Cogswell et al. 2004; Wagner and Nebreda 2009). DLK has been also reported to activate JNK (chapter 1.3). In this study the role of the putative phosphorylation sites of DLK on the activation of JNK was investigated (Fig. 3.4). Mutation in the ATP-binding site of DLK (K185A) which prevents DLK autophosphorylation, diminished the phosphorylation of JNK by DLK. Mutation at Serin-302 residue of DLK decreased the phosphorylation of JNK by DLK, where mutation at Serin-298 residue had no effect. Taken together these data suggest that DLK needs to be phosphorylated at Serin-302 residue to be catalytically active.

Knowing the importance of Serin-302 residue in the phosphorylation and activation of DLK necessitated establishing a reliable detection method to detect this phosphorylation site. A phospho-Serin-302 specific antibody was produced which detects the phosphorylated Serin-302 residue in DLK protein. Using this antibody the phosphorylated overexpressed DLKwt and DLK S298A mutant were detected in an immunoblot analysis. DLK S302A and DLK S302/298A mutants were not detectable. Due to a mutation in ATP-binding site DLK K185A mutant was remained unphosphorylated, too (Fig. 3.5). These data show that the generated antibody specifically recognizes the

phosphorylation on Serin-302 residue of DLK and provides a tool for determining DLK activity.

The involvement of a variety of cytokines in the pathogenesis of both T1DM and T2DM has been widely reported (chapter 1.2). As discussed in section 4.1.b., when activated, DLK inhibits the transcriptional activity of the β-cell protective factor CREB. In this study the regulation of DLK by two major pro-inflammatory cytokines, TNFα and IL-1β, involved in DM pathogenesis was investigated. The expression level of the endogenous DLK was unaffected by the cytokines (Fig. 3.6). CsA which activates DLK (Plaumann, Blume et al. 2008) and inhibits the CREB/CRE-directed gene transcription (Schwaninger, Blume et al. 1993; Kruger, Schwaninger et al. 1997)caused no increase in DLK protein expression. Forskolin, a diterpene natural product, which activates adenylyl cyclase had no significant effect on DLK protein expression. The cAMP signaling pathway plays an outstanding role in function and proliferation of pancreatic β-cells. The insulin secretagogue hormone glucagon-like peptide-1 (GLP-1) activates the adenylyl cyclase enzyme for cAMP production (Drucker 1998; Holst 1999; Kieffer and Habener 1999; Holz and Chepurny 2003). cAMP activates the cAMP-dependent protein kinase A (PKA) which directly induces the CREB/CRE-directed gene transcription (Montminy 1997; Daniel, Walker et al. 1998).

The phosphorylation of DLK was also investigated (Fig. 3.7). CsA significantly increased the phosphorylation of DLK. Where IL-1β caused no significant increase in DLK phosphorylation, TNFα phosphorylated the endogenous DLK in HIT cells. The activated DLK phosphorylates and activates the downstream kinase JNK, which is well known to be involved in apoptosis (Gallo and Johnson 2002). The activated JNK triggers the dissociation of DLK from JIP scaffold protein (Nihalani, Meyer et al. 2001; Nihalani, Wong et al. 2003), which might lead to DLK activation and the inhibition of CREB/CRE-directed gene transcription by DLK. Thus, the phosphorylation of DLK by TNFα might mediate the deleterious effects of TNFα in pancreatic β-cells. Forskolin also caused a significant increase in DLK phosphorylation. Beside PKA, EPAC (exchange protein activated by cAMP, also known as cAMPGEF: cAMP-regulated guanine nucleutide exchange factor) has been also identified to mediate the cAMP signaling (de Rooij, Zwartkruis et al. 1998; Kawasaki, Springett et al. 1998). Both PKA and EPAC induce calcium-induced calcium release from endoplasmic reticulum via ryanodin receptor, and consequently ATP production in mitochondria. They might also activate some other kinases such as CaMK, PI-3K, PKB (Akt), ERK1/2, and atypical PKC-ξ (Holz 2004).The mechanism/s by which cAMP might increase DLK phosphorylation needs further investigation, but what can be mentioned here is that glucose-induced membrane depolarization in one hand triggers the

CREB/CRE-directed gene transcription, on the other hand might inhibit DLK activity through induction of calcineurin. In contrast, cAMP signaling might show a dual activity, triggering the CREB/CRE-dependent gene transcription mediated by PKA and the activation of DLK by some other kinase which have been induced by PKA and/or EPAC, and consequently inhibition of CREB transcriptional activity. A witness to this idea could be the report in which DLKwt inhibited the CRE-directed gene transcription induced by membrane depolarization as well as cAMP induced gene transcription, while the DLK K185A mutant did not inhibit the membrane depolarization-induced gene transcription but inhibited the cAMP-induced transcription (Oetjen, Lechleiter et al. 2006), proposing a probable participation of cAMP-signaling pathway in the phosphorylation of DLK which is independent of the ATP-binding site.

4.1.b. Nuclear localization of DLK

A well know characteristic of the eukaryotic cells is the separation of the genetic materials and the transcriptional machinery of the nucleus from the translational machinery and metabolic system of the cytoplasm by the nuclear envelope. This segregation simplifies the regulation of cellular processes such as signal transduction, gene expression and cell cycle control and progress. The precise regulation of these phenomena is dependent on a bidirectional transport between the cytoplasm and the nucleus. Such a crucial process needs molecular machinery which recognizes the cargo in one compartment, translocates it through the nuclear envelope, and releases it in the other compartment. This kind of nuclear transport system was first identified around 30 years ago by characterizing a nuclear targeting signal in the simian virus 40 (SV40) large T-antigen (Kalderon, Richardson et al. 1984; Kalderon, Roberts et al. 1984). Since then, several nucleocytoplasmic transport pathways have been proposed, of which the classical nuclear import pathway is the best globally accepted. The transportation of the macromolecules into and out of the nucleus occurs through the structures called nuclear pore complexes (NPCs) (Stoffler, Fahrenkrog et al. 1999; Allen, Cronshaw et al. 2000; Fahrenkrog and Aebi 2002; Fahrenkrog and Aebi 2003). The ions and small proteins (<40kDa) diffuse passively through the pore complexes, but the bigger proteins use soluble carrier proteins, called karyopherins (Radu, Blobel et al. 1995) to translocate actively through the nuclear envelope. The karyopherins who are involved in the import and export of the cargo into and out of the nucleus are termed importins (Gorlich, Prehn et al. 1994)and exportins (Stade, Ford et al. 1997), respectively. The Ran GTPase is the source of energy for this active transportation (Quimby and Dasso 2003). The Ran guanine nucleotide exchange factor (RanGEF) in the nucleus and the Ran GTPase

activating protein (Ran GAP) in the cytoplasm modulates the Ran nucleotide states (Bischoff and Ponstingl 1991; Becker, Melchior et al. 1995; Corbett, Koepp et al. 1995; Klebe, Prinz et al. 1995). By this regulatory effect Ran is asymmetrically distributed in the cell, with more RanGTP in the nucleus and more RanGDP in the cytoplasm (Kalab, Weis et al. 2002; Smith, Slepchenko et al. 2002) allowing a directional nuclear transportation. In the absence of RanGTP the import receptors bind the cargo in the cytoplasm and release the protein in the nucleus upon binding of the RanGTP to the complex. In the other way, the export receptors bind the protein in nucleus upon binding to RanGTP and release the cargo in the cytoplasm after the hydrolysis of GTP to GDP. The importin discriminates between its cargo containing the amino acid targeting sequences called nuclear localization signal (NLS), and the other cellular proteins. The NLS consists of either one (monopartite) or two (bipartite) stretches of basic amino acids (Kalderon, Richardson et al. 1984; Dingwall and Laskey 1991; Robbins, Dilworth et al. 1991). In classical import pathway importin-α binds to the protein containing NLS in the cytoplasm and interacts then with importin-β (Gorlich, Kostka et al. 1995). Importin-β mediates the interaction of the complex to the nuclear pore. After nuclear translocation, RanGTP binds to and makes conformational changes in importin-β, leading to the release of importin-α-cargo complex (Lee, Matsuura et al. 2005). The binding of nucleoporin Nup2 and the importin-α export receptor Cse1/RanGTP to an autoinhibitory region on importin-α results in the release of cargo from importin-α and export of importin-α to the cytoplasm (Kutay, Bischoff et al. 1997; Hood and Silver 1998; Kobe 1999; Gilchrist, Mykytka et al. 2002; Harreman, Hodel et al. 2003; Matsuura, Lange et al. 2003; Matsuura and Stewart 2004; Matsuura and Stewart 2005) (Fig. 4.2).

Recently, a bipartite NLS in DLK has been identified in our group whose mutation prevents nuclear localization of DLK induced by pro-inflammatory cytokines (unpublished data). In this study the interaction of DLK NLS with nuclear importins was investigated (Fig. 3.8). The DLKwt protein interacted with importin-α, but neither with importin-β nor transportin. DLK NLS1 mutant showed very weak interaction to importin-α and no interaction to importin-β and transportin. DLK NLS2 mutant also showed no interaction to any of the importins. DLK-PP mutant, which is unable to homodimerize, also interacts to importin-α but neither to importin-β nor transportin, indicating that DLK does not need to be dimerized to interact with the importins. These data show that DLK use a classic NLS to interact to the classic import pathway component for nuclear localization.

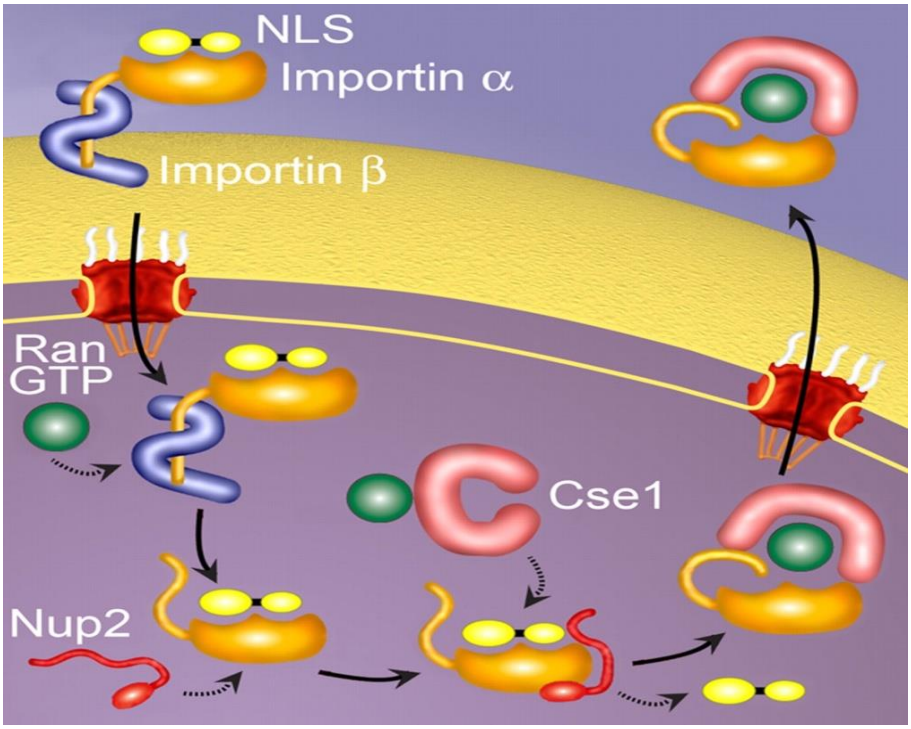

Figure 4. 2 The classical nuclear import cycle. In the cytoplasm the protein containing NLS binds to the Importin-α/importin-β heterodimer. Importin-α recognizes the NLS and importin-β interacts with the nuclear pore during translocation. When translocated into the nucleus, RanGTP binding causes a conformational change in importin-β resulting in the release of IBB (importin-β binding) region of the importin-α. Nucleoporin Nup2, export receptor Cse1, and an autoinhibitory domain work together to deliver and release the cargo in the nucleus. Finally, the export receptor Cse1 in complex with RanGTP recycles back the importin-α to the cytoplasm (Lange, Mills et al. 2007).

DLK in its inactive monomeric form is bound to JIP/IB-1 (JNK interacting protein/islet brain-1) and dissociates and homodimerizes upon phosphorylation of JIP/IB-1 by JNK (Nihalani, Meyer et al. 2001; Nihalani, Wong et al. 2003). In addition, the previous work of our group showed that nuclear localization of DLK is needed to inhibit the CREB-dependent gene transcription and to induce apoptosis in pancreatic β-cells (unpublished data). Thus, signals activating JNK such as pro-inflammatory cytokines may be amplified by the induction of DLK activity and nuclear localization.

In this study the nuclear localization of DLK driven by the pro-inflammatory cytokine TNFα was investigated in pancreatic β-cell line HIT (Fig. 3.9). TNFα triggers the nuclear localization of DLKwt in HIT cells, which proves the previous work of this group (unpublished data). TNFα also increases the nuclear localization of the DLK-PP mutant. The nuclear transport of the DLK-PP mutant under TNFα treatment is significantly

increased in comparison to non-treated cells, but is significantly less than DLKwt induced by TNFα. As previously reported, DLKwt inhibits the transcriptional activity of the CREB coactivator TORC (transducer of regulated CREB activity) while DLK-PP mutant showed no inhibitory effect (Phu do, Wallbach et al. 2011). These data suggest that, first a functional NLS is involved in the interaction of DLK protein with importin-α to initiate the nuclear transportation process, second the homodimerization of DLK is not necessary for the interaction with importin-α, but the disruption in DLK homodimerization changes its optimal nuclear translocation behavior, which might affect the regulatory role of DLK in gene transcription.

4.2 The effect of DLK on cell apoptosis and diabetes

4.2.a. DLK and the activation of caspase-3 in HIT cells

Pro-inflammatory cytokines have been reported to induce apoptosis in βTC1 cells as well as rat and human pancreatic islet cells (Rabinovitch, Suarez-Pinzon et al. 1994; Iwahashi, Hanafusa et al. 1996; Delaney, Pavlovic et al. 1997) (chapter 1.2). In this study the role of pro-inflammatory cytokines in the apoptosis of pancreatic β-cell line HIT was investigated (Fig. 3.10). The cleavage/activation of caspase-3 was detected as a sign of the apoptosis. IL-1β and IFNγ alone showed a slightly increase in the activation of caspase-3 which was not significant compared to the non-treated cells. The combination of the IL-1β and IFNγ caused no increase in the cleavage of caspase-3, neither. Although the role of IL-1β alone or in combination with IFNγ in the induction of apoptosis in pancreatic islets has been reported (Eizirik and Mandrup-Poulsen 2001), such an effect could not be detected in HIT cells. TNFα treatment of the cells led to an increase in the activation of caspase-3, which had been hypothesized before (Fig. 1.4). The combination of TNFα and IFNγ resulted in a synergistic effect on the cleavage of caspase-3, debating the importance of the mixture of the pro-inflammatory cytokines in the induction of apoptosis in β-cells.

The intermediary role of DLK in TNFα and TNFα/IFNγ combination induced apoptosis was also investigated. The protein amount of DLK was down regulated using an anti-DLK RNAi (Fig. 3.11) and the cells were treated with different combination of the cytokines. The down regulation of DLK was less than 50% which was not enough to be taken part in the conclusion. In addition, the transfection method itself caused an increase in the activation of caspase-3, which might be just magnified by cytokines. Thus, another down regulation approach is needed to be more effective in the down regulation of DLK and less toxic in the case of induction of cell apoptosis.

4.2.b. Animal experimentation

Using DLK-heterozygote mice and their wild-type littermates of C57BL/6J strain, the probable participation of DLK in diet-induced diabetes was investigated. Several criteria were measured during the experiment, such as body weight, blood glucose and the glycated hemoglobin (HbA1c) (Fig. 3.12). The idea was to induce diabetes in two distinct ways of feeding. First, glucotoxicity induced diabetes by carbohydrate-rich diet (CRD) (Kluth, Mirhashemi et al. 2011), and second obesity dependent insulin resistance and pro-inflammatory cytokines destruction of β-cells through high-fat diet (HFD) (Sauter, Schulthess et al. 2008). No changes in body weight and blood glucose were observed in any of the genotypes under CRD and HFD compared to wild-type mice under normal diet (ND) (Fig. 3.12 A and B), meaning that overt diabetes has not been established. The plasma level of HbA1c was measured higher in heterozygote mice under HFD compared to ND (Fig. 3.12 D), but there was no difference between HbA1c level in wild-type and heterozygote under HFD (Fig. 3.12 E). These data suggest that this model using the DLK heterozygote mice of C57BL/6J strain is not a reliable model for concluding the role of DLK in diet-induced diabetes. A β-cell specific DLK knock-out mice model might be valuable for further investigation (see below).

4.3 Generation of the conditional DLK knock-out mice

DLK is an exception in MLK family, whose existence is pivotal for the survival, since the global knock-out of the both alleles of DLK in mice results in perinatal death (Brancho, Ventura et al. 2005; Hirai, Cui de et al. 2006; Bisson, Tremblay et al. 2008). Using a tissue specific knock-out mice model could be a good alternative to overcome this problem (Nagy 2000). In this model DLK is flanked by two loxP sites, the recognition site for Cre recombinase, in one sex, and in the other sex the Cre recombinase is expressed under the control of a promoter of interest, in this case rat insulin promoter to be specifically expressed in pancreatic β-cells (Cre mice are from Pedro-Herrera). The newborn mice resulted from the breeding of these two mice express flanked DLK in the whole body and the Cre recombinase only in pancreatic β-cells. The Cre recombinase cuts out the flanked DLK and results in mice which are knock-out for DLK in β-cells.

4.3.a. Sequencing of genomic DLK in 129Sv mouse strain

Most of the gene-targeting experiments in mice are performed in 129Sv-derived embryonic stem (ES) cell lines, since these cell lines are more reliable at colonizing the germ line than the lines derived from other strains (van der Weyden, Adams et al. 2002). Since the genomic DLK sequence of 129Sv strain was not available in the scientific

resources the DNA extracted from 129Sv mouse was sequenced using primer nucleotides for DLK and compared to the sequence of DLK in C57BL/6J strain. Since no differences were observed in the sequenced area the available sequence of C57BL/6J strain can be used as well for the future analysis.

4.3.b. Generation of targeting knock-out vector for DLK

The use of the *Red* genes encoded proteins of bacteriophage λ permits the efficient homologous recombination in *E. coli (Zhang, Buchholz et al. 1998; Muyrers, Zhang et al. 1999; Datsenko and Wanner 2000; Murphy, Campellone et al. 2000; Yu, Ellis et al. 2000; Lee, Yu et al. 2001; Swaminathan, Ellis et al. 2001)*. Two *Red* genes are involved in the recombination process: *exo*, which encodes the 5'-3' exonuclease (Exo) that makes 3' single-strand DNA (ssDNA) overhang on the 5' end of the linear double-strand DNA (dsDNA), and *bet*, which encodes a pairing protein (Beta) that catalyzes the annealing of the 3' ssDNA overhang generated by Exo to the complementary DNA strand on the vector. The activity of RecBCD exonuclease causes the unstability of the linear dsDNA in *E*. coli. The λ-encoded protein Gam participates in the successful recombination by inhibition of RecBCD (Stahl 1998; Poteete 2001). The recombination functions of the bacteriophage λ can be expressed by a plasmid (Zhang, Buchholz et al. 1998; Murphy, Campellone et al. 2000), or by the integration of a defective prophage into the *E*. coli genome (Yu, Ellis et al. 2000). When the prophage is integrated, *E*. coli expresses the recombination genes under the control of λ P_L promoter. The promoter is under the control of temperature-sensitive λ cI857 repressor. At 32°C the repressor prevents the initiation of the expression of the proteins by promoter. Shifting the temperature to 42°C for 10-15 min removes the inhibition of promoter by the repressor and results in the very high level of recombination proteins' expression. Based on these properties a protocol was established for generating the conditional knock-out vector (Liu, Jenkins et al. 2003)(chapter 3.4).

In this study the gap-repair protocol (Liu, Jenkins et al. 2003) was used to generate the conditional cko vector. A map was prepared for each step and the restriction digestion was performed according to the prepared map (Fig. 3.14 – Fig. 3.20). The accuracy of the recombination was proved via step by step sequencing. The excision of the neo cassette by the induction of Cre recombinase depicts the existence of the functional loxP sites (Fig. 3.19). The presence of a neo cassette allows the selection of the injected ES cells (Fig. 3.20). The exons 3-7 of DLK are flanked by loxP sites, which can be removed by Cre recombinase to generate a cell specific cko model in which DLK lacks the functional catalytic part of its protein.

Summary

Diabetes mellitus type 2 is the most increasing metabolic disease worldwide. The disease is recognized by the disability of endocrine pancreas to afford the high metabolic demand which has been raised due to insulin resistance followed by hyperglycemia. This failure might be addressed to both β-cell dysfunction and β-cell mass decline.

CRE- (cAMP response element) binding protein (CREB) is a transcriptional factor which plays an outstanding role in the survival and maintenance of β-cells. The mitogen activated protein kinase kinase kinase (MAPKKK) DLK (dual leucine zipper kinase) has been shown to inhibit the membrane depolarization-induced transcriptional activity of CREB and its coactivator CRTC. DLK phosphorylates and activates the stress activated protein kinase JNK (C-Jun N-terminal kinase). In this study the regulation of DLK by prediabetic signals was investigated in two ways. First the regulation of DLK kinase activity by prediabetic signals, and second the subcellular translocation of DLK induced by pro-inflammatory cytokines. Two point mutations were generated in the putative phosphorylation sites of DLK (Serin-298 and Serin-302) and the participation of these phosphorylation sites in the activity of DLK was investigated. Mutation in Serin-302 residue abolished the inhibitory effect of DLK on CRE- and CBP-dependent gene transcription. The Serin-302 mutant was also unable to phosphorylate and activate JNK. These data suggest that Serin-302 residue is an important residue in the kinase activity of DLK. An antibody against DLK was produced which recognizes the phosphorylation of DLK specifically at Serin-302 residue. This antibody provides a valuable tool for investigating the activity of DLK. By use of this antibody we showed that pro-inflammatory cytokine TNFα alone and in combination with IFNγ activate DLK by phosphorylation of DLK at Serin-302 residue.

Previous study showed that pro-inflammatory cytokines TNFα and IL-1β induce nuclear localization of DLK in β-cell line HIT. In this study the interaction of DLK protein with nuclear receptors (α-importin, β-importin, and transportin) was investigated. The results showed that DLK interacts with α-importin but neither with β-importin nor with transportin. The mutation in DLK bipartite NLS destroyed the interaction with α-importin. These data show that DLK contains a functional bipartite NLS which interacts with the classic nuclear localization component α-importin which transports DLK into the nucleus. The mutation in leucine zipper sequence of DLK (DLK-PP) which prevents the homodimerization of DLK had no effect on the interaction of DLK with α-importin but decreased the nuclear localization induced by TNFα compared to DLKwt. This data

suggest that the homodimerization of DLK is not necessary for the interaction with nuclear receptor, but has an obvious effect on the stimulated nuclear translocation of the protein.

The role of DLK in the establishment of diet-induced diabetes was investigated using DLK heterozygote mice and their wild-type littermates. The data showed no establishment of diabetes in neither in wild-type nor in heterozygote mice.

DLK knock-out mice die perinatally. To investigate the role of DLK in function and survival of β-cells in an animal model, a targeting knock-out vector was designed and generated in this study. In this vector the exons 3 to 6 of DLK are flanked by two loxP sites which are recognized by Cre recombinase. The mice generated using this targeting vector, will be mated with the mice expressing Cre recombinase under the control of rat insulin promoter. The next generation express Cre recombinase in β-cells where it can cut out the loxP flanked DLK, resulting in the β-cell-specific DLK knock-out mice.

Conclusion

These data show that DLK is regulated in two ways by prediabetic signals:

1. TNFα induced the phosphorylation and thus the activation of DLK.
2. TNFα and IL-β induce the nuclear translocation of DLK, whereby only nuclear DLK inhibits CREB-dependent gene transcription and induces β-cell apoptosis.

Thus, it's feasible that the β-cell specific inhibition of DLK provides a novel therapeutic target for the treatment of diabetes mellitus type 2.

Zusammenfassung

Diabetes mellitus Typ 2 ist die metabolische Krankheit mit dem höchsten Prävalenzanstieg weltweit. Die Krankheit wird durch die Unfähigkeit des endokrinen Pankreas charakterisiert, adäquat auf metabolische Bedürfnisse zu reagieren. Die periphere Insulinresistenz, die aufgrund der Fehlfunktion des endokrinen Pankreas nicht ausreichend kompensiert werden kann, resultiert in erhöhten Blutzuckerspiegeln. Die Dysfunktion der β - Zellen und die Abnahme der β- Zelldichte können als Ursachen für die Fehlfunktion des endokrinen Pankreas angesehen werden.

CREB (cAMP response element binding protein) ist ein Transkriptionsfaktor, der eine bedeutsame Rolle für die Aufrechterhaltung der β- Zellen spielt.

Die mitogen-aktivierte protein kinase kinase kinase (MAPKKK) DLK (dual leucine zipper kinase) inhibiert die durch die Membrandepolarisation induzierte transkriptionelle Aktivität von CREB und des Koaktivators CRTC. DLK phosphoryliert und aktiviert die JNK (C-Jun N-terminal kinase). In dieser Studie wurde die Regulation der DLK durch die prädiabetischen Signale auf zwei Wegen untersucht: Es wurden die Regulation der DLK Kinase Aktivität durch prädiabetische Signale und die subzelluläre Lokalisation der DLK untersucht. Die Bedeutung der Phosphorylierung von Serin-298 und Serin-302 in der katalytischen Domäne (der DLK) für die Kinaseaktivität wurde mittels Punktmutation in Alanin erzeugt. Mutation des Serin- 302 Rest hebt den inhibitorischen Effekt der DLK auf der CRE- und CBP- abhängigen Gentranskription auf. Zusätzlich war diese Mutante unfähig JNK zu phosphorylieren und damit zu aktivieren. Diese Daten weisen darauf hin, dass das Serin-302 eine entscheidende Rolle für die katalytische Aktivität der DLK spielt.

Es wurde ein Antikörper erzeugt, der spezifisch am Serin-302 phosphoryliertes DLK erkennt. (Dieser Antikörper stellt ein nützliches Instrument zur Untersuchung der Aktivität der DLK dar.) Durch Verwendung des Antikörpers wurde gezeigt, dass das proinflammatorische Zytokin TNF-alpha alleine und in Kombination mit IFNγ aktiviert. Eine vorherige Studie in der β-Zell Linie HIT hatte gezeigt, dass die proinflammatorischen Zytokine TNFα und IL-1β eine nukleare Lokalisation der DLK induzieren. In dieser Studie wurde die Interaktion von DLK mit den Rezeptoren für den Kernimport (Importin-α, Importin-β und Transportin) untersucht. Die Ergebnisse zeigen, dass DLK mit Importin- α interagiert, aber weder mit Importin-β noch mit Transportin. Die Mutation in der zweigeteilten Kernerkennungssequenz (NLS) der DLK, hebt die Interaktion mit Importin-α auf. Diese Daten zeigen, dass DLK eine funktionelle zweigeteilte NLS besitzt, welche mit der klassischen nukleären Lokalisationskomponente Importin- α interagiert. Die Mutation in der Leuzin Zipper Sequenz der DLK (DLK-PP), die eine Homodimerization der DLK

verhindert, hat keinen Effekt auf die Interaktion der DLK mit dem Importin-α. Diese Mutation reduziert jedoch, verglichen mit der DLKwt, die TNFα stimulierte nukleare Lokalisation der DLK-PP.

Diese Daten weisen darauf hin, dass die Homodimerization der DLK nicht für die Interaktion mit Importin-α erforderlich ist, aber Stimulus- induzierte nukleare Lokalisation von DLK verhindert.

Die Rolle der DLK bei der Etablierung der Diät-induzierten Diabetes wurde durch heterozygote DLK Mäuse und ihren Wurfgeschwistern vom Wildtyp untersucht.

Weder im Wildtyp Mäusen noch in DLK heterozygoten Mäusen konnte die Induktion von Diabetes durch Diät erreicht werden.

DLK Knock-out Mäuse sterben perinatal. Um die Rolle der DLK für Funktion und Überleben der β-Zellen im Tiermodell zu untersuchen, sollte ein β-zellspezifischer targeting Knock-out Vektor entworfen und generiert werden. In diesem konditionellen DLK Knock-out Vektor sind die Exons 3 bis 6 der DLK von zwei loxP Sequenzen flankiert.Die mit dem targeting Vektor generierten Mäusen werden mit den Mäusen gepaart, welche unter der Kontrolle des Ratten Insulinpromoters, die Cre- Rekombinase expremieren. In den aus dieser Kreuzung entstehenden Mäusen, schneidet die ausschließlich in den β- Zellen exprimierte Cre-Rekombinase die von den loxP-Sequenzen flankierten DLK Exons 3 bis 6 aus, sodass die DLK spezifisch in den β-Zellen ausgeschaltet wird. Dieses führt zu β-zellspezifischen DLK Knock-out Mäusen.

Schlussfolgerung

Diese Daten zeigen, dass die DLK auf zwei Wegen von den prädiabetischen Signalen reguliert wird:

1) TNFα induziert die Phosphorylierung und folglich die Aktivierung der DLK.
2) TNFα und IL- β induzieren die nukleare Translokation der DLK, wodurch die CREB-abhängige Gentranskription gehemmt und die β-Zell Apoptosis induziert wird.

Die wenn möglich β-zellspezifische DLK stellt demnach ein neuartiges Ziel für die Therapie des Diabetes mellitus dar.

References

Aguirre, V., E. D. Werner, et al. (2002). "Phosphorylation of Ser307 in insulin receptor substrate-1 blocks interactions with the insulin receptor and inhibits insulin action." J Biol Chem **277**(2): 1531-1537.

Al-Lamki, R. S., J. Wang, et al. (2001). "Expression of tumor necrosis factor receptors in normal kidney and rejecting renal transplants." Lab Invest **81**(11): 1503-1515.

Allen, T. D., J. M. Cronshaw, et al. (2000). "The nuclear pore complex: mediator of translocation between nucleus and cytoplasm." J Cell Sci **113 (Pt 10)**: 1651-1659.

Ammendrup, A., A. Maillard, et al. (2000). "The c-Jun amino-terminal kinase pathway is preferentially activated by interleukin-1 and controls apoptosis in differentiating pancreatic beta-cells." Diabetes **49**(9): 1468-1476.

Arner, P. (2003). "The adipocyte in insulin resistance: key molecules and the impact of the thiazolidinediones." Trends Endocrinol Metab **14**(3): 137-145.

Bach, E. A., J. W. Tanner, et al. (1996). "Ligand-induced assembly and activation of the gamma interferon receptor in intact cells." Mol Cell Biol **16**(6): 3214-3221.

Ban, N., Y. Yamada, et al. (2000). "Activating transcription factor-2 is a positive regulator in CaM kinase IV-induced human insulin gene expression." Diabetes **49**(7): 1142-1148.

Banerjee, M. and M. Saxena (2012). "Interleukin-1 (IL-1) family of cytokines: role in type 2 diabetes." Clin Chim Acta **413**(15-16): 1163-1170.

Beck-Nielsen, H. (2002). "[Insulin resistance: organ manifestations and cellular mechanisms]." Ugeskr Laeger **164**(16): 2130-2135.

Becker, J., F. Melchior, et al. (1995). "RNA1 encodes a GTPase-activating protein specific for Gsp1p, the Ran/TC4 homologue of Saccharomyces cerevisiae." J Biol Chem **270**(20): 11860-11865.

Bending, D., P. Zaccone, et al. (2012). "Inflammation and type one diabetes." Int Immunol **24**(6): 339-346.

Bennett, M., K. Macdonald, et al. (1998). "Cell surface trafficking of Fas: a rapid mechanism of p53-mediated apoptosis." Science **282**(5387): 290-293.

Bergeron, P., M. Douziech, et al. (1997). "Inhibition of cell growth by overexpression of the ZPK gene." Biochem Biophys Res Commun **231**(1): 153-155.

Bischoff, F. R. and H. Ponstingl (1991). "Catalysis of guanine nucleotide exchange on Ran by the mitotic regulator RCC1." Nature **354**(6348): 80-82.

Bisson, N., M. Tremblay, et al. (2008). "Mice lacking both mixed-lineage kinase genes Mlk1 and Mlk2 retain a wild type phenotype." Cell Cycle **7**(7): 909-916.

Black, R. A., C. T. Rauch, et al. (1997). "A metalloproteinase disintegrin that releases tumour-necrosis factor-alpha from cells." Nature **385**(6618): 729-733.

Blonska, M., P. B. Shambharkar, et al. (2005). "TAK1 is recruited to the tumor necrosis factor-alpha (TNF-alpha) receptor 1 complex in a receptor-interacting protein (RIP)-dependent manner and cooperates with MEKK3 leading to NF-kappaB activation." J Biol Chem **280**(52): 43056-43063.

Bonny, C., A. Oberson, et al. (2001). "Cell-permeable peptide inhibitors of JNK: novel blockers of beta-cell death." Diabetes **50**(1): 77-82.

Bonny, C., A. Oberson, et al. (2000). "IB1 reduces cytokine-induced apoptosis of insulin-secreting cells." J Biol Chem **275**(22): 16466-16472.

Bradley, J. R. (2008). "TNF-mediated inflammatory disease." J Pathol **214**(2): 149-160.

Brancho, D., J. J. Ventura, et al. (2005). "Role of MLK3 in the regulation of mitogen-activated protein kinase signaling cascades." Mol Cell Biol **25**(9): 3670-3681.

Briaud, I., M. K. Lingohr, et al. (2003). "Differential activation mechanisms of Erk-1/2 and p70(S6K) by glucose in pancreatic beta-cells." Diabetes **52**(4): 974-983.

Brindle, P. K. and M. R. Montminy (1992). "The CREB family of transcription activators." Curr Opin Genet Dev **2**(2): 199-204.

Briscoe, J., N. C. Rogers, et al. (1996). "Kinase-negative mutants of JAK1 can sustain interferon-gamma-inducible gene expression but not an antiviral state." EMBO J **15**(4): 799-809.

Campbell, I. L., A. Iscaro, et al. (1988). "IFN-gamma and tumor necrosis factor-alpha. Cytotoxicity to murine islets of Langerhans." J Immunol **141**(7): 2325-2329.

Cardozo, A. K., F. Ortis, et al. (2005). "Cytokines downregulate the sarcoendoplasmic reticulum pump Ca2+ ATPase 2b and deplete endoplasmic reticulum Ca2+, leading to induction of endoplasmic reticulum stress in pancreatic beta-cells." Diabetes **54**(2): 452-461.

Carlson, C. J., S. Koterski, et al. (2003). "Enhanced basal activation of mitogen-activated protein kinases in adipocytes from type 2 diabetes: potential role of p38 in the downregulation of GLUT4 expression." Diabetes **52**(3): 634-641.

Carswell, E. A., L. J. Old, et al. (1975). "An endotoxin-induced serum factor that causes necrosis of tumors." Proc Natl Acad Sci U S A **72**(9): 3666-3670.

Carter, D. B., M. R. Deibel, Jr., et al. (1990). "Purification, cloning, expression and biological characterization of an interleukin-1 receptor antagonist protein." Nature **344**(6267): 633-638.

Corbett, A. H., D. M. Koepp, et al. (1995). "Rna1p, a Ran/TC4 GTPase activating protein, is required for nuclear import." J Cell Biol **130**(5): 1017-1026.

Daniel, P. B., W. H. Walker, et al. (1998). "Cyclic AMP signaling and gene regulation." Annu Rev Nutr **18**: 353-383.

Datsenko, K. A. and B. L. Wanner (2000). "One-step inactivation of chromosomal genes in Escherichia coli K-12 using PCR products." Proc Natl Acad Sci U S A **97**(12): 6640-6645.

Daviau, A., J. P. Couture, et al. (2011). "Loss of DLK expression in WI-38 human diploid fibroblasts induces a senescent-like proliferation arrest." Biochem Biophys Res Commun **413**(2): 282-287.

de Rooij, J., F. J. Zwartkruis, et al. (1998). "Epac is a Rap1 guanine-nucleotide-exchange factor directly activated by cyclic AMP." Nature **396**(6710): 474-477.

Decker, T., P. Kovarik, et al. (1997). "GAS elements: a few nucleotides with a major impact on cytokine-induced gene expression." J Interferon Cytokine Res **17**(3): 121-134.

Delaney, C. A., D. Pavlovic, et al. (1997). "Cytokines induce deoxyribonucleic acid strand breaks and apoptosis in human pancreatic islet cells." Endocrinology **138**(6): 2610-2614.

Dinarello, C. A. (1991). "Interleukin-1 and interleukin-1 antagonism." Blood **77**(8): 1627-1652.

Dinarello, C. A., M. Y. Donath, et al. (2010). "Role of IL-1beta in type 2 diabetes." Curr Opin Endocrinol Diabetes Obes **17**(4): 314-321.

Dingwall, C. and R. A. Laskey (1991). "Nuclear targeting sequences--a consensus?" Trends Biochem Sci **16**(12): 478-481.

Docherty, K. and A. R. Clark (1994). "Nutrient regulation of insulin gene expression." FASEB J **8**(1): 20-27.

Donath, M. Y. and P. A. Halban (2004). "Decreased beta-cell mass in diabetes: significance, mechanisms and therapeutic implications." Diabetologia **47**(3): 581-589.

Donath, M. Y. and T. Mandrup-Poulsen (2008). "The use of interleukin-1-receptor antagonists in the treatment of diabetes mellitus." Nat Clin Pract Endocrinol Metab **4**(5): 240-241.

Donath, M. Y., J. Storling, et al. (2003). "Inflammatory mediators and islet beta-cell failure: a link between type 1 and type 2 diabetes." J Mol Med (Berl) **81**(8): 455-470.

Dorow, D. S., L. Devereux, et al. (1993). "Identification of a new family of human epithelial protein kinases containing two leucine/isoleucine-zipper domains." Eur J Biochem **213**(2): 701-710.

Douziech, M., G. Grondin, et al. (1998). "Zonal induction of mixed lineage kinase ZPK/DLK/MUK gene expression in regenerating mouse liver." Biochem Biophys Res Commun **249**(3): 927-932.

Drews, G., P. Krippeit-Drews, et al. (2010). "Electrophysiology of islet cells." Adv Exp Med Biol **654**: 115-163.

Dripps, D. J., B. J. Brandhuber, et al. (1991). "Interleukin-1 (IL-1) receptor antagonist binds to the 80-kDa IL-1 receptor but does not initiate IL-1 signal transduction." J Biol Chem **266**(16): 10331-10336.

Drucker, D. J. (1998). "Glucagon-like peptides." Diabetes **47**(2): 159-169.

Dudek, N. L., H. E. Thomas, et al. (2006). "Cytotoxic T-cells from T-cell receptor transgenic NOD8.3 mice destroy beta-cells via the perforin and Fas pathways." Diabetes **55**(9): 2412-2418.

Ealick, S. E., W. J. Cook, et al. (1991). "Three-dimensional structure of recombinant human interferon-gamma." Science **252**(5006): 698-702.

Eggers, A., G. Siemann, et al. (1998). "Gene-specific transcriptional activity of the insulin cAMP-responsive element is conferred by NF-Y in combination with cAMP response element-binding protein." J Biol Chem **273**(29): 18499-18508.

Eisenbarth, G. S. (1986). "Type I diabetes mellitus. A chronic autoimmune disease." N Engl J Med **314**(21): 1360-1368.

Eisenberg, S. P., R. J. Evans, et al. (1990). "Primary structure and functional expression from complementary DNA of a human interleukin-1 receptor antagonist." Nature **343**(6256): 341-346.

Eizirik, D. L., G. S. Korbutt, et al. (1992). "Prolonged exposure of human pancreatic islets to high glucose concentrations in vitro impairs the beta-cell function." J Clin Invest **90**(4): 1263-1268.

Eizirik, D. L. and T. Mandrup-Poulsen (2001). "A choice of death--the signal-transduction of immune-mediated beta-cell apoptosis." Diabetologia **44**(12): 2115-2133.

Eizirik, D. L., S. Sandler, et al. (1994). "Cytokines suppress human islet function irrespective of their effects on nitric oxide generation." J Clin Invest **93**(5): 1968-1974.

El-Sheikh, A., W. L. Suarez-Pinzon, et al. (1999). "Both CD4(+)and CD8(+)T cells are required for IFN-gamma gene expression in pancreatic islets and autoimmune diabetes development in biobreeding rats." J Autoimmun **12**(2): 109-119.

Eliseev, R. A., B. Vanwinkle, et al. (2004). "Diazoxide-mediated preconditioning against apoptosis involves activation of cAMP-response element-binding protein (CREB) and NFkappaB." J Biol Chem **279**(45): 46748-46754.

Engelman, J. A., A. H. Berg, et al. (2000). "Tumor necrosis factor alpha-mediated insulin resistance, but not dedifferentiation, is abrogated by MEK1/2 inhibitors in 3T3-L1 adipocytes." Mol Endocrinol **14**(10): 1557-1569.

Fahrenkrog, B. and U. Aebi (2002). "The vertebrate nuclear pore complex: from structure to function." Results Probl Cell Differ **35**: 25-48.

Fahrenkrog, B. and U. Aebi (2003). "The nuclear pore complex: nucleocytoplasmic transport and beyond." Nat Rev Mol Cell Biol **4**(10): 757-766.

Fan, G., S. E. Merritt, et al. (1996). "Dual leucine zipper-bearing kinase (DLK) activates p46SAPK and p38mapk but not ERK2." J Biol Chem **271**(40): 24788-24793.

Federici, M., M. Hribal, et al. (2001). "High glucose causes apoptosis in cultured human pancreatic islets of Langerhans: a potential role for regulation of specific Bcl family genes toward an apoptotic cell death program." Diabetes **50**(6): 1290-1301.

Feve, B. and J. P. Bastard (2009). "The role of interleukins in insulin resistance and type 2 diabetes mellitus." Nat Rev Endocrinol **5**(6): 305-311.

Fountoulakis, M., M. Zulauf, et al. (1992). "Stoichiometry of interaction between interferon gamma and its receptor." Eur J Biochem **208**(3): 781-787.

Galcheva-Gargova, Z., B. Derijard, et al. (1994). "An osmosensing signal transduction pathway in mammalian cells." Science **265**(5173): 806-808.

Gallo, K. A. and G. L. Johnson (2002). "Mixed-lineage kinase control of JNK and p38 MAPK pathways." Nat Rev Mol Cell Biol **3**(9): 663-672.

Gao, Z., A. Zuberi, et al. (2003). "Aspirin inhibits serine phosphorylation of insulin receptor substrate 1 in tumor necrosis factor-treated cells through targeting multiple serine kinases." J Biol Chem **278**(27): 24944-24950.

Germain, L., J. Fradette, et al. (2000). "The mixed lineage kinase leucine-zipper protein kinase exhibits a differentiation-associated localization in normal human skin and induces keratinocyte differentiation upon overexpression." J Invest Dermatol **115**(5): 860-867.

Gery, I., R. K. Gershon, et al. (1972). "Potentiation of the T-lymphocyte response to mitogens. I. The responding cell." J Exp Med **136**(1): 128-142.

Giannoukakis, N., Z. Mi, et al. (2000). "Prevention of beta cell dysfunction and apoptosis activation in human islets by adenoviral gene transfer of the insulin-like growth factor I." Gene Ther **7**(23): 2015-2022.

Gilchrist, D., B. Mykytka, et al. (2002). "Accelerating the rate of disassembly of karyopherin.cargo complexes." J Biol Chem **277**(20): 18161-18172.

Gorlich, D., S. Kostka, et al. (1995). "Two different subunits of importin cooperate to recognize nuclear localization signals and bind them to the nuclear envelope." Curr Biol **5**(4): 383-392.

Gorlich, D., S. Prehn, et al. (1994). "Isolation of a protein that is essential for the first step of nuclear protein import." Cell **79**(5): 767-778.

Gough, D. J., K. Sabapathy, et al. (2007). "A novel c-Jun-dependent signal transduction pathway necessary for the transcriptional activation of interferon gamma response genes." J Biol Chem **282**(2): 938-946.

Gould, S. J. and S. Subramani (1988). "Firefly luciferase as a tool in molecular and cell biology." Anal Biochem **175**(1): 5-13.

Granowitz, E. V., B. D. Clark, et al. (1991). "Interleukin-1 receptor antagonist competitively inhibits the binding of interleukin-1 to the type II interleukin-1 receptor." J Biol Chem **266**(22): 14147-14150.

Gray, P. W. and D. V. Goeddel (1982). "Structure of the human immune interferon gene." Nature **298**(5877): 859-863.

Greenlund, A. C., M. A. Farrar, et al. (1994). "Ligand-induced IFN gamma receptor tyrosine phosphorylation couples the receptor to its signal transduction system (p91)." EMBO J **13**(7): 1591-1600.

Greenlund, A. C., M. O. Morales, et al. (1995). "Stat recruitment by tyrosine-phosphorylated cytokine receptors: an ordered reversible affinity-driven process." Immunity **2**(6): 677-687.

Greenlund, A. C., R. D. Schreiber, et al. (1993). "Interferon-gamma induces receptor dimerization in solution and on cells." J Biol Chem **268**(24): 18103-18110.

Guest, C. B., M. J. Park, et al. (2008). "The implication of proinflammatory cytokines in type 2 diabetes." Front Biosci **13**: 5187-5194.

Gysemans, C. A., L. Ladriere, et al. (2005). "Disruption of the gamma-interferon signaling pathway at the level of signal transducer and activator of transcription-1 prevents immune destruction of beta-cells." Diabetes **54**(8): 2396-2403.

Gysemans, C. A., D. Pavlovic, et al. (2001). "Dual role of interferon-gamma signalling pathway in sensitivity of pancreatic beta cells to immune destruction." Diabetologia **44**(5): 567-574.

Habener, J. F., C. P. Miller, et al. (1995). "cAMP-dependent regulation of gene transcription by cAMP response element-binding protein and cAMP response element modulator." Vitam Horm **51**: 1-57.

Haefliger, J. A., T. Tawadros, et al. (2003). "The scaffold protein IB1/JIP-1 is a critical mediator of cytokine-induced apoptosis in pancreatic beta cells." J Cell Sci **116**(Pt 8): 1463-1469.

Haeusgen, W., T. Herdegen, et al. (2011). "The bottleneck of JNK signaling: molecular and functional characteristics of MKK4 and MKK7." Eur J Cell Biol **90**(6-7): 536-544.

Harada, H., E. Takahashi, et al. (1994). "Structure and regulation of the human interferon regulatory factor 1 (IRF-1) and IRF-2 genes: implications for a gene network in the interferon system." Mol Cell Biol **14**(2): 1500-1509.

Harreman, M. T., M. R. Hodel, et al. (2003). "The auto-inhibitory function of importin alpha is essential in vivo." J Biol Chem **278**(8): 5854-5863.

Heim, M. H., I. M. Kerr, et al. (1995). "Contribution of STAT SH2 groups to specific interferon signaling by the Jak-STAT pathway." Science **267**(5202): 1347-1349.

Hibi, M., A. Lin, et al. (1993). "Identification of an oncoprotein- and UV-responsive protein kinase that binds and potentiates the c-Jun activation domain." Genes Dev **7**(11): 2135-2148.

Hirai, S., F. Cui de, et al. (2006). "The c-Jun N-terminal kinase activator dual leucine zipper kinase regulates axon growth and neuronal migration in the developing cerebral cortex." J Neurosci **26**(46): 11992-12002.

Hirai, S., M. Izawa, et al. (1996). "Activation of the JNK pathway by distantly related protein kinases, MEKK and MUK." Oncogene **12**(3): 641-650.

Hirai, S., M. Katoh, et al. (1997). "MST/MLK2, a member of the mixed lineage kinase family, directly phosphorylates and activates SEK1, an activator of c-Jun N-terminal kinase/stress-activated protein kinase." J Biol Chem **272**(24): 15167-15173.

Hirai, S., A. Kawaguchi, et al. (2005). "Expression of MUK/DLK/ZPK, an activator of the JNK pathway, in the nervous systems of the developing mouse embryo." Gene Expr Patterns **5**(4): 517-523.

Holst, J. J. (1999). "Glucagon-like peptide-1, a gastrointestinal hormone with a pharmaceutical potential." Curr Med Chem **6**(11): 1005-1017.

Holz, G. G. (2004). "Epac: A new cAMP-binding protein in support of glucagon-like peptide-1 receptor-mediated signal transduction in the pancreatic beta-cell." Diabetes **53**(1): 5-13.

Holz, G. G. and O. G. Chepurny (2003). "Glucagon-like peptide-1 synthetic analogs: new therapeutic agents for use in the treatment of diabetes mellitus." Curr Med Chem **10**(22): 2471-2483.

Holzman, L. B., S. E. Merritt, et al. (1994). "Identification, molecular cloning, and characterization of dual leucine zipper bearing kinase. A novel serine/threonine protein kinase that defines a second subfamily of mixed lineage kinases." J Biol Chem **269**(49): 30808-30817.

Hood, J. K. and P. A. Silver (1998). "Cse1p is required for export of Srp1p/importin-alpha from the nucleus in Saccharomyces cerevisiae." J Biol Chem **273**(52): 35142-35146.

Hotamisligil, G. S. (2006). "Inflammation and metabolic disorders." Nature **444**(7121): 860-867.

Hotamisligil, G. S., P. Arner, et al. (1995). "Increased adipose tissue expression of tumor necrosis factor-alpha in human obesity and insulin resistance." J Clin Invest **95**(5): 2409-2415.

Hsieh, Y. C., Y. H. Chen, et al. (2005). "Role of cAMP-response element-binding protein phosphorylation in hepatic apoptosis under protein kinase C alpha suppression during sepsis." Shock **24**(4): 357-363.

Hsu, H., J. Huang, et al. (1996). "TNF-dependent recruitment of the protein kinase RIP to the TNF receptor-1 signaling complex." Immunity **4**(4): 387-396.

Hu, J., S. K. Roy, et al. (2001). "ERK1 and ERK2 activate CCAAAT/enhancer-binding protein-beta-dependent gene transcription in response to interferon-gamma." J Biol Chem **276**(1): 287-297.

Hugl, S. R., M. F. White, et al. (1998). "Insulin-like growth factor I (IGF-I)-stimulated pancreatic beta-cell growth is glucose-dependent. Synergistic activation of insulin receptor substrate-mediated signal transduction pathways by glucose and IGF-I in INS-1 cells." J Biol Chem **273**(28): 17771-17779.

Hutchings, P., H. Rosen, et al. (1990). "Transfer of diabetes in mice prevented by blockade of adhesion-promoting receptor on macrophages." Nature **348**(6302): 639-642.

Ichijo, H., E. Nishida, et al. (1997). "Induction of apoptosis by ASK1, a mammalian MAPKKK that activates SAPK/JNK and p38 signaling pathways." Science **275**(5296): 90-94.

Igarashi, K., G. Garotta, et al. (1994). "Interferon-gamma induces tyrosine phosphorylation of interferon-gamma receptor and regulated association of protein tyrosine kinases, Jak1 and Jak2, with its receptor." J Biol Chem **269**(20): 14333-14336.

Inada, A., Y. Hamamoto, et al. (2004). "Overexpression of inducible cyclic AMP early repressor inhibits transactivation of genes and cell proliferation in pancreatic beta cells." Mol Cell Biol **24**(7): 2831-2841.

Isaacs, A. and J. Lindenmann (1957). "Virus interference. I. The interferon." Proc R Soc Lond B Biol Sci **147**(927): 258-267.

Ishizuka, N., K. Yagui, et al. (1999). "Tumor necrosis factor alpha signaling pathway and apoptosis in pancreatic beta cells." Metabolism **48**(12): 1485-1492.

Iwahashi, H., T. Hanafusa, et al. (1996). "Cytokine-induced apoptotic cell death in a mouse pancreatic beta-cell line: inhibition by Bcl-2." Diabetologia **39**(5): 530-536.

Jambal, P., S. Masterson, et al. (2003). "Cytokine-mediated down-regulation of the transcription factor cAMP-response element-binding protein in pancreatic beta-cells." J Biol Chem **278**(25): 23055-23065.

Jansson, D., A. C. Ng, et al. (2008). "Glucose controls CREB activity in islet cells via regulated phosphorylation of TORC2." Proc Natl Acad Sci U S A **105**(29): 10161-10166.

Jhala, U. S., G. Canettieri, et al. (2003). "cAMP promotes pancreatic beta-cell survival via CREB-mediated induction of IRS2." Genes Dev **17**(13): 1575-1580.

Jiang, Y., J. D. Woronicz, et al. (1999). "Prevention of constitutive TNF receptor 1 signaling by silencer of death domains." Science **283**(5401): 543-546.

Jones, S. J., E. C. Ledgerwood, et al. (1999). "TNF recruits TRADD to the plasma membrane but not the trans-Golgi network, the principal subcellular location of TNF-R1." J Immunol **162**(2): 1042-1048.

Kahn, B. B. and J. S. Flier (2000). "Obesity and insulin resistance." J Clin Invest **106**(4): 473-481.

Kahn, S. E. (2001). "Clinical review 135: The importance of beta-cell failure in the development and progression of type 2 diabetes." J Clin Endocrinol Metab **86**(9): 4047-4058.

Kahn, S. E., R. L. Hull, et al. (2006). "Mechanisms linking obesity to insulin resistance and type 2 diabetes." Nature **444**(7121): 840-846.

Kaiser, N., A. P. Corcos, et al. (1991). "Monolayer culture of adult rat pancreatic islets on extracellular matrix: modulation of B-cell function by chronic exposure to high glucose." Endocrinology **129**(4): 2067-2076.

Kalab, P., K. Weis, et al. (2002). "Visualization of a Ran-GTP gradient in interphase and mitotic Xenopus egg extracts." Science **295**(5564): 2452-2456.

Kalderon, D., W. D. Richardson, et al. (1984). "Sequence requirements for nuclear location of simian virus 40 large-T antigen." Nature **311**(5981): 33-38.

Kalderon, D., B. L. Roberts, et al. (1984). "A short amino acid sequence able to specify nuclear location." Cell **39**(3 Pt 2): 499-509.

Kallunki, T., T. Deng, et al. (1996). "c-Jun can recruit JNK to phosphorylate dimerization partners via specific docking interactions." Cell **87**(5): 929-939.

Kaneto, H., D. Kawamori, et al. (2004). "Oxidative stress and the JNK pathway as a potential therapeutic target for diabetes." Drug News Perspect **17**(7): 447-453.

Karaskov, E., C. Scott, et al. (2006). "Chronic palmitate but not oleate exposure induces endoplasmic reticulum stress, which may contribute to INS-1 pancreatic beta-cell apoptosis." Endocrinology **147**(7): 3398-3407.

Karin, M. and A. Lin (2002). "NF-kappaB at the crossroads of life and death." Nat Immunol **3**(3): 221-227.

Kawasaki, H., G. M. Springett, et al. (1998). "A family of cAMP-binding proteins that directly activate Rap1." Science **282**(5397): 2275-2279.

Khoo, S., T. B. Gibson, et al. (2004). "MAP kinases and their roles in pancreatic beta-cells." Cell Biochem Biophys **40**(3 Suppl): 191-200.

Kieffer, T. J. and J. F. Habener (1999). "The glucagon-like peptides." Endocr Rev **20**(6): 876-913.

Kim, S., H. S. Kim, et al. (2007). "Essential role for signal transducer and activator of transcription-1 in pancreatic beta-cell death and autoimmune type 1 diabetes of nonobese diabetic mice." Diabetes **56**(10): 2561-2568.

Klebe, C., H. Prinz, et al. (1995). "The kinetic mechanism of Ran--nucleotide exchange catalyzed by RCC1." Biochemistry **34**(39): 12543-12552.

Kluth, O., F. Mirhashemi, et al. (2011). "Dissociation of lipotoxicity and glucotoxicity in a mouse model of obesity associated diabetes: role of forkhead box O1 (FOXO1) in glucose-induced beta cell failure." Diabetologia **54**(3): 605-616.

Kobe, B. (1999). "Autoinhibition by an internal nuclear localization signal revealed by the crystal structure of mammalian importin alpha." Nat Struct Biol **6**(4): 388-397.

Kotenko, S. V., L. S. Izotova, et al. (1995). "Interaction between the components of the interferon gamma receptor complex." J Biol Chem **270**(36): 20915-20921.

Kruger, M., M. Schwaninger, et al. (1997). "Inhibition of CREB- and cAMP response element-mediated gene transcription by the immunosuppressive drugs cyclosporin A and FK506 in T cells." Naunyn Schmiedebergs Arch Pharmacol **356**(4): 433-440.

Kutay, U., F. R. Bischoff, et al. (1997). "Export of importin alpha from the nucleus is mediated by a specific nuclear transport factor." Cell **90**(6): 1061-1071.

Kutlu, B., A. K. Cardozo, et al. (2003). "Discovery of gene networks regulating cytokine-induced dysfunction and apoptosis in insulin-producing INS-1 cells." Diabetes **52**(11): 2701-2719.

Kyriakis, J. M., P. Banerjee, et al. (1994). "The stress-activated protein kinase subfamily of c-Jun kinases." Nature **369**(6476): 156-160.

Lange, A., R. E. Mills, et al. (2007). "Classical nuclear localization signals: definition, function, and interaction with importin alpha." J Biol Chem **282**(8): 5101-5105.

Larsen, C. M., M. Faulenbach, et al. (2009). "Sustained effects of interleukin-1 receptor antagonist treatment in type 2 diabetes." Diabetes Care **32**(9): 1663-1668.

Larsen, C. M., M. Faulenbach, et al. (2007). "Interleukin-1-receptor antagonist in type 2 diabetes mellitus." N Engl J Med **356**(15): 1517-1526.

Leahy, J. L. (1990). "Natural history of beta-cell dysfunction in NIDDM." Diabetes Care **13**(9): 992-1010.

Leahy, J. L., S. Bonner-Weir, et al. (1992). "Beta-cell dysfunction induced by chronic hyperglycemia. Current ideas on mechanism of impaired glucose-induced insulin secretion." Diabetes Care **15**(3): 442-455.

Leahy, J. L., L. M. Bumbalo, et al. (1994). "Diazoxide causes recovery of beta-cell glucose responsiveness in 90% pancreatectomized diabetic rats." Diabetes **43**(2): 173-179.

Ledgerwood, E. C., J. S. Pober, et al. (1999). "Recent advances in the molecular basis of TNF signal transduction." Lab Invest **79**(9): 1041-1050.

Lee, E. C., D. Yu, et al. (2001). "A highly efficient Escherichia coli-based chromosome engineering system adapted for recombinogenic targeting and subcloning of BAC DNA." Genomics **73**(1): 56-65.

Lee, S. J., Y. Matsuura, et al. (2005). "Structural basis for nuclear import complex dissociation by RanGTP." Nature **435**(7042): 693-696.

Lehuen, A., J. Diana, et al. (2010). "Immune cell crosstalk in type 1 diabetes." Nat Rev Immunol **10**(7): 501-513.

Leung, I. W. and N. Lassam (2001). "The kinase activation loop is the key to mixed lineage kinase-3 activation via both autophosphorylation and hematopoietic progenitor kinase 1 phosphorylation." J Biol Chem **276**(3): 1961-1967.

Lillie, J. W. and M. R. Green (1989). "Transcription activation by the adenovirus E1a protein." Nature **338**(6210): 39-44.

Ling, Z., R. Kiekens, et al. (1996). "Effects of chronically elevated glucose levels on the functional properties of rat pancreatic beta-cells." Diabetes **45**(12): 1774-1782.

Lingohr, M. K., R. Buettner, et al. (2002). "Pancreatic beta-cell growth and survival--a role in obesity-linked type 2 diabetes?" Trends Mol Med **8**(8): 375-384.

Liu, D., A. K. Cardozo, et al. (2002). "Double-stranded RNA cooperates with interferon-gamma and IL-1 beta to induce both chemokine expression and nuclear factor-kappa B-dependent apoptosis in pancreatic beta-cells: potential mechanisms for viral-induced insulitis and beta-cell death in type 1 diabetes mellitus." Endocrinology **143**(4): 1225-1234.

Liu, F. and M. R. Green (1990). "A specific member of the ATF transcription factor family can mediate transcription activation by the adenovirus E1a protein." Cell **61**(7): 1217-1224.

Liu, P., N. A. Jenkins, et al. (2003). "A highly efficient recombineering-based method for generating conditional knockout mutations." Genome Res **13**(3): 476-484.

Liu, Y. J. (2005). "IPC: professional type 1 interferon-producing cells and plasmacytoid dendritic cell precursors." Annu Rev Immunol **23**: 275-306.

Loweth, A. C., G. T. Williams, et al. (1998). "Human islets of Langerhans express Fas ligand and undergo apoptosis in response to interleukin-1beta and Fas ligation." Diabetes **47**(5): 727-732.

Maclean, N. and R. F. Ogilvie (1955). "Quantitative estimation of the pancreatic islet tissue in diabetic subjects." Diabetes **4**(5): 367-376.

Maedler, K. (2008). "Beta cells in type 2 diabetes - a crucial contribution to pathogenesis." Diabetes Obes Metab **10**(5): 408-420.

Maedler, K., A. Fontana, et al. (2002). "FLIP switches Fas-mediated glucose signaling in human pancreatic beta cells from apoptosis to cell replication." Proc Natl Acad Sci U S A **99**(12): 8236-8241.

Maedler, K., D. M. Schumann, et al. (2006). "Low concentration of interleukin-1beta induces FLICE-inhibitory protein-mediated beta-cell proliferation in human pancreatic islets." Diabetes **55**(10): 2713-2722.

Maedler, K., P. Sergeev, et al. (2002). "Glucose-induced beta cell production of IL-1beta contributes to glucotoxicity in human pancreatic islets." J Clin Invest **110**(6): 851-860.

Maedler, K., G. A. Spinas, et al. (2001). "Distinct effects of saturated and monounsaturated fatty acids on beta-cell turnover and function." Diabetes **50**(1): 69-76.

Maedler, K., G. A. Spinas, et al. (2001). "Glucose induces beta-cell apoptosis via upregulation of the Fas receptor in human islets." Diabetes **50**(8): 1683-1690.

Maedler, K., J. Storling, et al. (2004). "Glucose- and interleukin-1beta-induced beta-cell apoptosis requires Ca2+ influx and extracellular signal-regulated kinase (ERK) 1/2 activation and is prevented by a sulfonylurea receptor 1/inwardly rectifying K+ channel 6.2 (SUR/Kir6.2) selective potassium channel opener in human islets." Diabetes **53**(7): 1706-1713.

Major, C. D. and B. A. Wolf (2001). "Interleukin-1beta stimulation of c-Jun NH(2)-terminal kinase activity in insulin-secreting cells: evidence for cytoplasmic restriction." Diabetes **50**(12): 2721-2728.

Mantovani, A., M. Locati, et al. (2001). "Decoy receptors: a strategy to regulate inflammatory cytokines and chemokines." Trends Immunol **22**(6): 328-336.

March, C. J., B. Mosley, et al. (1985). "Cloning, sequence and expression of two distinct human interleukin-1 complementary DNAs." Nature **315**(6021): 641-647.

Marshak, S., G. Leibowitz, et al. (1999). "Impaired beta-cell functions induced by chronic exposure of cultured human pancreatic islets to high glucose." Diabetes **48**(6): 1230-1236.

Mata, M., S. E. Merritt, et al. (1996). "Characterization of dual leucine zipper-bearing kinase, a mixed lineage kinase present in synaptic terminals whose phosphorylation state is regulated by membrane depolarization via calcineurin." J Biol Chem **271**(28): 16888-16896.

Matsui, N., G. Sarkar, et al. (1996). "Identification of a dual leucine zipper kinase involved in rat fracture repair." Biochem Biophys Res Commun **229**(2): 571-576.

Matsuura, Y., A. Lange, et al. (2003). "Structural basis for Nup2p function in cargo release and karyopherin recycling in nuclear import." EMBO J **22**(20): 5358-5369.

Matsuura, Y. and M. Stewart (2004). "Structural basis for the assembly of a nuclear export complex." Nature **432**(7019): 872-877.

Matsuura, Y. and M. Stewart (2005). "Nup50/Npap60 function in nuclear protein import complex disassembly and importin recycling." EMBO J **24**(21): 3681-3689.

Mayr, B. and M. Montminy (2001). "Transcriptional regulation by the phosphorylation-dependent factor CREB." Nat Rev Mol Cell Biol **2**(8): 599-609.

Mayr, B. M., G. Canettieri, et al. (2001). "Distinct effects of cAMP and mitogenic signals on CREB-binding protein recruitment impart specificity to target gene activation via CREB." Proc Natl Acad Sci U S A **98**(19): 10936-10941.

McGarry, J. D. and R. L. Dobbins (1999). "Fatty acids, lipotoxicity and insulin secretion." Diabetologia **42**(2): 128-138.

McKenzie, M. D., N. L. Dudek, et al. (2006). "Perforin and Fas induced by IFNgamma and TNFalpha mediate beta cell death by OT-I CTL." Int Immunol **18**(6): 837-846.

Merritt, S. E., M. Mata, et al. (1999). "The mixed lineage kinase DLK utilizes MKK7 and not MKK4 as substrate." J Biol Chem **274**(15): 10195-10202.

Micheau, O. and J. Tschopp (2003). "Induction of TNF receptor I-mediated apoptosis via two sequential signaling complexes." Cell **114**(2): 181-190.

Miller, B. J., M. C. Appel, et al. (1988). "Both the Lyt-2+ and L3T4+ T cell subsets are required for the transfer of diabetes in nonobese diabetic mice." J Immunol **140**(1): 52-58.

Miyauchi, K., Y. Takiyama, et al. (2009). "Upregulated IL-18 expression in type 2 diabetic subjects with nephropathy: TGF-beta1 enhanced IL-18 expression in

human renal proximal tubular epithelial cells." Diabetes Res Clin Pract **83**(2): 190-199.

Montminy, M. (1997). "Transcriptional regulation by cyclic AMP." Annu Rev Biochem **66**: 807-822.

Murphy, K. C., K. G. Campellone, et al. (2000). "PCR-mediated gene replacement in Escherichia coli." Gene **246**(1-2): 321-330.

Muyrers, J. P., Y. Zhang, et al. (1999). "Rapid modification of bacterial artificial chromosomes by ET-recombination." Nucleic Acids Res **27**(6): 1555-1557.

Nadeau, A., G. Grondin, et al. (1997). "In situ hybridization analysis of ZPK gene expression during murine embryogenesis." J Histochem Cytochem **45**(1): 107-118.

Nagata, K., A. Puls, et al. (1998). "The MAP kinase kinase kinase MLK2 co-localizes with activated JNK along microtubules and associates with kinesin superfamily motor KIF3." EMBO J **17**(1): 149-158.

Nagy, A. (2000). "Cre recombinase: the universal reagent for genome tailoring." Genesis **26**(2): 99-109.

Nair, J. S., C. J. DaFonseca, et al. (2002). "Requirement of Ca2+ and CaMKII for Stat1 Ser-727 phosphorylation in response to IFN-gamma." Proc Natl Acad Sci U S A **99**(9): 5971-5976.

Nguyen, H., C. V. Ramana, et al. (2001). "Roles of phosphatidylinositol 3-kinase in interferon-gamma-dependent phosphorylation of STAT1 on serine 727 and activation of gene expression." J Biol Chem **276**(36): 33361-33368.

Nihalani, D., S. Merritt, et al. (2000). "Identification of structural and functional domains in mixed lineage kinase dual leucine zipper-bearing kinase required for complex formation and stress-activated protein kinase activation." J Biol Chem **275**(10): 7273-7279.

Nihalani, D., D. Meyer, et al. (2001). "Mixed lineage kinase-dependent JNK activation is governed by interactions of scaffold protein JIP with MAPK module components." EMBO J **20**(13): 3447-3458.

Nihalani, D., H. N. Wong, et al. (2003). "Recruitment of JNK to JIP1 and JNK-dependent JIP1 phosphorylation regulates JNK module dynamics and activation." J Biol Chem **278**(31): 28694-28702.

Nishitoh, H., M. Saitoh, et al. (1998). "ASK1 is essential for JNK/SAPK activation by TRAF2." Mol Cell **2**(3): 389-395.

Oetjen, E., R. Blume, et al. (2007). "Inhibition of MafA transcriptional activity and human insulin gene transcription by interleukin-1beta and mitogen-activated

protein kinase kinase kinase in pancreatic islet beta cells." Diabetologia **50**(8): 1678-1687.

Oetjen, E., T. Diedrich, et al. (1994). "Distinct properties of the cAMP-responsive element of the rat insulin I gene." J Biol Chem **269**(43): 27036-27044.

Oetjen, E., D. Grapentin, et al. (2003). "Regulation of human insulin gene transcription by the immunosuppressive drugs cyclosporin A and tacrolimus at concentrations that inhibit calcineurin activity and involving the transcription factor CREB." Naunyn Schmiedebergs Arch Pharmacol **367**(3): 227-236.

Oetjen, E., A. Lechleiter, et al. (2006). "Inhibition of membrane depolarisation-induced transcriptional activity of cyclic AMP response element binding protein (CREB) by the dual-leucine-zipper-bearing kinase in a pancreatic islet beta cell line." Diabetologia **49**(2): 332-342.

Oetjen, E., K. M. Thoms, et al. (2005). "The immunosuppressive drugs cyclosporin A and tacrolimus inhibit membrane depolarization-induced CREB transcriptional activity at the coactivator level." Br J Pharmacol **144**(7): 982-993.

Oyadomari, S., E. Araki, et al. (2002). "Endoplasmic reticulum stress-mediated apoptosis in pancreatic beta-cells." Apoptosis **7**(4): 335-345.

Paludan, S. R. (1998). "Interleukin-4 and interferon-gamma: the quintessence of a mutual antagonistic relationship." Scand J Immunol **48**(5): 459-468.

Parkash, J., M. A. Chaudhry, et al. (2005). "Tumor necrosis factor-alpha-induced changes in insulin-producing beta-cells." Anat Rec A Discov Mol Cell Evol Biol **286**(2): 982-993.

Pennica, D., J. S. Hayflick, et al. (1985). "Cloning and expression in Escherichia coli of the cDNA for murine tumor necrosis factor." Proc Natl Acad Sci U S A **82**(18): 6060-6064.

Pestka, S., S. V. Kotenko, et al. (1997). "The interferon gamma (IFN-gamma) receptor: a paradigm for the multichain cytokine receptor." Cytokine Growth Factor Rev **8**(3): 189-206.

Phillips, J. M., N. M. Parish, et al. (2009). "Type 1 diabetes development requires both CD4+ and CD8+ T cells and can be reversed by non-depleting antibodies targeting both T cell populations." Rev Diabet Stud **6**(2): 97-103.

Phu do, T., M. Wallbach, et al. (2011). "Regulation of the CREB coactivator TORC by the dual leucine zipper kinase at different levels." Cell Signal **23**(2): 344-353.

Pine, R. (1997). "Convergence of TNFalpha and IFNgamma signalling pathways through synergistic induction of IRF-1/ISGF-2 is mediated by a composite GAS/kappaB promoter element." Nucleic Acids Res **25**(21): 4346-4354.

Platanias, L. C. (2005). "Mechanisms of type-I- and type-II-interferon-mediated signalling." Nat Rev Immunol **5**(5): 375-386.

Plaumann, S., R. Blume, et al. (2008). "Activation of the dual-leucine-zipper-bearing kinase and induction of beta-cell apoptosis by the immunosuppressive drug cyclosporin A." Mol Pharmacol **73**(3): 652-659.

Poitout, V. and R. P. Robertson (2002). "Minireview: Secondary beta-cell failure in type 2 diabetes--a convergence of glucotoxicity and lipotoxicity." Endocrinology **143**(2): 339-342.

Poteete, A. R. (2001). "What makes the bacteriophage lambda Red system useful for genetic engineering: molecular mechanism and biological function." FEMS Microbiol Lett **201**(1): 9-14.

Pukel, C., H. Baquerizo, et al. (1988). "Destruction of rat islet cell monolayers by cytokines. Synergistic interactions of interferon-gamma, tumor necrosis factor, lymphotoxin, and interleukin 1." Diabetes **37**(1): 133-136.

Quimby, B. B. and M. Dasso (2003). "The small GTPase Ran: interpreting the signs." Curr Opin Cell Biol **15**(3): 338-344.

Rabinovitch, A., W. Suarez-Pinzon, et al. (1999). "Transfection of human pancreatic islets with an anti-apoptotic gene (bcl-2) protects beta-cells from cytokine-induced destruction." Diabetes **48**(6): 1223-1229.

Rabinovitch, A., W. L. Suarez-Pinzon, et al. (1994). "DNA fragmentation is an early event in cytokine-induced islet beta-cell destruction." Diabetologia **37**(8): 733-738.

Radu, A., G. Blobel, et al. (1995). "Identification of a protein complex that is required for nuclear protein import and mediates docking of import substrate to distinct nucleoporins." Proc Natl Acad Sci U S A **92**(5): 1769-1773.

Rana, A., K. Gallo, et al. (1996). "The mixed lineage kinase SPRK phosphorylates and activates the stress-activated protein kinase activator, SEK-1." J Biol Chem **271**(32): 19025-19028.

Rasmussen, R. K., J. Rusak, et al. (1998). "Mixed-lineage kinase 2-SH3 domain binds dynamin and greatly enhances activation of GTPase by phospholipid." Biochem J **335 (Pt 1)**: 119-124.

Rhodes, C. J. (2005). "Type 2 diabetes-a matter of beta-cell life and death?" Science **307**(5708): 380-384.

Robbins, J., S. M. Dilworth, et al. (1991). "Two interdependent basic domains in nucleoplasmin nuclear targeting sequence: identification of a class of bipartite nuclear targeting sequence." Cell **64**(3): 615-623.

Robertson, R. P., J. Harmon, et al. (2004). "Beta-cell glucose toxicity, lipotoxicity, and chronic oxidative stress in type 2 diabetes." Diabetes **53 Suppl 1**: S119-124.

Robertson, R. P., L. K. Olson, et al. (1994). "Differentiating glucose toxicity from glucose desensitization: a new message from the insulin gene." Diabetes **43**(9): 1085-1089.

Robertson, R. P., H. J. Zhang, et al. (1992). "Preservation of insulin mRNA levels and insulin secretion in HIT cells by avoidance of chronic exposure to high glucose concentrations." J Clin Invest **90**(2): 320-325.

Robitaille, K., A. Daviau, et al. (2008). "Calphostin C-induced apoptosis is mediated by a tissue transglutaminase-dependent mechanism involving the DLK/JNK signaling pathway." Cell Death Differ **15**(9): 1522-1531.

Rossetti, L., A. Giaccari, et al. (1990). "Glucose toxicity." Diabetes Care **13**(6): 610-630.

Rui, L., V. Aguirre, et al. (2001). "Insulin/IGF-1 and TNF-alpha stimulate phosphorylation of IRS-1 at inhibitory Ser307 via distinct pathways." J Clin Invest **107**(2): 181-189.

Sako, Y. and V. E. Grill (1990). "Coupling of beta-cell desensitization by hyperglycemia to excessive stimulation and circulating insulin in glucose-infused rats." Diabetes **39**(12): 1580-1583.

Sakuma, H., A. Ikeda, et al. (1997). "Molecular cloning and functional expression of a cDNA encoding a new member of mixed lineage protein kinase from human brain." J Biol Chem **272**(45): 28622-28629.

Saldeen, J. (2000). "Cytokines induce both necrosis and apoptosis via a common Bcl-2-inhibitable pathway in rat insulin-producing cells." Endocrinology **141**(6): 2003-2010.

Sambrook, J., E. F. Fritsch, et al. (1989). Molecular cloning : a laboratory manual. Cold Spring Harbor, N.Y., Cold Spring Harbor Laboratory.

Sanger, F., S. Nicklen, et al. (1977). "DNA sequencing with chain-terminating inhibitors." Proc Natl Acad Sci U S A **74**(12): 5463-5467.

Santerre, R. F., R. A. Cook, et al. (1981). "Insulin synthesis in a clonal cell line of simian virus 40-transformed hamster pancreatic beta cells." Proc Natl Acad Sci U S A **78**(7): 4339-4343.

Sarvetnick, N., D. Liggitt, et al. (1988). "Insulin-dependent diabetes mellitus induced in transgenic mice by ectopic expression of class II MHC and interferon-gamma." Cell **52**(5): 773-782.

Sauter, N. S., F. T. Schulthess, et al. (2008). "The antiinflammatory cytokine interleukin-1 receptor antagonist protects from high-fat diet-induced hyperglycemia." Endocrinology **149**(5): 2208-2218.

Schroder, K., P. J. Hertzog, et al. (2004). "Interferon-gamma: an overview of signals, mechanisms and functions." J Leukoc Biol **75**(2): 163-189.

Schwaninger, M., R. Blume, et al. (1995). "Involvement of the Ca(2+)-dependent phosphatase calcineurin in gene transcription that is stimulated by cAMP through cAMP response elements." J Biol Chem **270**(15): 8860-8866.

Schwaninger, M., R. Blume, et al. (1993). "Inhibition of cAMP-responsive element-mediated gene transcription by cyclosporin A and FK506 after membrane depolarization." J Biol Chem **268**(31): 23111-23115.

Screaton, R. A., M. D. Conkright, et al. (2004). "The CREB coactivator TORC2 functions as a calcium- and cAMP-sensitive coincidence detector." Cell **119**(1): 61-74.

Shoelson, S. E., L. Herrero, et al. (2007). "Obesity, inflammation, and insulin resistance." Gastroenterology **132**(6): 2169-2180.

Sims, J. E. (2002). "IL-1 and IL-18 receptors, and their extended family." Curr Opin Immunol **14**(1): 117-122.

Sims, S. H., Y. Cha, et al. (1993). "A novel interferon-inducible domain: structural and functional analysis of the human interferon regulatory factor 1 gene promoter." Mol Cell Biol **13**(1): 690-702.

Smith, A. E., B. M. Slepchenko, et al. (2002). "Systems analysis of Ran transport." Science **295**(5554): 488-491.

Srinivasan, S., E. Bernal-Mizrachi, et al. (2002). "Glucose promotes pancreatic islet beta-cell survival through a PI 3-kinase/Akt-signaling pathway." Am J Physiol Endocrinol Metab **283**(4): E784-793.

Stade, K., C. S. Ford, et al. (1997). "Exportin 1 (Crm1p) is an essential nuclear export factor." Cell **90**(6): 1041-1050.

Stahl, F. W. (1998). "Recombination in phage lambda: one geneticist's historical perspective." Gene **223**(1-2): 95-102.

Stoffler, D., B. Fahrenkrog, et al. (1999). "The nuclear pore complex: from molecular architecture to functional dynamics." Curr Opin Cell Biol **11**(3): 391-401.

Subramaniam, P. S., B. A. Torres, et al. (2001). "So many ligands, so few transcription factors: a new paradigm for signaling through the STAT transcription factors." Cytokine **15**(4): 175-187.

Suk, K., S. Kim, et al. (2001). "IFN-gamma/TNF-alpha synergism as the final effector in autoimmune diabetes: a key role for STAT1/IFN regulatory factor-1 pathway in pancreatic beta cell death." J Immunol **166**(7): 4481-4489.

Sun, D. and A. Ding (2006). "MyD88-mediated stabilization of interferon-gamma-induced cytokine and chemokine mRNA." Nat Immunol **7**(4): 375-381.

Swaminathan, S., H. M. Ellis, et al. (2001). "Rapid engineering of bacterial artificial chromosomes using oligonucleotides." Genesis **29**(1): 14-21.

Tajiri, Y., C. Moller, et al. (1997). "Long-term effects of aminoguanidine on insulin release and biosynthesis: evidence that the formation of advanced glycosylation end products inhibits B cell function." Endocrinology **138**(1): 273-280.

Takeuchi, M., M. Rothe, et al. (1996). "Anatomy of TRAF2. Distinct domains for nuclear factor-kappaB activation and association with tumor necrosis factor signaling proteins." J Biol Chem **271**(33): 19935-19942.

Teramoto, H., O. A. Coso, et al. (1996). "Signaling from the small GTP-binding proteins Rac1 and Cdc42 to the c-Jun N-terminal kinase/stress-activated protein kinase pathway. A role for mixed lineage kinase 3/protein-tyrosine kinase 1, a novel member of the mixed lineage kinase family." J Biol Chem **271**(44): 27225-27228.

Thomas, H. E., R. Darwiche, et al. (2002). "Interleukin-1 plus gamma-interferon-induced pancreatic beta-cell dysfunction is mediated by beta-cell nitric oxide production." Diabetes **51**(2): 311-316.

Tibbles, L. A., Y. L. Ing, et al. (1996). "MLK-3 activates the SAPK/JNK and p38/RK pathways via SEK1 and MKK3/6." EMBO J **15**(24): 7026-7035.

Toyoshima, F., T. Moriguchi, et al. (1997). "Fas induces cytoplasmic apoptotic responses and activation of the MKK7-JNK/SAPK and MKK6-p38 pathways independent of CPP32-like proteases." J Cell Biol **139**(4): 1005-1015.

Tsien, R. Y. (1998). "The green fluorescent protein." Annu Rev Biochem **67**: 509-544.

Unger, R. H. (1995). "Lipotoxicity in the pathogenesis of obesity-dependent NIDDM. Genetic and clinical implications." Diabetes **44**(8): 863-870.

Uysal, K. T., S. M. Wiesbrock, et al. (1997). "Protection from obesity-induced insulin resistance in mice lacking TNF-alpha function." Nature **389**(6651): 610-614.

Valledor, A. F., E. Sanchez-Tillo, et al. (2008). "Selective roles of MAPKs during the macrophage response to IFN-gamma." J Immunol **180**(7): 4523-4529.

van der Weyden, L., D. J. Adams, et al. (2002). "Tools for targeted manipulation of the mouse genome." Physiol Genomics **11**(3): 133-164.

Ventura, J. J., P. Cogswell, et al. (2004). "JNK potentiates TNF-stimulated necrosis by increasing the production of cytotoxic reactive oxygen species." Genes Dev **18**(23): 2905-2915.

Wagner, E. F. and A. R. Nebreda (2009). "Signal integration by JNK and p38 MAPK pathways in cancer development." Nat Rev Cancer **9**(8): 537-549.

Walker, K. Z., K. O'Dea, et al. (1996). "Body fat distribution and non-insulin-dependent diabetes: comparison of a fiber-rich, high-carbohydrate, low-fat (23%) diet and a 35% fat diet high in monounsaturated fat." Am J Clin Nutr **63**(2): 254-260.

Walter, M. R., W. T. Windsor, et al. (1995). "Crystal structure of a complex between interferon-gamma and its soluble high-affinity receptor." Nature **376**(6537): 230-235.

Wang, H., G. Kouri, et al. (2005). "ER stress and SREBP-1 activation are implicated in beta-cell glucolipotoxicity." J Cell Sci **118**(Pt 17): 3905-3915.

Webster, N., J. R. Jin, et al. (1988). "The yeast UASG is a transcriptional enhancer in human HeLa cells in the presence of the GAL4 trans-activator." Cell **52**(2): 169-178.

Weir, G. C. and S. Bonner-Weir (2004). "Five stages of evolving beta-cell dysfunction during progression to diabetes." Diabetes **53 Suppl 3**: S16-21.

Welsh, N. (1996). "Interleukin-1 beta-induced ceramide and diacylglycerol generation may lead to activation of the c-Jun NH2-terminal kinase and the transcription factor ATF2 in the insulin-producing cell line RINm5F." J Biol Chem **271**(14): 8307-8312.

Wesche, H., C. Korherr, et al. (1997). "The interleukin-1 receptor accessory protein (IL-1RAcP) is essential for IL-1-induced activation of interleukin-1 receptor-associated kinase (IRAK) and stress-activated protein kinases (SAP kinases)." J Biol Chem **272**(12): 7727-7731.

White, M. F. (2003). "Insulin signaling in health and disease." Science **302**(5651): 1710-1711.

Xu, Z., A. C. Maroney, et al. (2001). "The MLK family mediates c-Jun N-terminal kinase activation in neuronal apoptosis." Mol Cell Biol **21**(14): 4713-4724.

Yang, J., Y. Lin, et al. (2001). "The essential role of MEKK3 in TNF-induced NF-kappaB activation." Nat Immunol **2**(7): 620-624.

Yu, D., H. M. Ellis, et al. (2000). "An efficient recombination system for chromosome engineering in Escherichia coli." Proc Natl Acad Sci U S A **97**(11): 5978-5983.

Yuan, M., N. Konstantopoulos, et al. (2001). "Reversal of obesity- and diet-induced insulin resistance with salicylates or targeted disruption of Ikkbeta." Science **293**(5535): 1673-1677.

Zhang, Y., F. Buchholz, et al. (1998). "A new logic for DNA engineering using recombination in Escherichia coli." Nat Genet **20**(2): 123-128.

Curriculum Vitae

Educational Background

Oct 1999-Oct 2003	Bachelors of Science in Biology, Department of Biology, Faculty of Science, University of Tehran
Oct 2003-Jan 2007	Master of science in Pharmacology-Toxicology, Department of Pharmacology, Faculty of Medicine, University of Tehran/ Medical Sciences
July2009	PhD student in Biological Science, University of Göttingen, Department of Pharmacology.
2012	Clinical Pharmacology and Toxicology, UKE, Hamburg

Honors and Achievements

2003	The **Second** rank in **Toxicology** in the Iranian National Exam for Entering Nationwide M.Sc. Programs in Pharmacological Sciences.

Publications

2008	Protective Effects of Lithium on Acetic Acid-Induced Colitis in Rats (Dig Dis Sci. 2008 Dec 10)
2008	Morphine is protective against doxorubicin induced cardiotoxicity in rat (Toxicology. 2008 Jan 14;243(1-2):96-104.)
2010	The modulatory effect of lithium on doxorubicin-induced cardiotoxicity in rat. (Eur J Pharmacol. 2010 Sep 1;641(2-3):193-8. Epub 2010 Jun 9.)